INFORMATION TO USERS

This manuscript has been reproduced from the microfilm master. UMI films the text directly from the original or copy submitted. Thus, some thesis and dissertation copies are in typewriter face, while others may be from any type of computer printer.

The quality of this reproduction is dependent upon the quality of the copy submitted. Broken or indistinct print, colored or poor quality illustrations and photographs, print bleedthrough, substandard margins, and improper alignment can adversely affect reproduction.

In the unlikely event that the author did not send UMI a complete manuscript and there are missing pages, these will be noted. Also, if unauthorized copyright material had to be removed, a note will indicate the deletion.

Oversize materials (e.g., maps, drawings, charts) are reproduced by sectioning the original, beginning at the upper left-hand corner and continuing from left to right in equal sections with small overlaps.

Photographs included in the original manuscript have been reproduced xerographically in this copy. Higher quality 6" x 9" black and white photographic prints are available for any photographs or illustrations appearing in this copy for an additional charge. Contact UMI directly to order.

Bell & Howell Information and Learning
300 North Zeeb Road, Ann Arbor, MI 48106-1346 USA
800-521-0600

UMI®

A *diatribe* in quantum chemistry

by

Vassiliki-Alexandra Glezakou

A dissertation submitted to the graduate faculty

in partial fulfillment of the requirement for the degree of

DOCTOR OF PHILOSOPHY

Major: Physical Chemistry

Major Professor: Mark Stephen Gordon

Iowa State University

Ames, Iowa

2000

UMI Number: 9962817

UMI®

Bell & Howell Information and Learning Company
300 North Zeeb Road
P.O. Box 1346
Ann Arbor, MI 48106-1346

Graduate College

Iowa State University

This is to certify that the Doctoral dissertation of

Vassiliki-Alexandra Glezakou

has met the dissertation requirements of Iowa State University

Committee Member

Committee Member

Committee Member

Committee Member

Major Professor

For the Major Program

For the Graduate College

To the loving memory of my father Theodoros and my aunt Evanggelia

To my nephews Nicola and Teodoro

Στήν πολύτιμη μνήμη τοῦ πατέρα μου Θεοδώρου καί τῆς θείας μου Ευαγγελίας

Στούς ἀνηψιούς μου Νικόλα καί Θεόδωρο

TABLE OF CONTENTS

ACKNOWLEDGEMENTS

I would like to thank some of the people who influenced my education and my personality, starting with my 5th Grade Teacher, Mr. Evanggelos Tatlas, from whom I had my first Chemistry class. I am thankful to Professors Dimitris Katakis and Kyriakos Viras of University of Athens, Greece, and Dr. Michel Dupuis for their advice and assistance when it was much needed.

Simple words fail to express my gratitude to my Major Advisor, Professor Mark S. Gordon, who is responsible for many good things in my life. He is one of those rare people that combine the technical expertise of an excellent scientist and a tireless group leader, and the compassion of a parent.

I would like to thank Professors James W. Evans, David K. Hoffman, Glenn R. Luecke, Klaus Ruedenberg and Lee Keith Woo for gracing my thesis committee, and for being the wonderful Teachers they are. In particular I thank Dr. Luecke and his family, who often provided a surrogate home along with his technical advice.

Eternally thankful to Professor Constantine Stassis, for his "glorified" lectures, which had the deepest impact on me, his encouragement, his advice and his friendship.

The late Professor Therese Cotton will always have a special place in my heart, for encouraging me even when she was fighting her own difficult battle.

Dr. Michael W. Schmidt has been the "bonus" for joining the "Gordon Gang". In him, I found a valuable advisor and a great friend. I only wish he made his coffee stronger!

Many, many thanks to my "support group" Dr. Stephen T. Elbert, Professor Michio Okumura and my "sibling-in-science" Dr. Jerry A. Boatz and his family, for standing by me and lending a sympathetic ear to my thesis-induced (and not only) whining.

To my friends Dr. Galina Chaban and Professor Nikita Matsunaga who welcomed me to the group, the ever-expanding Gordon Group, and soon-to-be-Dr. Troy Konshak with whom I shared the hardships of graduate school, I wish the best. Dr. David M. Halstead of the Scalable Computing Laboratory had been a great help and quick with a joke on many an occasion, for which I thank him a lot.

Last, but not least, I would like to acknowledge my family. I can never thank enough my Mother Maria for all she has done and still does for me, and for teaching me to be strong and independent. I feel blessed for my two sisters Ourania-Heleni and Niki, who rarely complained for my hovering presence about them, mesmerized by their physics, math, anatomy and comic books. Very patiently, they read, taught and explained things to me, and spoiled me with their love and affection.

ΕΥΧΑΡΙΣΤΙΕΣ

Θά ἤθελα νά εὐχαριστήσω ὅλους ὅσους συνετέλεσαν στήν παιδεία μου καί τήν διαμόρφωση τῆς προσωπικότητάς μου, ἀρχίζοντας μέ τόν κ. Ε. Τάτλα, τόν δάσκαλο μου τῆς 5ης Δημοτικοῦ, ἀπό τόν ὁποῖον ἄκουσα τήν πρώτη διάλεξη Χημείας. Ὀφείλω θερμές εὐχαριστίες στούς Καθηγητές Δημήτριο Κατάκη καί Κυριάκο Βύρα τοῦ Πανεπιστημίου Ἀθηνῶν τῆς Ἑλλάδος, καθώς καί στόν Δρ. Michel Dupuis ὅταν χρειάστηκα τήν συμβουλή καί βοηθειά τους.

Ἁπλες λέξεις ἀδυνατοῦν νά περιγράψουν τήν εὐγνωμοσύνη μου πρός τόν Καθηγητή μου Mark. S. Gordon, ὁ ὁποῖος εὐθύνεται γιά πολλά καλά γεγονότα στήν ζωή μου. Εἶναι ἕνας ἀπό τούς λίγους ἀνθρώπους οἱ ὁποῖοι συνδυάζουν τήν τεχνική κατάρτηση ἑνός ἐξαιρετικοῦ ἐπιστήμονα, καί τήν καλωσύνη γονέα, πρός τούς μαθητές του.

Θά ἤθελα νά εὐχαριστήσω τά μέλη τῆς ἐξεταστικῆς μου ἐπιτροπῆς, κυρίους Καθηγητές James W. Evans, David. K.Hoffman, Glenn. R. Luecke, Klaus. Ruendenberg καί Lee Keith Woo γιά τήν ἐξαιρετική τιμή τοῦ νά συμμετέχουν στήν ἐπιτροπή τῆς διατριβῆς μου. Ἰδιαιτέρως εὐχαριστῶ τόν Dr. Luecke, τοῦ ὁποίου ἡ οἰκογένεια μέ περιέβαλλε μέ στοργή καθ' ὅλη τήν διάρκεια τῆς ἐδῶ παραμονῆς μου.

Ἐγκάρδιες εὐχαριστίες στόν Καθηγητή Κωνσταντίνο Στάσση, γιά τίς "δεδοξασμένες" διαλέξεις του, πού μέ ἐπηρέασαν βαθύτατα, γιά τήν συνεχή ἐνθάρυνση, τίς συμβουλές, καί τήν φιλία του.

Ἡ ἀνάμνηση τῆς τέως Καθηγήτριας Therese Cotton θά μέ συνοδευει πάντοτε, γιά τό ἐνδιαφέρον μέ τό ὁποῖο μέ περιέβαλλε, ἀκόμη καί κατά τίς πλέον δύσκολες στιγμές τῆς ζωῆς της.

Ὁ Δρ. Michael W. Schmidt εἶναι πραγματική ἐπιβράβευση γιά ὅσους ἐπιλεγουν τήν ἐρευνητική ὁμάδα Gordon. Στό πρόσωπό του ἀναγνωρίζω ἕνα πολύτιμο συνεργάτη καί σύμβουλο, καί ἕνα ἀγαπημενο φίλο. Τό μόνο πράγμα πού θά ἀλλαζα σ'αὐτόν εἶναι ...ἡ πυκνότητα τοῦ καφέ του!

Ἄπειρες εὐχαριστίες στήν "ὁμάδα υποστήριξης", Δρ. Stephen T. Elbert, Καθηγητή Michio Okumura, τόν "ἀδελφόν ἐν ἐπιστήμῃ" Δρ. Jerry A. Boatz καί τήν οἰκογένειά του γιά

τήν ἀμείωτη συμπαράστασή τους κατά τήν διάρκεια τῶν "κρίσεων λόγῳ διατριβῆς", καί ὄχι μόνον.

Στούς καλούς μου φίλους Δρ. Galina Chaban καί Καθηγητή Nikita Matsunaga πού μέ καλωσόρισαν στήν ὁμάδα, τήν μονίμως αὐξανόμενη ὁμάδα Gordon, καθώς καί τόν Troy G. Konshak μέ τόν ὁποῖο μοιραστήκαμε πολλές ἀπό τίς δυσκολίες τοῦ διδακτορικοῦ, εὔχομαι ὅ,τι τό καλύτερο. Εὐχαριστῶ τόν Δρ. David M. Halstead τοῦ Scalable Computing Laboratory γιά τήν κατ' ἐπανάληψη βοήθειά του καί τά ἀστεῖα του.

Τελειώνοντας, θά ἤθελα νά εὐχαριστήσω τήν οἰκογενειά μου. Ἁπλες λέξεις ἀδυνατοῦν νά ἐκφράσουν τήν εὐγνωμοσύνη μου πρός τήν Μητέρα μου Μαρία, γιά ὅ,τι ἔχει κάνει καί συνεχίζει νά κάνει γιά μένα. Νιώθω ἀπέραντη εὐγνωμοσύνη γιά τήν παρουσία στήν ζωή μου τῶν δύο ἀδελφῶν μου, Οὐρανίας-Ἑλένης καί Νίκης, πού σπανίως παραπονέθηκαν γιά τήν μόνιμη παρουσία μου κοντά στά βιβλία τους. Μέ ἄπειρη ὑπομονή μοῦ διάβασαν, ἐξήγησαν τό ἄγνωστο, καί μέ "κακόμαθαν" μέ τήν ἀγάπη καί στοργή τους.

Βασιλική-Ἀλεξάνδρα Γκλεζάκου

Ames, Iowa , Spring 2000.

Author's note on the title:

diatribe / 'diə ,tribe / from the Greek word διατριβή, which means the detailed, in depth study of a subject.

"...Chemistry especially has always had irresistible attractions for me from the enormous, the illimitable power which the knowledge of it confers. Chemists - I assert it emphatically - might sway, if they pleased, the destinies of humanitiy. ... "

Count Fosco

From "The Woman in White" by Wilkie Collins

"If, in some cataclysm, all of scientific knowledge were to be destroyed, and only one sentence passed on to the next generation of creatures, what statement would contain the most information in the fewest words? I believe it is the *atomic hypothesis* (or *the atomic fact*, or whatever you wish to call it), that *all things are made of atoms – little particles that move around in perpetual motion, attracting each other when they are a little distance apart, but repelling upon being squeezed into one another.* In that one sentence, you will see, there is an enormous amount of information about the world, if just a little imagination and thinking are applied."

Richard Feynman

From his first lecture on basic physics at Caltech, Fall 1961.

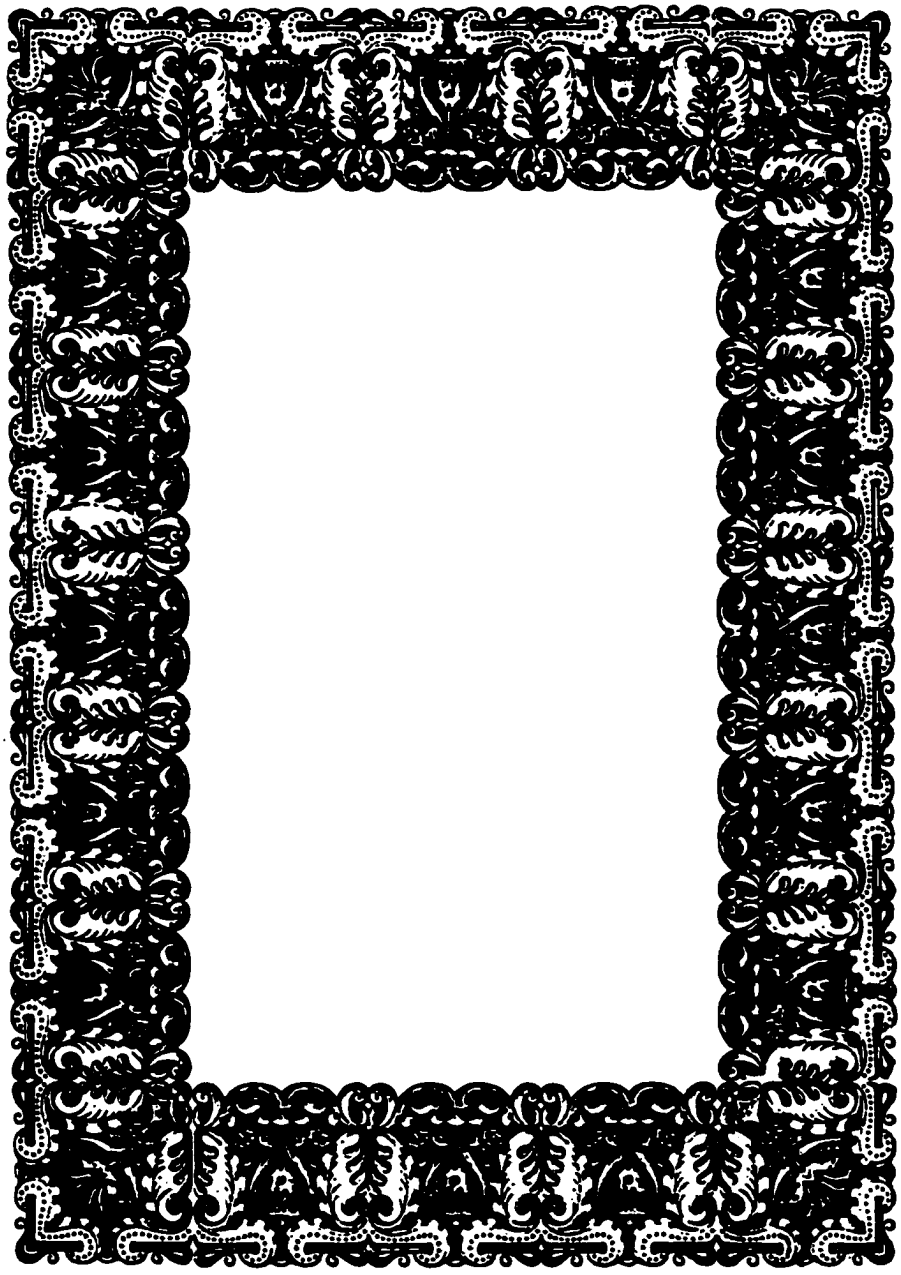

Full view of an electron enlarged 10,000-fold. Note that the electron extends beyond the edge of frame in all directions.
Also, note that the area within the frame is ~h.

CHAPTER 1: INTRODUCTION AND METHODS

At a glance...

The motivation behind this work is the interest in fundamental problems in chemistry solved by applications of theoretical and computational methods. This work is a selective presentation of some of the projects undertaken during my studies, and they have been published or are to be submitted for publication. The general theme of this work is the chemistry of Ti(I), high energy materials and new materials, but throughout this compilation, a variety of topics is being discussed:

- Computational thermochemistry with emphasis on:
  - transition metal chemistry and in particular that of Ti and/or Si compounds
  - explosive annulenes ($C_{36}H_{16}$, $C_{32}Si_4H_{16}$ and $C_{72}H_{32}$), that thermally rearrange to nanostructures.
- Study of Ti/C clusters (Ti_8C_{12}, Metcars) and reaction channels of Ti(I) with Ethene to TiC_2, the basic building blocks of Metcars.
- Study of the B/H_2 system, a high-energy material, with potential use as a rocket fuel, and a prototype of diabatic behaviour.

Dissertation organization

Chapter 1 is an introduction to the methods and commonly used technical terms.

Chapter 2 is a study in *ab initio* computational thermochemistry of Ti and Si containing cyclobutanes, providing thermochemical information that in general is scarce in

the literature. Many of the Si or transition metal containing compounds are quite elusive to obtain, but very desirable to study, since they are closely related to catalytic or chemical vapour deposition (CVD) processes.

Chapter 3 is a thermochemical study of C_{18}-annulenes and their Si-doped analogues.

Chapter 4 focuses on the reaction of Ti(I) with C_2H_4:

$Ti(I) + C_2H_4 \rightarrow ? \rightarrow TiC_2, Ti_2C_2, Ti_2C_3 \rightarrow ? \rightarrow Ti_8C_{12}$

The scarcity of experimental studies of neutral transition metals with small hydrocarbons, a prototypical reaction for many hetero- and homogeneous processes, makes theoretical studies even more essential.

Chapter 5 is a study of the system B/H_2 with state-of-the-art *ab initio* calculations, providing a deeper understanding of the fundamental long and short range interactions and an evaluation of its use as a high energy material. Accurate potential energy surfaces and their detailed characterization are in great demand in the field of dynamics for dynamical studies.

Chapter 6 summarizes the conclusions for the previous chapters.

Let us now proceed with a short introduction to the theoretical methods and terminology.

The fundamental equation

In quantum mechanics, all the properties of any physical system can be determined once the Lagrangian is known. The Lagrangian requires that the field Ψ which describes the physical problem be known at any instant. Mathematically, this statement is equivalent to solving the non-relativistic, time-dependent Schrödinger equation[2], under the assumption that the velocities involved are much smaller than the speed of light:

$$-\frac{\hbar}{i}\frac{\partial\Psi}{\partial t} = \hat{\mathcal{H}}\Psi(Q,t) \tag{1}$$

where $\hat{\mathcal{H}}$ is a many-electron Hamiltonian operator, Ψ is a many-electron, vector field or wavefunction, Q a generalized space coordinate and t the time coordinate.

In most cases, the theoretical chemist deals with stationary problems and therefore solving the time-independent problem is sufficient. The separation of the spatial variables from the time is a common method for simplifying any equation with many variables. Yet, the numerical challenge encountered when addressing electronic structure problems from first principles is intimidating. In the case of a may-electron system, such a task involves the simultaneous solution of many second-order differential equations with singular potentials and many variables. Consequently, the use of approximations that take advantage of our chemical knowledge and intuition is inevitable in solving the non-relativistic Schrödinger equation.

The simplest approximation that was applied, is the Born-Oppenheimer approximation[3], in which the motion of the nuclei is decoupled from that of the electrons. It is based on the difference in mass between electrons and nuclei ($\sim 10^3$-10^{-5}) and assumes that the light electrons follow the heavier nuclei instantaneously during the motion of the latter. The total wavefunction is written as a product of an electronic and a nuclear component:

$$\Psi(Q) = \psi_{el}(r;R)\Theta(R) \tag{2}$$

where r and R are generalized position vectors of the electrons and nuclei respectively. The electronic part is then parametrized with respect to the position of the nuclei ("fixed" geometry).

The total, non-relativistic, time independent Hamiltonian, in the absence of external fields, is:

$$\hat{\mathcal{H}} = \hat{\mathcal{H}}_{el} + \hat{\mathcal{T}}_{nuc} \tag{3}$$

where

$$\hat{\mathcal{T}}_{nuc} = -\sum_{\mu} \frac{1}{2m_{\mu}} \nabla_{\mu}^{2} \tag{3.1}$$

is the nuclear kinetic energy, and

$$\hat{\mathcal{H}}_{el} = -\sum_{i} \frac{1}{2} \nabla_{i}^{2} - \sum_{\mu,i} \frac{Z_{\mu}}{|r_{\mu} - r_{i}|} + \sum_{i<l} \frac{1}{|r_{i} - r_{j}|} + \sum_{\mu<\nu} \frac{Z_{\mu} Z_{\nu}}{|r_{\mu} - r_{\nu}|} \tag{3.2}$$

The problem is then reduced to solving the electronic equation parametrized with respect to the nuclear coordinates:

$$\hat{\mathcal{H}}_{el}(r;R)\psi_{el}(r;R) = E_{el}(R)\psi_{el}(r;R) \tag{4}$$

The nuclear wavefunction is a solution to the equation:

$$\{\hat{\mathcal{T}}_{nuc}(R) + E_{el}(R)\}\Theta(R) = \mathcal{E}\Theta(R) \tag{5}$$

The notion of potential energy surfaces, or that of electronic structure and the shape of the molecules ("molecular geometry") is a consequence of the Born-Oppenheimer approximation. As we will see later on, this approximation breaks down when two such potential surfaces cross and often a different approach is necessary.

However, the problem at hand is still too complicated to solve and further approximations are introduced in order to obtain a qualitatively correct solution. Such an approach is the Hartree-Fock method[4].

The Hartree-Fock approximation

According to the Pauli exclusion principle[5], a physically acceptable wavefunction has to be antisymmetric with respect to the interchange of the coordinates of any two electrons. An "obvious" choice for such a trial function is a Slater determinant[6], an antisymmetrized linear combination of Hartree products. The Hartree-Fock approximation is a variational method, and the energy, as a function of a trial wavefunction, is minimized with respect to this function:

$$E[\Phi] = \frac{\left\langle \Phi \mid \hat{\mathcal{H}} \mid \Phi \right\rangle}{\langle \Phi \mid \Phi \rangle} \geq \mathcal{E}_0 \tag{6}$$

with the calculated energy $E[\Phi]$ being an upper bound to the exact ground state energy E_0, as the variational principle dictates.

The integral over Slater determinants can be ultimately reduced to zero-, one-, and two-electron integrals over one-electron functions, and the electronic Hamiltonian for a many-electron system can be written as follows:

$$\hat{\mathcal{H}}_{el} = \sum_i \hat{h}_i + \sum_{i<j} \hat{g}_{ij} + \hat{h}_0 \tag{7}$$

The zero-electron term

$$\hat{h}_0 = \sum_{\mu<\nu} \frac{Z_\mu Z_\nu}{|r_\mu - r_\nu|} = \sum_{\mu<\nu} \frac{Z_\mu Z_\nu}{r_{\mu\nu}} \tag{7.1}$$

is a constant within the Born-Oppenheimer approximation for fixed nuclear positions, which is ignored until the end of the computations and simply added in at the end.

The one-electron term

$$\hat{h}_i = -\frac{1}{2}\nabla_i^2 - \sum_{\mu}\frac{Z_\mu}{r_{i\mu}} \tag{7.2}$$

which includes the electrons' kinetic energy and the potential energy between nuclei and electrons, depends on the coordinates of one electron only and is totally symmetric in the electron coordinates.

The two-electron term

$$\hat{g}_{ij} = \frac{1}{r_{ij}} \tag{7.3}$$

describes the interaction between any two electrons. This term is more complicated than the previous one, and introduces non-vanishing contributions due to the antisymmetric character of the wavefunction.

Ultimately, one has to solve the Hartree-Fock Equations, a set of linear, one-particle equations:

$$\hat{\mathcal{F}}(1)|\varphi_i(1)\rangle = \varepsilon_i|\varphi_i(1)\rangle \quad \text{i=1,2,...,N (number of electrons)} \tag{8}$$

where

$$\hat{\mathcal{F}}(1) = \hat{h}(1) + \sum_{\mu}\left[\hat{\mathcal{J}}_\mu(1) - \hat{\mathcal{K}}_\mu(1)\right] \equiv \hat{h}(1) + v^{HF}(1) \tag{8.1}$$

is the Fock operator, a Hermitian integrodifferential operator. $v^{HF}(1)$ is the average potential of (N-1) electrons, $\{|\varphi_i(1)\rangle\}_i$ are column vectors (MO's, molecular orbitals) that diagonalize the Fock matrix, and $\{\varepsilon_i\}_i$ are their eigenvalues.

Since the Fock operator depends on the molecular orbitals that have to be determined, one must solve iteratively until self-consistency is achieved. As a further approximation, the

molecular orbitals are taken to be linear combinations of the atomic orbitals (LCAO's)[7], and "belong" to the molecule as a whole:

$$|\varphi_i\rangle = \sum_{\alpha} c_{\alpha i}\chi_{\alpha} \tag{9}$$

The atomic orbitals $\{\chi_a\}$ are centered on each atom and they are linear combinations of basis functions, in the majority of the cases GTO's (Gaussian Type Orbitals), as proposed originally by Boys[8]:

$$\chi_v(r) = \mathcal{N}x^l y^m z^n \exp(-\alpha r^2) \tag{9.1}$$

where $\mathcal{N}$ is a normalization factor, l, m, n integers and α a number determined from atomic calculations.

Notice that within the Born-Oppenheimer model, the Hartree-Fock method is exact within the non-relativistic limit, with the only approximation introduced being that of the single-determinant wavefunction. Nevertheless, for practical purposes a second approximation is unavoidable, that being the finite number of basis functions that can be used.

Correlation energy

The Hartee-Fock approximation is a very useful tool, because it gives a qualitatively correct picture for most stationary problems, and its shortcomings are known and well understood. The model neglects correlation however, by virtue of the orbital approximation. The correlation energy is defined to be the difference in energy between the exact energy and the Hartree-Fock limit[9]:

$$\varepsilon^{corr} = \mathcal{E}^{exact} - E^{HF} \tag{10}$$

The Hartree-Fock wavefunction does include part of the correlation through the Fermi hole, which couples the motion of same spin electrons only, but neglects the interaction between opposite spins, as well as the instantaneous interactions between electron pairs (dynamic correlation). Nevertheless, it provides of a means for systematic recovery of the correlation, through use of the virtual space (the group of unoccupied orbitals).

Size-consistency and size-extensivity

These terms are often used interchangeably, but are quite different in nature. Size-extensivity is a more formal property, and it means that a method scales properly with the number of particles. It therefore applies even to atoms. Size-consistency on the other hand, implies a balanced description of a system at its equilibrium (geometry) and "at infinity". Note that this criterion is defined in terms of a fragmentation process, and a different fragmentation scheme may give different results. Size-consistency is not a more general concept, in the contrary, it is more restricted in the sense that it requires that electron correlation be described consistently even within a chosen fragmentation process.

Correlation methods

Following are the most popular methods that correct for correlation.

(i) Rayleigh-Schrödinger Perturbation Theory.

Correlation energy can be incorporated perturbatively through Rayleigh-Schrodinger perturbation theory (RSPT), as applied first by Möller and Plesset[10] (also known as MPPT). The Hartee-Fock Hamiltonian is taken to be the zero-th order Hamiltonian for an N-electron

system. The most common correction is through the second order (MP2), but higher order corrections (MP3, MP4 or MP5) are often included. Perturbation theory is not variational, but it is size-consistent, regardless of where the expansion is terminated. MP2 corrections will recover up to about 80% of the dynamic correlation[11].

(ii) Configuration Interaction Methods

1. *Configuration interaction (CI)*[11]. In this approach, single, or double or higher order excitations from a judiciously chosen space, into the virtual space are considered. The CI-wavefunction is written as a linear combination of the excitation determinants (equation (11)), and the coefficients, $\{C_{\alpha I}\}$ are optimized to minimize the CI-energy.

$$|\Psi_{CI}\rangle = c_0|\Phi_0\rangle + \sum_{ia} c_i^a|\Phi_i^a\rangle + \sum_{\substack{i<j \\ a<b}} c_{ij}^{ab}|\Phi_{ij}^{ab}\rangle + \sum_{\substack{i<j<k \\ a<b<c}} c_{ijk}^{abc}|\Phi_{ijk}^{abc}\rangle + \ldots \qquad (11)$$

where $|\Phi_I\rangle = \sum_{\mu} c_{\mu i}|\varphi_i\rangle$

If all possible excitations are included, it is called full CI, which is feasible for only a few small systems. The most common CI wavefunction computed is with single and double excitations (CISD)[11].

2. *Multiconfiguration Self Consisitent Field Theory*. Hartree-Fock becomes inadequate in processes where bonds break or form, or in cases of near-degeneracies, where more than one electronic configurations become equally important (quasi-degenerate). In such instances, the use of multi-configuration wavefunctions (MCSCF)[12] is imperative. The wavefunction is written as a linear combination of determinants, just like in (11), but the orbital $\{c_{\mu I}\}$ and the linear coefficients $\{C_{\alpha I}\}$ are simultaneously optimized. The number of quasi-degenerate configurations included is generally much smaller than in the CI case. This method recovers what is called non-dynamic (or static) correlation. The number of correlated

orbitals define an active space and when all possible configurations within this space are included, the method is referred to as Fully Optimized Reaction Space (FORS)[13], also known as Complete Active Space (CAS)[14]. This type of wavefunction is the reference used throughout the study of the system B/H_2.

(iii) Coupled-Cluster Methods

The basic idea of the cluster expansion was first introduced by Sinanoğlu[14], in an effort to characterize correlation treatments more general than separated electron pairs. The wavefuntions is written as:

$$\Psi = (1 + C_1 + C_2 + \cdots)\Psi_0 \tag{12}$$

where the coefficients $\{C_K\}$ represent excitation amplitudes between electron pairs. Size-extensivity is the result of unconnected pairs (unlinked by Sinanoğlu's term, or disconnected). The modern coupled cluster techniques include a variety of implementations[15,16,17].

MCSCF can be also combined with configuration interaction, for example multi-reference configuration interaction (MRCI)[12a], or a perturbative treatment, such as the multiconfigurational quasidegenerate second order perturbation theory (MCQDPT2)[18] or CASPT2[19] to provide both qualitatively and quantitatively correct results. In general, it is desirable to approach the full CI limit with complete basis sets, an improbable quest except for atoms or 2-3 atom-systems. As the computing power increases, so does the size of the problems that scientists would like to tackle. Most of the time this is not possible and many methods try to approach this result through successive corrections. This approach finds a wide applicability in computational thermochemistry[20].

Computational thermochemistry

Although most practical work is done in the condensed phase, in many cases, the thermochemistry of a reaction does not change much qualitatively, in the gas phase[21]. Thermochemical predictions can therefore be of great importance, as in the case of transition metal elements or more unusual systems. There are many ways to predict thermochemical properties:

- Empirical estimates
  - group additivity schemes
  - molecular mechanics models
  - chemical reasoning
- Quantum mechanical models
  - semiempirical MO methods
  - *ab initio* MO methods
  - density functional methods
  - quantum Monte Carlo
- Hybrid methods.

The general consensus is that users of thermochemical data will rely increasingly upon *ab initio* calculations with empirical corrections to account for accuracy shortcomings. Of course, empirical corrections are acceptable only (i) if the errors introduced are systematic and cancel out and (ii) there are enough experimental data to support their implementation.

One way of applying corrections systematically is through isodesmic[21,22] and/or homodesmic[22] reactions. Both schemes are based on the cancellation of errors on both sides of a chemically balanced equation where the total number of formal bonds is conserved. An

isodesmic reaction preserves the number and formal type of chemical bonds. A homodesmic reaction preserves both the number and type, as well as the formal groups.

An example of a homodesmic reaction would be:

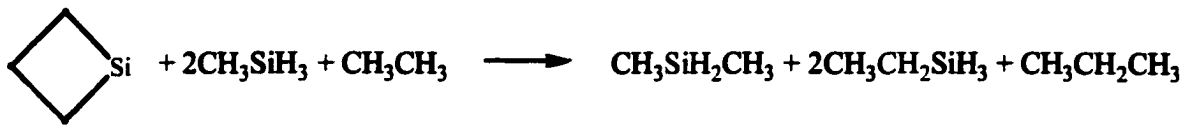

An example of an isodesmic reaction is:

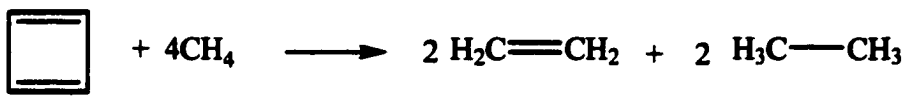

A simpler isodesmic scheme would be to simply terminate any C-C fragments with hydrogens.

A very successful hybrid scheme is the G2 method developed by Pople and co-workers[23,24]. G2 is a composite model, in which the results of several calculations of increasing sophistication are used to extract the corrections that approach the result of a very expensive calculation. The few empirical corrections do not depend on the chemical composition and therefore are more general and quite accurate (on the order of ~5 kcal mol^{-1}). The G2 scheme or more economical versions of it see Chapter 3, combined with the appropriate homodesmic and isodesmic reactions, are used for the thermochemical predictions throughout this work.

References

1. GAMESS by: Schmidt, M. W.; Baldridge, K. K.; Boatz, J. A.; Elbert, S. T.; Gordon, M. S.; Jensen, J. H.; Koseki, S.; Matsunaga, N.; Nguyen, K. A.; Su, S.; Windus, T. L.; Dupuis, M.; Montogomery, J. A. *J. Comp. Chem.* **1993**, 14, 1347.
2. (a) Schrödinger, E. *Ann. Physik* **1926**, 79, pages 361, 489, 734. (b) *ibid* **1926**, 80, 473. (c) *ibid* **1926**, 81, 109.
3. Born, M.; Oppenheimer, J. R. *Ann. Physik* **1927**, 84, 457.
4. (a) Hartree, D. R. *Proc. Cambridge Phil. Soc.* **1928**, *24*, pages 89, 111, 426. (b) Fock, V. *Physik* **1930**, 61, 126.
5. Pauli, W. *Z. Physik* **1925**, 31, 765.
6. Slater, J. C. *Phys. Rev.* **1930**, 35, 210. (b) Fock, V. *Z. Physik* **1930**, 62, 795.
7. Roothaan, C. C. J. *Rev. Mod. Phys.* **1960**, 32, 179.
8. Boys, S. F. *Proc. Roy. Soc.* (London), **1950**, A200, 542.
9. Löwdin, P.-O. *Adv. Chem. Phys.* **1959**, 2, 207.
10. Möller, C.; Plesset, M. S. *Phys. Rev.* **1934**, 46, 618.
11. Szabo A.; Ostlund S. N. in *Modern Quantum Chemistry*, McGraw-Hill, New York, **1989**.
12. (a) Werner, H.-J. in Advances in Chemical Physics: Ab Initio Methods in Quantum Chemistry Part II, K.P. Lawley editor, John Wiley & Sons, New York, **1987**, 69, 1. (b) Shepard R. reference (a), p.63. (c) Roos, B.O. reference (a), p.399.
13. (a) Sundberg, K. R.; Rüdenberg K. in *Quantum Science*, ed. Calais, J. L.; Goscinski, O.; Linderberg, J.; Ohrn, Y., Plenum, New York, **1976**, p 505. (b) Cheung, L. M.; Sundberg, K. R.; Rüdenberg, K. *Int. J. Quantum Chem.* **1979**, 16, 1103. (c) Rüdenberg, K.; Schmidt, M. W.; Gilbert, M. M.; Elbert, S. T. *Chem. Phys.* **1982**, 71, 41, 51 and 65.

14. (a)Sinanoğlu, O. *J. Chem. Phys.* **1962**, *36*, 706. (b) Sinanoğlu, O. *ibid* 3198.

15. (a) Foudation of the CC methods: Čížek J. *J. Chem. Phys.* **1966**, *45*, 4256. (b) Coupled-pair many electron theory, CPMET of Paldus and Čížek: Čížek, J. *Int. J. Quantum Chem.* **1971**, *5*, 359.

16. Spin-orbital CCD equations: (a) Hurley, A. C. *"Elctron Correlation in Small Molecules"*, Academic Press, New York, **1965**. (b) Taylor, P. R.; Backsay, G. B.; Hush, N. S.; Hurley, A. C. *Chem. Phys. Lett.* **1976**, *41*, 444.

17. Derivation and practical implementation of CCSD: Purvis, G.D.; Bartlett, R. J. J. *Chem. Phys.* **1982**, *76*, 1910.

18. Roos, B. O.; Taylor, P. R.; Siegbahn, P. E. M. *Chem. Phys.* **1980**, 48, 157.

19. (a) Nakano, H. *J. Chem. Phys.* **1993**, 99, 7983. (b) Nakano, H. *Chem. Phys. Lett.* **1993**, 201, 372.

20. (a) Anderson, K.; Malmquist, P.-Å.; Roos, B. O. *J. Chem. Phys.* **1992**, 96, 1218. (b) Anderson, K.; Malmquist, P.-Å.; Roos, B. O. *J. Phys. Chem.* **1990**, 94, 5483.

21. ACS Symposium Series 677, *"Computational Thermochemistry. Prediction and Estimation of Molecular Thermodynanics"*, Eds. Irikura, K. K. and Frurip, D.J. **1996**.

22. (a) Hehre, W. J.; Radom, L.; Schleyer, P. v. R.; Pople, J. A. *Ab Initio Molecular Orbital Theory*, Wiley New York, **1986**. (b) Hehre, W. J.; Ditchfield, R.; Radom, L.; Pople, J. A. J. *Am. Chem. Soc.* **1970**, 92, 4796.

23. George, P.; Trachtman, M.; Bock, C. W.; Brett, A. M. *Tetrahedron* **1976**, 32, 317.

24. Curtiss, L. A.; Raghavachari, K.; Trucks, G. W.; Pople, J. A. *J. Chem. Phys.* **1991**, 94, 7221.

CHAPTER 2: STRUCTURE, BONDING, AND HEATS OF FORMATION OF SILATITANACYCLOBUTANES

A paper published in and reprinted with permission of

The Journal of Physical Chemistry A, 1997, *101(46)*,Pages 8714-8719

Vassiliki-Alexandra Glezakou and Mark S. Gordon

Department of Chemistry, Iowa State University, Ames, IA 50011-3111

Abstract

The MP2/TZVP geometries and the standard heats of formation at 0 and 298.15K of 1,2- and 1,3-silatitanacyclobutanes and a number of smaller Ti and/or Si containing alkanes are calculated using the G2-model. The G2-procedure was suitably modified to allow for treatment of first row transition elements and was directly applied to the reference compounds, which were subsequently connected to the two rings via the appropriate homodesmic reactions. The expected accuracy should be on the order of 3 kcal mol^{-1}. Bonding and structural characteristics are discussed in terms of Boys localized orbitals and Bader density analysis.

Introduction

Metallacyclobutanes[1] are known for a wide variety of reactivities with both organic and inorganic reagents, playing a key role in a wide spectrum of important reactions including methylene transfer to organic carbonyls[2, 3a], formation of enolates[2b, 3], electron transfer from activated halides[4], olefin metathesis[5], ring-opening polymerization[6] and

complexation with metal halides[7]. Their reactivity is influenced by kinetic and thermodynamic factors, the metal center and its ligands and the substituents[8]. Correlated photoelectron spectroscopy (PES)[9] is often employed to address electronic structure related questions.

Unfortunately, metallacyclobutanes are not particularly stable for high quality PES studies. On the other hand, the analogous silametallacyclobutanes show considerable thermal stability and have been chemically, structurally and spectroscopically characterized for a number of transition metals[9] (M=Ti, Zr, Nb and Mo) and Th[10]. From the early transition metals, only Ti has been characterized by X-ray diffraction, while tetravalent Zr, Nb and Mo offer more stable analogues for study. They all crystallize in a monoclinic unit cell of $P2_1/m$ symmetry.

We are interested in the thermochemical properties as well as the reaction behaviour (ring opening) of these cyclic systems. As a first step, and given the lack of thermochemical data, the MP2 structures and heats of formation obtained using homodesmic reactions[11] are reported for the 1-sila-2- and 1-sila-3-metallacyclobutanes. In principle, reliable heats of formation could be directly calculated using a basis of triple zeta quality with extra diffuse and polarization functions at a high level of theory to account for correlation, for example, using higher orders of perturbation theory or extensive configuration interaction methods. Calculations at this level become very expensive. Instead, the heats of formation of a number of smaller Ti-containing alkane and silane reference compounds were calculated, using the Gaussian-2 model[12a]; these were subsequently combined in the homodesmic reactions from which the estimated G2-heats of formation of the cyclic systems were finally obtained.

Computational Details

The heats of formation of 1-sila-2- and 1-sila-3-titanacyclobutane were calculated from the appropriate homodesmic reactions (*vide infra*) involving two and three heavy atom fragments. A modified G2 procedure was employed for the direct evaluation of the heats of formation of these smaller molecules.

Three ab *initio* programs were employed for our calculations:

The GAMESS suite of programs[13] was used to perform self-consistent field (SCF) geometry optimizations and to obtain Boys localized molecular orbitals[14] using the built-in triple zeta[15a] plus polarization[15b] (TZVP) basis set. GAMESS was also used for exponent optimization for the higher order polarization functions on Ti.

The diffuse s, p and d polarization functions for Ti were extracted from the standard TZV basis in a even-tempered fashion; the resulting exponents are:

$\alpha_s = 0.0350$; $\alpha_p = 0.0239$; $\alpha_d = 0.0207$.

The f and g polarization functions were obtained by individual exponent optimizations on the ground ^3F state of Ti atom. These optimizations were performed with a singles and doubles configuration interaction (CISD) from a restricted Hartee-Fock (ROHF) wavefunction, in which only the $(4s)^2\,(3d)^2$ electrons were correlated. The optimized exponents are:

$\alpha_f = 0.591$; $\alpha_g = 0.390$

The (2f) and (3f) polarization sets were obtained following the even-scaling rule[17a], according to which atomic basis functions with the same angular momentum should have exponents in a geometric progression:

$(2f) = (1/2\ f_0, 2f_0)$[17b] and $(3f) = (1/4\ f_0, 1f_0, 4f_0)$[17b]

where f_0 refers to the original single f-exponent.

The **Gaussian 92** program[18] was used for second order perturbation theory (MP2) geometry optimizations[19] and analytic Hessians[20] (second derivatives of the energy) to locate the potential energy minima for the rings and smaller systems. Gaussian92 was also employed for the majority of the G2 steps (single-point calculations using second order perturbation theory with extended and diffuse polarization basis sets (MP2) and fourth order perturbation theory with corrections from single, double, triple and quadruple excitations (MP4SDTQ,)[21]; single-point energies using quadratic configuration interaction including contributions from singles, doubles and triples (QCISD(T)).

HONDO 8.4[23] was used for the MP2 and MP4SDTQ single-point calculations where basis sets with g polarization functions were involved.

All MP2 and MP4 single-point calculations were done at the MP2 (frozen core)/TZVP optimized geometries.

Modifications of the original G2 scheme were made in order to handle Ti. To date, the procedure has been applied only to main group elements with an accuracy of 2-3 kcal mol^{-1}. In our modified scheme, we kept the originally proposed basis sets for H, C and Si (ref 12a and refs therein), and used a TZV plus polarization (TZVP) basis set on Ti, expanding with higher angular momentum polarization functions to be consistent with the main group elements. This TZVP basis set was used throughout the MP2-optimization and Hessian runs. Table 1 summarizes the additions/changes made. For clarity, only Ti is listed in the column of modifications, but it is understood that the basis sets listed in column "Original G2" were still used for H, C and Si.

Results and Discussion

Theoretical prediction[24] of heats of formation generally involves the computation of bond dissociation energies, atomization energies and heats of reactions, and one can combine theoretical as well as experimental data for this purpose. Because more than one step is usually involved, care should be taken to minimize the systematic errors, while almost always empirical corrections are made for chemical accuracy. Even high quality calculations may lead to erroneous predictions, unless the appropriate reactions are considered. Large basis sets and treatment for electron correlation are the most important factors, both of which are computationally expensive. Because of the size of the ring compounds, in terms of numbers of electrons and basis functions, direct application of the G2 model on the cyclic compounds would be too demanding; therefore, in this study, we employ homodesmic reactions to optimize the cancellation of systematic errors, while the G2 procedure is applied directly to the smaller reference compounds to obtain their heats of formation.

I. Homodesmic reactions [11]

In this type of reaction, entire chemical groups are conserved upon going from reactants to products. Homodesmic reactions are expected to minimize the contribution to the heat of formation from electron correlation and basis set effects by forcing a cancellation of such errors. For the cyclic systems of interest the following homodesmic reaction were used:

$$+ SiH_3CH_3 + TiH_3CH_3 + CH_3CH_3 + SiH_3TiH_3 \longrightarrow \quad (1)$$

$$TiH_3CH_2CH_3 + SiH_3CH_2CH_3 + SiH_3TiH_2CH_3 + TiH_3SiH_2CH_3$$

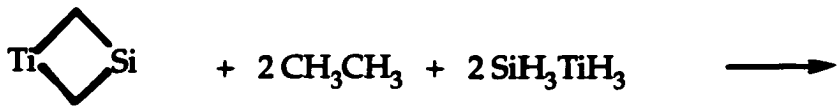

(2)

$$CH_3TiH_2CH_3 + 2\,TiH_3CH_2SiH_3 + CH_3SiH_2CH_3$$

The heats of formation of the cyclic systems can be calculated from the heats of reactions (1) and (2), once the heats of formation are known for the smaller reference species.

II. Geometries[25]

In Figure 1, the MP2/TZVP geometries of the cyclic systems (R1, R2) and of the fragments (F1 - F13) are shown. For geometries of C_1 symmetry, a bond distance average value is given; the local symmetry of XH_3 groups (X = C, Si, or Ti) is essentially C_{3V}.

Of the two silatitanacyclobutanes (R1, R2), the 1,3 - isomer is more stable by 21.5 kcal mol^{-1} at the MP2/TZVP level of theory, in agreement with the experimental evidence accompanying the synthesis of analogous systems[9].

At the same level of theory, structures (F4, F6) and (F5, F7) constitute two conformational pairs. As also reported before[26], SiH_3TiH_3 shows two close-lying minima, both of C_{3V} symmetry (structures F4, F6), differing by only 2.7 kcal mol^{-1}. In the lowest energy minimum (F6), the hydrogens on Si are inverted towards Ti forming three hydrogen bridges. Therefore, the Si - Ti bond shortens by .077 Å compared to the "conventional", ethane - like structure (F4). The analogous effect is observed in the $SiH_3TiH_2CH_3$ isomers (F5, F7), but the minima here are almost degenerate, F7 being more stable by only 1.4 kcal mol^{-1} [25]. Structures R1 and F8 also have Si directly bonded to Ti and Si-Ti bond distances similar to those in F4 and F5. Nonetheless, no bridging minima were

found for either of these species. It seems essential to have a SiH_3-unit rather than $-SiH_2-$ for any bridging to occur. This conclusion was further supported by an effort to use the CH_3-group for bridging in $TiH_3SiH_2CH_3$. The resulting minimum lies 4.6-kcal mol^{-1} higher than F8.

In calculating the heats of formation, only the lowest minima were considered.

III. G2 -energies and heats of formation

The zero-point G2-energy, is given by the formula[12]:

$$E_0(G2) = E_0(G1) + \Delta_1 + \Delta_2 + 1.14E\text{-}3\ n_{pair} \qquad \text{(III.1)}$$

$E_0(G1)$[12b] is the calculated G1-energy, computed at the MP4 and QCI levels of theory, and includes the vibrational zero-point energy corrections, as well as an empirical correction (HLC). The following formulae are the ones used for the G1/G2- energies, adjusted to our basis set modifications. In the adopted notation for the basis set, "triple zeta" is equivalent to 6-311 G for H, C and Si and TZV for Ti suitably extended with polarization functions:

- $E_0(G1)$ = E (MP4/triple zeta (f, d, p)) +
  [E (MP4/triple zeta + (f, d, p)) - E (MP4/triple zeta (f, d, p))] +
  [E (MP4/triple zeta (2fg, 2df,p)) - E (MP4/triple zeta (f, d, p))] +
  [E (QCISD (T)/triple zeta (f, d, p)) - E (MP4/triple zeta (f, d, p))] +
  HLC + ZPE (III.2)

where HLC is an empirical correction and ZPE the MP2 vibrational zero-point energy scaled by 0.943[27].

The corrections Δ_1 and Δ_2 are given by (III3) and (III.4):

- Δ_1 = [E (MP2/triple zeta + (3fg, 3df, 2p)) - E (MP2/triple zeta (f, d, p))] -

[E (MP2/triple zeta + (f, d, p)) - E (MP2/triple zeta (f, d, p))] -

[E (MP2/triple zeta (2fg, 2df,p)) - E (MP2/triple zeta (f, g, p))] (III.3)

- Δ_2 = [E (MP2/triple zeta + G (3fg, 3df, 2p)) -

E (MP2/triple zeta G (f, d, p))] (III.4)

The corrections (III.2, III.3, III.4) made on top of G1 (III.1) account for additivity assumptions of the diffuse and higher order polarization functions, while the last term re-adjusts the higher level correction.

The heats of reaction (ΔH_r) for the homodesmic reactions (1) and (2) were calculated at the MP2/TZVP level from the E_0(MP2) energies. The standard heats of formation, $\Delta H_{f,0K}$, for each of the fragments were calculated using the experimental energies of atomization[28]. The standard heats of formation at 298.15K were then calculated by adding the thermal corrections for vibrations, rotations and translations. Table 2 summarizes the results of our calculations. Both cyclic systems appear to be highly reactive. The calculated heats of formation at 298.15K are 91.3 and 74.3 kcal mol^{-1} for the 1,2- and 1,3-silatitanacyclobutane respectively. The 1,3-isomer is more stable by 17.0 kcal mol^{-1} and therefore should be a better candidate for synthesis and isolation, especially if bulkier substituents are used, which might further enhance this energy difference. All the Ti-containing reference compounds also feature high heats of formation, which are reported for the first time. The calculated values for CH_3CH_3, SiH_3CH_3 and CH_3 SiH_2CH_3 are in excellent agreement with experiment and certainly within the error of the method. For $SiH_3CH_2CH_3$, the G2 result is in very good accordance with previously reported theoretical result using MP2 isodesmic reactions[29]. This earlier work noted that the experimental

value[30] for this molecule should be revisited.

IV. Boys localization and Bader analysis[31]

In Figure 2, we show the Boys localized orbitals, *1*- *4* for the 1,2-ring and six -*7* for the 1,3-ring. These reveal some very interesting features, especially for the first system. The C-C bond in the first system is typical, but the others are indicative of considerable ring-strain. The Ti-Si and Ti-C bonds are bent outward, as one would expect for a strained system. Especially noteworthy is the observation that the C-Si bond is bent towards the interior of the ring, an unusual feature for a neutral molecule. We therefore employed a Bader analysis of the localized orbitals to determine the actual bond-path and bonding in these cyclic systems. This type of density analysis is discussed in full detail in reference 31 and especially in 31d. We are interested in critical *points* of the electron density, e.g. points where the gradient of the density is zero, $\rho(\mathbf{r})=0$. A *bond critical point* is a point at which the Hessian of the density has one positive and two negative eigenvalues. This implies that there is a bond path connecting the two atoms, and they are considered to be bonded. Bond critical points are indicated by the black dots in pictures *5* and *8*. A *ring critical point* is a point at which the Hessian has two positives and only one negative eigenvalues. According to this definition, both systems are rings with formal two-center bonds.

The ring-strain of the 1,2-isomer is obvious in both the curved path of the contour plots of the localized orbitals (*2* -*4*) and the bond path from the density analysis (*5*). As noted above, the Si-C bond is curved inward towards the interior of the ring. The corresponding Si-C localized orbital shows considerable delocalization (back bonding) on Ti: nearly 10% of the two electrons in this LMO are located on Ti. The Mulliken atomic populations in this orbital are 0.168 on Ti, 0.612 on Si and 1.33 on C. This may explain the

unusual location of the bond critical point of the Si-C bond closer to the less electronegative center (Si).

The increase in the length of the most strained bonds, measured by the length of the electron density bond path, as compared to the geometrical distances is on the order of 1-2%. The Ti-Si bond is increased by 0.0489Å, Si-C by 0.044Å and Ti-C by 0.017 (only 0.8%). The C-C bond remains essentially unchanged. In the 1,3-isomer, the geometric and bond path lengths are essentially the same.

Conclusions

In the present work, the MP2/TZVP geometries and the standard heats of formation at 0 and 298.15 K of 1-sila-2- and 1-sila-3-titanacyclobutanes obtained from the G2-energies and the appropriate homodesmic reactions are reported. A G2-procedure modified to include first-row transition metals has been used. Species that contain directly bonded Si and Ti exist in more than one close-lying minima and favour geometries with the hydrogens on Si inverted towards Ti. All the Ti-containing fragments have high enthalpies of formation, which are tabulated here for the first time. The 1-sila-3-titanacyclobutane is more stable than the 1,2-isomer by 17.0 kcal mol^{-1}, and with bulkier substituents would be easier to isolate. Boys localization and Bader analysis show considerable ring-strain in the 1,2-isomer and delocalization of the Si-C bond onto Ti.

Acknowledgements

This work was supported by the AFOSR grant No F49 620-95-1-0073. The authors would like to thank Dr. M.W. Schmidt and Dr. J.A. Boatz for helpful discussions. The authors are grateful to Dr. S.T. Elbert for providing access to the SGI Power Challenge of the Scalable Computing Laboratory (SCL), which is funded by Iowa State University and the Ames Laboratory-USDOE under Contract W-7405-Eng-82.

References and Notes

(1) Selective references: (a) Puddephatt, R.J. *Comments Inorg. Chem.* **1982**, *2* 69 and references therein. (b) Grubbs, R.H. In *Comprehensive Organometallic Chemistry* Wilkinson, G.; Stone, F.G.A.; Abel, E.W. Eds. Pergamon Press: Oxford, U.K., **1982**; Vol.8, Chapter 54, p 499, and references therein. (c) Chappel, S.D.; Cole-Hamilton, D.J. *Polyhedron Report Number 2: The Preparation and Properties of Metallacyclic Compounds of the Transition Elements;* Pergamon Press: Oxford, U.K., **1982**; Vol.1, p 739, and references therein. (d) Puddephat, R.J. *Coord. Chem. Rev.* **1980**, *33*, 149 and references therein.

(2) (a) Stille, J.R.; Grubbs, R.H. *J. Am. Chem. Soc.* **1986**, *108*, 855. (b) For a review: Brown-Wensley, K.A.; Buchwald, S.L.; Cannizzo, L.F.; Clawson, L.E.; Ho, S.; Meinhart, J.D.; Stille, J.R.; Staruss, D.; Grubbs, R.H. *Pure Appl. Chem.* **1983**, *55*, 1733.

(3) (a) Clawson, L.E.; Buchenwald, S.L.; Grubbs, R.H. *Tetrahedron Lett.* **1984**, *50*, 5733. (b) Stille, J.R.; Grubbs, R.H. *J. Am. Chem. Soc.* **1983**, *105*, 1664. (c) Chou, T.; Huang, S. *Bull. Inst. Chem. Acad. Sin.* **1984**, *31*, 44.

(4) Buchwald, S.L.; Anslyn, E.V.; Grubbs, R.H.*J. Am. Chem. Soc.* **1985**,*107*, 1766.

(5) (a) Straus, D.A.; Grubbs, R.H. *J. Mol. Catal.* **1985**, *28*, 9. (b) Lee, J.B.; Ott, K.C.; Grubbs, R.H. *J. Am. Chem. Soc.* **1982**, *104*, 7491.

(6) (a) Gilliom, L.R.; Grubbs, R.H. *J. Am. Chem. Soc.* **1986**,*108*, 733. (b) For a review on ring-opening polymerization: Calderon, J.J. *Macromol. Sci. Rev.* **1972**, *C7(1)*, 105.

(7) (a) Mackenzie, P.B.; Ott, K.C.; Grubbs, R.H. *Pure Appl. Chem.* **1984**,*56*, 59. (b) Park, J.W.; Mackenzie, P.B.; Schaefer, W.P.; Grubbs, R.H. *J. Am. Chem. Soc.* **1986**, *108*, 6402.

(8) Anslyn, E.V.; Grubbs, R.H. *J. Am. Chem. Soc.* **1987**, *109*, 4880 and references therein.

(9) Ciliberto, E.; Di Bella, S.; Gulino, A.; Fragalá, I.; Petersen, J.L.; Marks, T.J. *Organometallics* **1992**, *11*, 1727 and reference (6) therein.

(10) (a) Tikkanen, W.; Ziller, J.W. *Organometallics* **1991**, *10*, 2266. (b) Amorose, D.M.; Petersen, J.L. *Organometallics* **1991**, *10*, 2191. (c) Tikkanen, W.; Egan, J.W. Jr.; Petersen, J.L. *Organometallics* **1984**, *3*, 1646. (d) Tikkanen, W.; Liu, J. Z.; Egan, J.W. Jr.; Petersen, J.L. *Organometallics* **1984**, *3*, 825.

(11) George,P.; Trachtman, M.; Bock, C.W.; Brett, A.M. *Tetrahedron* **1976**, *32*, 317.

(12) (a) Curtiss, L.A.; Raghavachari, K.; Trucks, G.W.; Pople, J.A. *J. Chem. Phys.* **1991**, *94*, 7221. (b) Pople, J.A.; Head-Gordon, M.; Fox, D.J.; Raghavachari, K.; Curtiss, L.A. *J. Chem.Phys.* **1989**, *90* , 5622.

(13) Schmidt, M.W.; Baldridge, K.K.; Boatz, J.A.; Elbert, S.T.; Gordon, M.S.; Jensen, J.H.; Koseki, S.; Matsunaga, N.; Nguyen, K.A.; Su, S.J.; Windus, T.L.; Dupuis, M.; Montogomery,J.A. *J. Comput. Chem.* **1993**, *14*, 1347.

(14) Foster, J.M.; Boys, S.F. *Rev. Mod. Phys.* **1963**, *32*, 300.

(15) (a) TZV for Li-Ne, Dunning, T.H. *J. Chem. Phys.* **1971**, *55*, 716. (b) TZV for Na-Ar, McLean, A.D; Chandler, G.S. *J.Chem.Phys.* **1980**, *72*, 5639. (c) TZV for Sc-Zn (from HONDO 7.0), Wachter, A.J.H. *J. Chem. Phys.* **1970**, *52*, 1033. This is basically Wachter's basis (14s9p5d) extended to triple zeta quality by using (6d) contracted to [411] according to Rappé, A.K.; Smedley, T.A.; Goddard, W.A., III, *J. Phys. Chem.* **1981**, *85*, 2607. Also, the most diffuse s (α_s=0.0333) was substituted by an s with α_s=0.2090 to better describe the 3s-4s region, while another two p were added (α_p=0.1506 and α_p=0.0611) to acount for a 4p. (d) Single-polarization d-functions for C and Si from HONDO 7.0, α_d=0.720 and α_d=0.388 respectively.

(16) For a complete review on the even-tempered expasion of atomic basis sets, see the series of papers: (a) Ruedenberg, K.; Raffenetti, R.C.; Bardo, R.D. In *Proceedings of the 1972 Boulder Seminar Research Conference on Theoretical Chemistry,* Smith, D.W. Ed.; Wiley: New York, **1973**; p 164. (b) Raffenetti, R.C. *J. Chem. Phys.* **1973**, *59*, 5936. (c) Bardo, R.D.; Ruedenberg, K. *J. Chem. Phys.* **1973**, *59*, 5956. (d) Bardo, R.D.; Ruedenberg, K. *J. Chem. Phys.* **1973**, *59*, 5966. (e) Raffenetti, R.C.; Ruedenberg, K. *J.Chem. Phys.* **1973**, *59*, 5978. (f) Bardo, R.D.; Ruedenberg, K. *J. Chem. Phys.* **1974**, *60* , 918. (g) Bardo, R.D.; Ruedenbrg, K. *J. Chem. Phys.* **1974**, *60*, 932. (h) Feller, D.F.; Ruedenberg, K. *Theoret. Chim. Acta* **1979**, *52* , 231.

(17) (a) Raffenetti, R.C. *J. Chem. Phys.* **1973**, *58* , 4452. (b) Appropriate scaling scheme for substituting a single-polarization with double and triple-split, Frisch, M.J.; Pople, J.A.; Binkley, J.S. *J. Chem. Phys.* **1984**, *80* , 3265.

(18) *Gaussian 92*, Revision A, Frisch, M.J.; Trucks, G.W.; Head-Gordon, M.; Gill,

P.M.W.; Foresman,J.B.; Johnson, B.J.; Schlegel, H.B.; Robb, M.A. ; Replogle, E. S.; Gomberts, R.; Andres, J.L; Raghavachari, K.; Binkley, J.S.; Gonzalez, C.; Martin, R.L.; Fox, D.J.; DeFrees, D.J.; Baker, J.; Stewart, J.P.P.; Pople, J.A. Gaussian Inc., Pittsburgh PA, **1992**.

(19) (a) Frisch, M.J.; Head-Gordon, M.; Pople, J.A. *Chem. Phys. Lett.* **1990**, *166*, 275. (b) Frisch, M.J.; Head-Gordon, M.; Pople, J.A. *Chem. Phys. Lett.* **1990**, *166*, 281. (c) Pople, J.A.; Krishnan, R.; Schlegel, H.B.; Binkley, J.S. *Int. J. Quant. Chem. Symposia* **1979**, *13*, 325. (d) Handy, N.C.; Schaeffer, H.F.,III. *J. Chem. Phys.* **1980**, *72*, 4654.

(20) (a) Head-Gordon, M.; Trucks, G.W.; Frisch, M.J. *Chem. Phys. Lett.* **1992**, *196* , 624. (b) Amos, R.D. *Chem. Phys. Lett.* **1984**, *108* , 185.

(21) (a) Krishnan, R.; Pople, J.A. *Int. J. Quant. Chem. Symposia* **1978**, *14*, 91. (b) Krishnan, R.; Frisch, M.J.; Pople, J.A. *J. Chem. Phys.* **1980**, *72*, 4244.

(22) Pople, J.A.; Head-Gordon, M.; Raghavachari, K. *J. Chem. Phys.* **1987**, *87*, 5968.

(23) Dupuis, M.; Chin, S.; Marquez, A. *"CHEM-Station and HONDO"* in *"Relativistic and Electron Correlation Effects in Molecules and Clusters"*, Malli, G.L. Ed.; NATO ASI Series; Plenum Press, New York, **1993**, p 315.

(24) (a) Hehre, W.J.; Radom, L.; Schleyer, P.v.R.; Pople, J.A. In *Ab Initio Molecular Orbital Theory* , Wiley-Interscience: New York, **1986**. (b) Gordon, M.S.; Francisco, J.S.; Schlegel, H.B. In *Advances in Silicon Chemistry* , JAI Press Inc., **1993**; Vol. 2 , p 137,

(25) Comparisons of the structural isomers at the MP2 level do not include the zero-point corrections. When included, the relative difference remains, except in the case of (F5,F7) where it practically vanishes. In the latter case, the bridged isomer is considered in

the subsequent computations for consistency with (F4,F6).

(26) Kudo, T.; Gordon, M.S. *J. Phys. Chem.* **1995**, *99*, 9340.

(27) Pople, J.A.; Scott, A. P.; Wong, M.W.; Radom, L. *Isr. J. of Chem.* **1993**, *33*, 345. We used the scaling-factor for MP2-fundamentals rather than the suggested one for MP2-zero-point energies (0.9646), since it is the harmonic frequencies that are calculated.

(28) *JANAF Thermochemical Tables* , **1985**, Vol. 14, 3rd Ed., Supplement No 1.

(29) Gordon, M.S.; Boatz, J.A.; Walsch, R. *J. Phys. Chem.* **1989**, *93*, 1584.

(30) Wagman, D.D.; Evans, W.H.; Parker, V.B.; Schumm, R.H.; Halow, I.; Bailey, S. M.; Churney, K.L.; Nuttall, R.L. *J. Phys. Chem. Ref. Data Suppl.* **1982**, *11*, 2.

(31) (a) Bader, R.F.W.; Nguyen-Dang, T.T.; *Rep. Prog. Phys.* **1981**, *44*, 893. (b) Bader, R.F.W.; Nguyen-Dang, T.T. *Adv. Quantum Chem.* **1981**, *14*, 63. (c) Bader, R.F.W. *Acc. Chem. Res.* **1985**, *18*, 9. (d) Bader, R.F.W. In *Atoms in Molecules: A Quantum Theory*, International Series of Monographs on Chemistry, Vol. 22 ; Clarenton Press: Oxford, **1994**.

(32) Doncaster, A.M.; Walsh, R.J. *J. Chem. Soc., Faraday Trans. 2* **1986**, *82*, 707.

Table 1: Modified G2 procedure to include transition metals.

Original G2	Modified G2
(H, C, Si)	(Ti)
HF geometries, frequencies/6-31G(d,p)	--
MP2(FU) geometries/6-31G(d,p)	MP2(FZC) geometries, frequencies/H, C, Ti, TZVP
The following calculations refer to single-point frozen core energies at MP2(FZC) geometries	
MP4SDTQ/6-311G(d,p)	MP4SDTQ/Ti, TZV(f)
MP4SDTQ/6-311+G(d,p)	MP4SDTQ/Ti, TZV+(f)
MP4SDTQ/6-311G(2df,p)	MP4SDTQ/Ti, TZV)2fg)
QCISD(T)/6-311G(d,p)	QCISD(T)/Ti, TZV(f)
Higher level correction (HLC)	HLC
MP2/6-311+G(3df,2p)	MP2/Ti, TZV+(3gf)

Table 2: Zero-point MP2, G1 and G2 energies and standard heats of formation.

Molecule	E_0(MP2)[a]	ZPE[b]	E_0(G1)[a]	E_0(G2)[a]	$\Delta H^\circ_{f,0K}$ [c]	$\Delta H^\circ_{f,298.15K}$ [c]	Experiment [c]
H	-0.49981		-0.50000	-0.50000	+51.6[d]	+52.1[d]	
C	-37.74684		-37.78464	-37.78420	+170.0[d]	+171.3[d]	
Si	-288.89587		-288.93378	-288.93325	+106.6[d]	+107.6[d]	
Ti	-848.41785		-848.46411	-848.46259	+112.6[d]	+113.2[d]	
CH_3CH_3	-79.50196	72.02	-79.62558	-79.63001	-16.4	-20.2	-20.24 ± .05[e]
SiH_3CH_3	-330.51865	59.12	-330.65429	-330.65682	-3.1	-7.0	-6.9±1.0[e]
TiH_3CH_3	-889.91247	48.43	-890.06144	-890.06264	+80.4	+77.9	
SiH_3TiH_3	-1140.90469	41.44	-1141.06831	-1141.06712	+107.7	+103.7	
$SiH_3CH_2CH_3$	-369.68342	86.90	-369.87342	-369.87714	-3.5	-8.9	-34.2[f]
$CH_3SiH_2CH_3$	-369.70192	87.00	-369.89212	-369.89698	-16.0	-21.1	-22.6 ± 1.0[e]
$TiH_3CH_2CH_3$	-929.07740	76.25	-929.28054	-929.28309	+79.9	+75.4	
$CH_3TiH_2CH_3$	-929.10586	75.74	-929.30792	-929.31029	+62.8	+58.8	
$SiH_3TiH_2CH_3$	-1180.09909	68.01	-1180.31819	-1180.31826	+88.0	+83.1	
$TiH_3SiH_2CH_3$	-1180.08433	67.06	-1180.30094	-1180.30234	+97.9	+93.5	
$TiH_3CH_2SiH_3$	-1180.10358	64.53	-1180.31884	-1180.31828	+87.9	+83.1	
	-1218.10234	76.80			+96.3	+91.3	
	-1218.13953	73.94			+79.0	+74.3	

[a] Energies in Hartrees. [b] Vibrational zero-point energies in mHartrees, scaled by 0.943. [c] Heats of formation in kcal mol^{-1}.
[d] Reference 28. [e] Reference 32. [f] Reference 30.

Figure 1. MP2/TZVP geometries of the silatitanacyclobutanes (R1 and R2) and the reference compounds (F1-F13). For C1 symmetries, the average bond distances are given.

(Figure 1 is divided here into parts 1a, 1b and 1c)

H C Si Ti

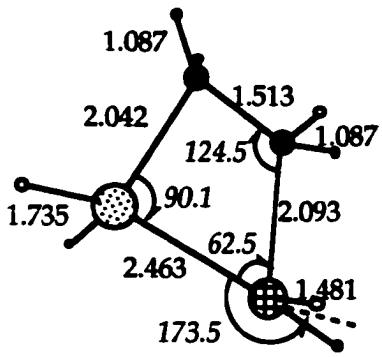

R1, C_S

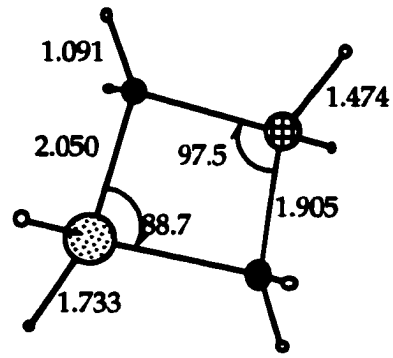

R2, C_{2V}

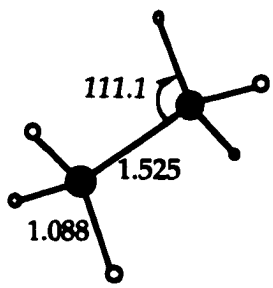

F1, D_{3D}

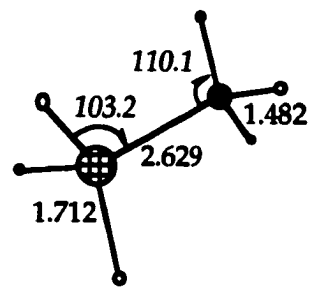

F2, C_{3V}

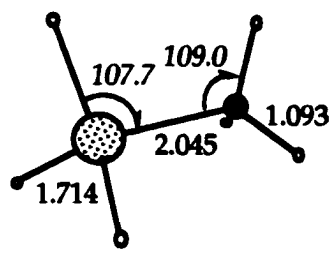

F3, C_{3V}

1a

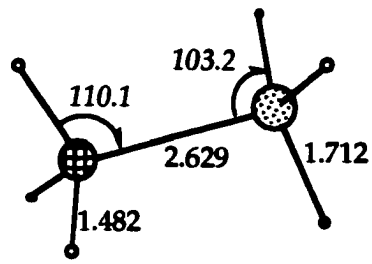

F4, C_{3V}

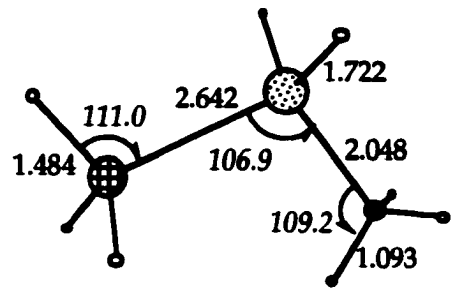

F5, C_1

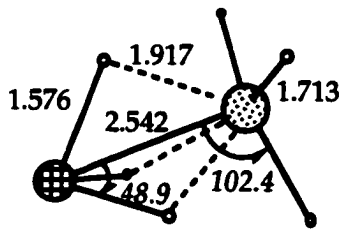

F6, C_{3V}

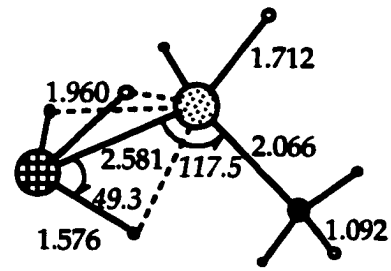

F7, C_{3V}

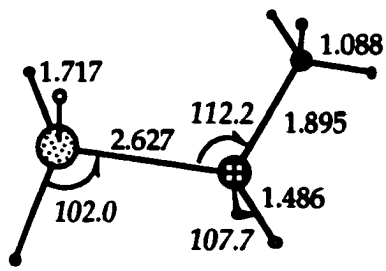

F8, C_S

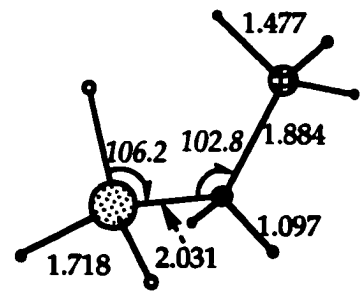

F9, C_1

1b

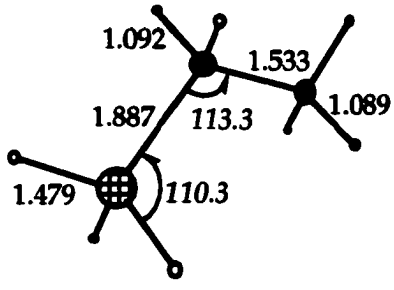

F10, C_S

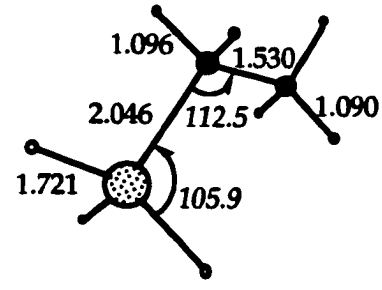

F11, C_S

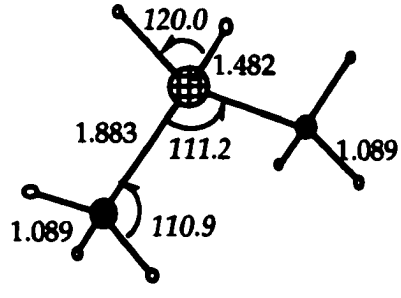

F12, C_1

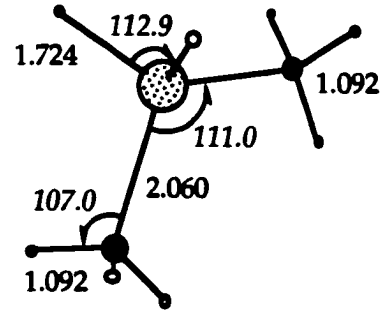

F13, C_1

1c

Figure 2. Boys localized orbitals for 1-sila-titanacyclobutane (1-4) and 1-sila-2-titanacyclobutane (6,7). 5 and 6 show the real bond path and the bond critical points from the Bader analysis. Red (+) and blue (-) correspond to opposite signs of the wave function. (Figure 2 is divided into parts 2a and 2b)

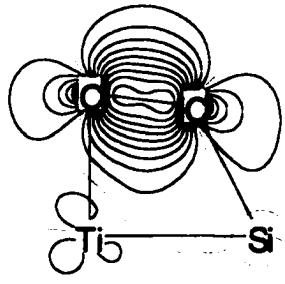

1

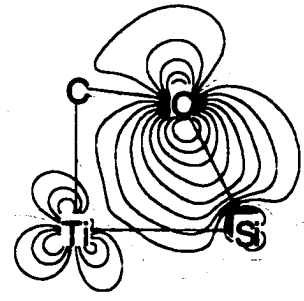

2

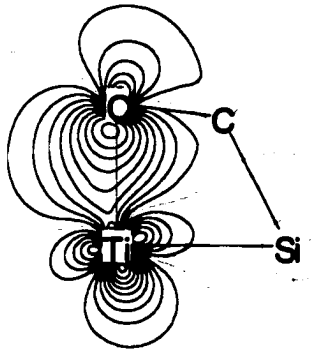

3

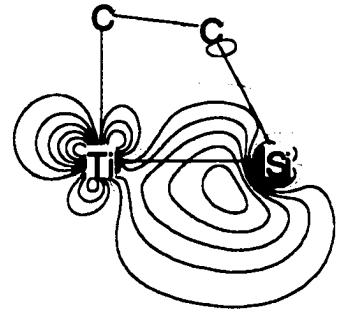

4

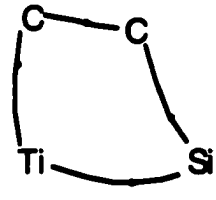

5

2a

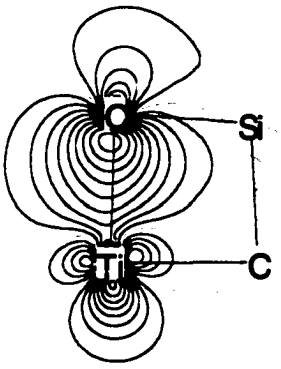

6

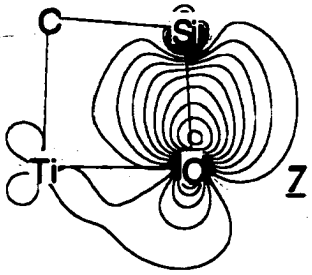

7

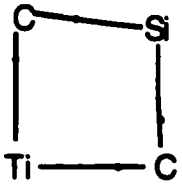

8

CHAPTER 3: STRUCTURE AND THERMODYNAMICS OF CARBON- AND CARBON/SILICON-PRECURSORS TO NANOSTRUCTURES

A paper to be submitted for publication to *The Journal of the American Chemical Society.*

Vassiliki-Alexandra Glezakou and Mark S. Gordon

Iowa State University, Department of Chemistry, Ames IA 50011.

Jerry A. Boatz

AFRL/PRS, Edwards AFB, CA 93524-7680

Abstract

The structures at the Hartree-Fock level, as well as energetics and heats of formation are reported in this paper for the unsaturated system $C_{36}H_{16}$ and its Si-doped analogue $C_{32}Si_4H_{16}$, and several smaller, unsaturated fragments. The results are based on homodesmic and isodesmic reactions and the G2(MP2,SVP) method with a double valence plus polarization basis. A possible initial reactive channel is examined, which could lead to the formation of the onion-type nanostructures.

Introduction

In this paper, the structure and standard heat of formation of the annulene derivative, $C_{36}H_{16}$ (1,2:5,6:11,12:15,16-Tetrabenzo-3,7,9,13,17,19-hexadehydro[20]annulene) and that of its Si-doped isomer $C_{32}Si_4H_{16}$ ((1,2:5,6:11,12:15,16-Tetrabenzo-3,7,9,13,17,19-

hexadehydro-8,9,18,19-tetrasila[20]annulene) is reported. The synthesis and properties of the parent system were reported recently[1]: this system is quite stable and inert to irradiation, but readily explodes in vacuum under mild heating to give pure carbon nanotubes. X-ray diffraction studies and semi-empirical MNDO-PM3 calculations suggest a chiral conformation with an isomerization barrier through a planar structure only 7.5 kcal mol^{-1} higher than the ground state. As various experiments suggest[2], this material may present new opportunities in C- or non-C-nanostructures.

The current work explores:

(a) the thermodynamics of the parent molecule.

(b) the structural and thermodynamic effects of the partial substitution in the C-backbone by Si.

(c) A possible reactive channel for the first step in the explosive transformation to nano-structures and a comparison to the "chicken-wire" isomer $C_{36}H_{16}$.

The present theoretical treatment is also a performance test of reduced requirements *ab initio* calculations for large systems or systems with delocalized electrons where very often various levels of calculations have contradicting results[3].

The system $C_2Si_2H_2$ has a number of closely lying, but quite different in structure isomers. It appears that at least some have a triplet ground state, a fact totally neglected in the literature. Due to the importance of better understanding of the Si-C bonding, we devoted a more detailed, multi-reference study to this system[4].

Computational details

The G2 methodology[5] is one of the theoretical chemical models that aim at providing reliable energies (within ~5 kcal mol^{-1}) through a series of *ab initio* calculations that include correlation. In this procedure, the quadratic configuration interaction with single and double excitations and perturbative triples,QCISD(T)/6-311+G(3df,2p), level of theory is approximated through various levels of second- and fourth-order perturbation theory and a variety of increasingly larger basis sets. However, even in this regime, the calculations may soon become impossible for large systems. Therefore, a number of alternative "G2-like" schemes with reduced basis set and level of theory requirements[6] have been devised that appear to give the same level of accuracy, but in a more economical manner.

The G2(MP2,SVP)[6b] theory was chosen for the present work, with a split-valence plus polarization (SVP, 6-31G(d)) basis set employed for the optimizations at the Hartree-Fock level and for the second order derivatives of the energy. A second optimization is performed at the MP2-FU//6-31G(d) (full core) level of theory. The final G2(MP2,SVP) energy combines single point calculations at the MP2 geometries and includes two steps:

I. an MP2 calculation with an extended basis set to obtain the effect of the large basis sets

II. a quadratic configuration interaction with singles, doubles and (iterative triples) (QCISD(T)), which incorporates dynamic correlation effects.

The total G2(MP2, SVP) energy is given by the following formula:

$$E_0=E[QCISD(T)/6\text{-}31G(d)] + \Delta_{MP2,SVP} + HLC + E(ZPE) \quad (1)$$

where

$$\Delta_{MP2,SVP}=E[MP2/6\text{-}311+G(3df,2p)] - E[MP2/6\text{-}31G(d)]$$

is the change in the second order perturbation theory (MP2) energy due to the basis set improvement.

The high level correction (HLC) is computed in the same manner as in the original G2 method, and the zero point energy (ZPE) correction is evaluated from the Hartree-Fock force fields scaled by 0.893[7]. This procedure has been shown to yield considerable savings in both disk space and CPU time without sacrificing the reliability of the original scheme.

All calulations were performed with the Gaussian94[8],GAMESS[9] and ACESII[10] quantum codes.

Homodesmic and isodesmic reactions

Homodesmic and isodesmic reactions[11] are schemes that help optimize the cancellation of systematic errors. They are balanced chemical reactions that break a large molecule into smaller fragments, on which high-level calculations are feasible. A homodesmic reaction balances the number and the formal type of the chemical bonds involved, maintaining at the same time the connectivity of atoms and groups. An isodesmic reaction usually preserves only the number of bond types, and hydrogens are used to terminate the fragments. The typical error of the "conventional" G2 procedure[4] for the computed heats of formation is 2-3kcal mol^{-1}, which increases with the number of heavy atoms. Raghavachari *et al.*[12] argue that isodesmic reactions are more reliable for larger systems, as long as G2-energies are used on both sides. In general, the homodesmic scheme is preferable, especially when G2 energies are not available, because the cancellation of errors is more uniform. Experimental heats of formation may also be used for reference

molecules in these schemes, in order to obtain more accurate heats of formation, for target molecules.

For the system $C_{36}H_{16}$ the gas, standard heat of formation is evaluated using the homodesmic reaction as shown in Figure 1. For the Si-doped systems, simpler isodesmic reactions are used, because these isomers have a more complicated morphology, as it will be shown below.

I. Structure, G2(MP2,SVP) energy and heat of formation of the primary fragments

The G2(MP2,SVP) energy for a number of small hydrocarbons and sila-hydrocarbons was calculated. These were subsequently used in the appropriate reactions, for the theoretical prediction of their gas phase standard heats of formation at 298.15K. The thermochemical data obtained in this section are used in sections II, III and IV, for the evaluation of the heats of formation of the larger systems. Table 1A lists the absolute energies of the primary fragments: Hartree-Fock optimized, HF//6-31G(d), and single-point MP2 energies. The zero-point correction to the energies (ZPE) and the thermal correction result from the harmonic HF frequencies. Figures 2,3 and 4 summarize the geometrical parameters of the all-C and C/Si fragments. The corresponding absolute energies are listed in Tables 1A and 1B.

The Si-containing molecules have open-shell ground states. The G2 procedure treats open-shell systems within the unrestricted formulation. We treated these systems with both UHF and ROHF methods for comparison. We call this modified G2(MP2, SVP) scheme R-G2 for restricted-G2, where the QCISD(T) step is replaced by a CCSD(T) calculation.

As can be evinced from the literature[6d,12a], the accuracy of many thermochemical predictions for benzene and larger aromatic systems, is not as good as that for smaller

compounds. "Conventional" G2 underestimates the standard heat of formation of benzene by 3.9 kcal mol^{-1}, while G3, the latest, more expensive flavor of the series, comes as close as -0.6 kcal mol^{-1} to the experimental value[6d]. In this study, the G2 energies were used in combination with the experimental atomization energies to calculate the standard heats of formation. This method gives quite good agreement with experiment for most cases, except for aromatic systems, as can be seen from Table 2. Diacetylene, benzene and phenyl acetylene were also calculated via the isodesmic reactions proposed by Raghavachari[12a, b]. For example, the following chemical (isodesmic) reaction can be written for benzene:

R1: $C_6H_6 + 6CH_4 \rightarrow 3C_2H_4 + 3C_2H_6$

This method underestimates the value for benzene by only 1.35 kcal mol^{-1} at the G2(MP2,SVP) level of computation.

The G2(MP2, SVP) energy of the fragments F3 and F4 (see Figure 1) of the homodesmic reaction could not be directly computed, due to linear dependencies caused by the diffuse functions at the E[MP2/6-311+G(3df,2p)] step. In analogy with benzene, the heats of formation of these fragments were therefore computed indirectly using the following isodesmic schemes at the MP2/6-31G(d) level of theory:

R2: $Ph\text{-}C\equiv C\text{-}Ph$ *(F3)* $+ 4CH_4 \rightarrow 2\,C_6H_6 + C_2H_2 + 2C_2H_6$

R3: $HC\equiv C_a\text{-}Ph\text{-}C\equiv C\text{-}CH$*(F4)* $+ 6CH_4 \rightarrow C_6H_6 + 3C_2H_2 + 3C_2H_6$

II. $C_{36}H_{16}$

The ground state (^1A) of $C_{36}H_{16}$ (other than "graphitic-like" structure) has a chiral conformation of D_2 symmetry. MNDO-PM3[1] calculations predict a barrier of 7.5 kcal mol-1 for enantiomerization through a planar structure of D_{2h} symmetry. In this work, the planar structure is also predicted to be a transistion state, with one very small imaginary frequency of 10.84 cm^{-1}. The energy difference between the D_2 minimum and the D_{2h} transition state is calculated to be 7.5 kcal mol^{-1} at RHF//6-31G(d) and 7.4 kcal mol^{-1} at MP2/6-31G(d). Both values are corrected for vibrational zero-point energies by the scaled harmonic Hartree-Fock frequencies. Naturally, the imaginary frequency was excluded from the correction in the case of the transition state. Figure 5a shows a set of selected parameters for these two structures.

Onion-like nanotubes are non-crystalline materials with basic units of graphene layers embedded between clusters of sp^3-hybridized C. This mixed hybridization of C's is one of their basic characteristics[13]. $C_{36}H_{16}$ has a graphene-like isomer (Tetrabenzo[b c, e f, k l, n,o]coronene, Figure 5b) which is by 289.9 kcal mol^{-1} (D_{2h}, MP2/RHF//6-31G(d), ZPE included) lower than the annulenic derivative.

In Figure 5b, the average geometrical parameters of the "graphitic" isomer $C_{36}H_{16}$ are given, as well as the isodesmic scheme used in the computation of its heat of formation. The cartesian coordinates for these two systems are available as supplementary material in Appendices I and II.

III. Si-doping and structural and electronic effects

Si-doped polymers have been proposed in the literature to interpret Si-surfaces[14]. In 1981 the first Si-Si containing polymer was synthesized[15a], the same year that the first Si=C

containing species was also isolated[15b]. Although Si and C are cogeners, Si- or Si-doped two-dimensional polymers still evade detection. Nonetheless, as chips become smaller and smaller, theoretical investigation of Si-doped systems, both small and large can be very helpful[16]. The readiness with which the all-carbon system transforms into onion-type nanotubes[13] (concentric spherical nanocapsules), may present researchers with a possible pathway to obtain Si-doped nanostructures, once the $C_{32}Si_4H_{16}$ parent has been synthesized.

Given the evasiveness of silicon containing species with multiple bonds, only four carbon atoms were substituted and in such a way that the linear diacetylenic units C_4 have single bonds between Si and Si. Optimization of the resulting system led to a twisted structure as before, except that the originally linear Si-C bonds rearranged to form two C_2Si_2 diamond-shaped rings, due to the instability of the Si-C multiple bonds[17,18]. As Murrel, Kroto, and Guest first pointed out[18a], the isomerization of silaacetylene to :Si=CH2 is substantially exothermic. Hopkinson and Lien[18b] discovered that the linear HsiCH is not even a minimum on the potential surface. However, Gordon and Pople[18c] found that a slightly bent structure of silaacetylene is in fact favoured. These findings are in accord with our findings for $C_{32}Si_4H_{16}$. The substitution leads to a rather radical change of the structure. In fact, we located three minima on the Hartree-Fock potential energy surface (PES). All structures are well-characterized minima with positive definite Hessians at the Hartree-Fock level. The triplet was optimized within the restricted open shell method. Appendices II-IV list the cartesian coordinates of the optimized geometries.

The first minimum located was a singlet state (^1A, D_2), Figure 6a. An attempt to locate the corresponding minimum of the triplet state led to the triplet state (^3A, C_1), Figure 7a. Since the two structures were considerably different, we re-optimized the singlet state

starting from the triplet geometry. This led to the global minimum on the singlet $C_{32}Si_4H_{16}$ PES, (^1A, C_1), Figure 8a. The global minimum is more stable by 50.3 kcal mol^{-1} compared to the D_2 singlet state and 18.9 kcal mol^{-1} more stable than the triplet at the MP2/6-31G(d)/HF//6-31G(d), including zero-point corrections. The main difference between the D_2 and C_1 structures is the collapse of the C_2Si_2 ring in the interior of the molecule to form a C_4Si_4 core. Note however, that while the central cluster maintains an almost C_{2v} local symmetry in the case of the triplet state, it adopts a highly asymmetric conformation with one dangling bond: Si51 is connected only to C48, Figure 8a.. In the case of the triplet, Si51 is connected to both C48 and C47, Figure 7a.

Schematically:

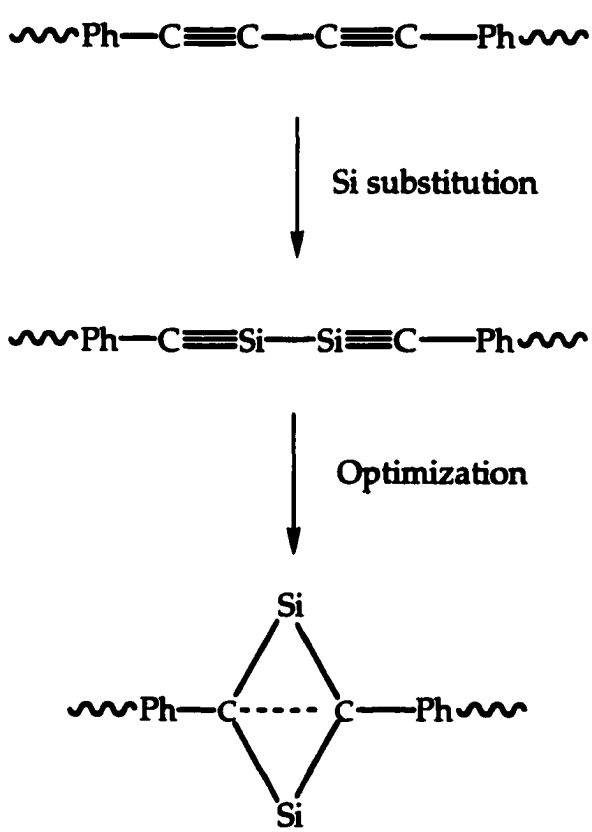

The standard heat of formation of the Si-doped species was calculated via the following isodesmic reaction, at the MP2/6-31G(d)//HF/6-31G(d) level of theory and geometries:

R4: $C_{32}Si_4H_{16} + 4H_2 \rightarrow 2Ph - C \equiv C - Ph + C_4Si_4H_4$

IV. Dimerization of $C_{36}H_{16}$

UV (337 nm N_2 laser) LD-TOF (laser desorption time-of-flight) and IR LD-FTMS (laser desorption Fourrier transform mass spectroscopy) experiments[1] on films of $C_{36}H_{16}$ indicate that the initial stages of its explosive transformation are very likely to involve oligomerization to up to 20 units. This idea was tested by exploring the dimerization of the parent system. The resulting dimer has a total of 1144 basis functions at the RHF//6-31G(d) level of theory, at which first and numerical second derivatives were computed. For simplicity, the symmetry was constrained to D_2, as in the monomer, resulting in 26 symmetry unique atoms and a total of 104 atoms (72 heavy).

The diacetylenic side units were chosen as the dimerization sites, as can be seen in Figure 9a. The choice was based on references in the literature[16] suggesting that polyacetylenes easily undergo side polymerization compatible with the mild heating *in vacuo* that triggers the explosive transformation. The following schematic depicts the reaction across the diacetylenic sides of the two monomers, where the triple bonds open up, in order to form an 8-membered ring between two allenic-type units:

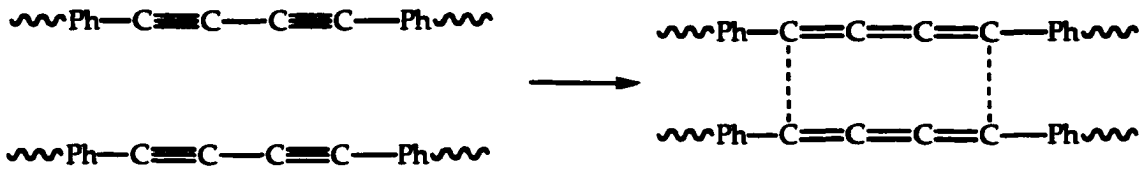

Because of the strain in the resulting 8-member ring, the final optimized structure acquires the following structure along the periphery of the 8-membered ring:

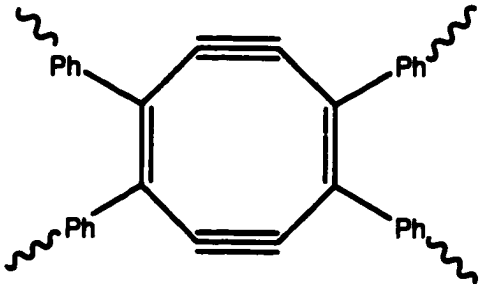

At the MP2/RHF//(6-31G(d) level of theory, with zero-point corrections from the HF frequencies scaled, this energy difference becomes -37.4 kcal mol^{-1}, the dimer being the lowest. The dimer is optimized within the constraints of the D_2 symmetry.

The optimized cartesian coordinates for $C_{72}H_{32}$ are listed in Appendix IV.

Discussion

In Figure 2, the Hartree-Fock (MP2-full core) geometries of the primary hydrocarbons are shown. Figures 3 and 4 show the structures for the Si-containing fragments. Table 1A summarizes the Hartree-Fock and MP2 absolute energies and zero-point correction, while Table 1B the energies needed for the evaluation of the G2(MP2,SVP) energies for these molecules. The open-shell fragments for the molecules of interest were computed at both the UHF/UMP2 and ROHF/ROMP2 levels of theory. In the latter case, the QCISD(T) calculation required for the G2-energy evaluation was substituted by a CCSD(T) calculation.

Because of the significance of the G2-method in thermochemical predictions, we feel that the open-shell part of the method should be revisited and made free of spin contamination, which in the case of $C_2Si_2H_2$, is ~10%. One way of going about this, is the R-G2 (restricted-G2) modification that we present here.

The system $C_2Si_2H_2$ is a particularly interesting prototype, for CVD processes. It is a highly unsaturated system with at least a dozen closely lying isomers. Understanding the bonding in this prototype could be quite important for tailoring Si-doped nanostructures. The slightly negative LUMO value and the asymetric character of the localized orbitals,even though the system itself posseses C_{2v} symmetry, are indicative of multi-reference character.

The agreement between the calculated heats of formation of the primary fragments and the available experimental data (Table 2) is quite good, about 1%. For aromatic systems, as observed by others also, the direct evaluation of heats of formation from the G2-energy is less accurate than indirect computation via isodesmic reactions where G2-energies are used on both sides of the reaction. The presence of one benzene ring induces an error of ~11% from direct evaluation. Use of the appropriate isodesmic scheme reduces this error to ~7%.

For the Si-containing species, there are no available experimental data. The computed heats of formation are comparable to the corresponding all-C systems. Si-substitution seems to decrease the heat of formation of the system by approximately 25.0 kcal mol^{-1} per Si atom.

The heats of formation of the fragments F3 and F4 (homodesmic reaction, Figure 1) were computed from the isodesmic reactions. The relative error as discussed above, is ~7%.

The calculated heat of formation for the $C_{36}H_{16}$ annulenic system (which has been synthesized[1]) is 372.4 kcal mol^{-1}. Figures 5c and 5d show the localized orbitals along the di-acetylenic sides of the molecule, very typical triple (5c) and single (5d) C-C bonds, which are

favoured by the twisted D_2 conformation. For the planar transition state, the number in parenthesis corresponds to the gas standard heat of formation at 0K. Its "graphitic" isomer has a computed heat of formation of 44.0 kcal mol^{-1}, 1.2 kcal mol-1 per C atom. The Si-containing molecule (higher singlet) has a heat of formation of 271.4 kcal mol^{-1}. For the lower singlet, no thermochemical prediction was possible,since the central cluster of C_4Si_4 has dangling bonds and would not be well represented by the G2 method. Table 4 summarizes the singlet-triplet splitting and the first Koopmans theorem ionization potential for these Si-doped systems. Figures 6b, 7b and 7c and 8b and 8c show the localized orbitals of D_2-singlet, C_1-triplet and C_1-singlet $C_{32}Si_4$ H_{16}. The unpaired electrons are localized on C45 and C46, while Si49 and Si50, which are the least obstructed sites, carry the lone pairs. In isolated $C_4Si_4H_4$, there is no steric hindrance, and localization places the lone electrons on the Si's rather than the C's, which being more electronegative, carry the lone pairs. Singlet coupling leads to the structure of 8a, which is actually the most stable of all $C_{32}Si_4H_{16}$ isomers.

Finally, dimerization of the all-carbon molecule, with the addition taking place along the longer (diacetylenic) sides of the parent molecule, results in the structure shown in Figure 9a. The dimer formation is actually exothermic by 37.4 kcal mol^{-1} at the MP2/HF//6-31G(d) level, corrected for zero-point vibrational energies. The dimer was optimized within the constraints of D_2 symmetry and has a heat of formation of 707.6 kcal mol^{-1}.

Acknowledgements

The authors wish to acknowledge Dr. M. W. Schmidt for the numerous enlightened discussions, and the Scalable Computing Laboratory of AmesLab for the computing resources. This project was supported by AFOSR Grant No F49620-99-1-0063.

References

1. Boese, R.; Matzger, A. J.; Vollhardt, K. P. C. *J. Amer. Chem. Soc.* **1997**,*119*, 2052.
2. (a) Diederich, F. in *Modern Acetylene Chemistry*; Stang, P. J.; Diederich, F. Eds.; VCH Weinheim, **1995**.(b) Tobe, Y.; Fujii, T.; Matsumoto, H.; Naemura, K. *Pure Appl. Chem.* **1996**, *68*, 239. (c) Kuwatani, Y.; Ueda, I. *Angew. Chem., Int. Ed. Engl.***1995**, *34*, 1892. (d) Zhou, Q.; Carroll, P. J.; Swager, T. M. *J. Org. Chem.* **1994**, *59*, 1294.
3. Diederich, F.; Rubin, Y. *Angew. Chem. Int. Ed. Engl.***1992**, *31*, 1101.
4. Glezakou, V.-A.; Gordon, M. S. paper in preparation.
5. Curtiss, L. A.; Raghavachari, K.; Trucks, G. W.; Pople, J. A *J. Chem. Phys.* **1991**,*94*, 7221.
6. (a) For G2(MP2), Curtiss, L. A.; Raghavachari, K.; Pople, J. A. *J. Chem. Phys.* **1993**, *98*, 1293.(b) For G2(MP2, SVP) Smith, B. J.; Radom, L. *J. Phys. Chem.* **1995**, *99*, 6468. (c) For G2(MP2, SV) Curtiss, L. A.; Redfern, P. C.; Smith, B.; Radom, L. *J. Chem. Phys.* **1996**, *104*, 5148. (d) For the conventional G3 method, see Curtiss, L. A.; Raghavachari, K.; Redfern, P. C.; Rassolov, V.; Pople, J. A. *J. Chem. Phys.* **1998**,*109*, 7764, and refs. (1-4) therein for the older G1 and G2 methods.
7. Pople, J. A.; Scott, A. P.; Wong, M. W.; Radom, L. *Isr. J. Chem.* **1993**, *33*, 345.

8. *Gaussian 94*, Revision D.1, Frisch, M.J.; Trucks, G.W.; Schlegel, H.B.; Gill, P.M.W.; Johnson, B.J.; Robb, M.A. ; Cheeseman, J. R.; Keith, T. A.; Petersson, G. A.; Montgomery, J. A.; Raghavachari, K.; Al-Laham, M. A.; Zakrzewski, V. G.; Ortiz, J. V.; Foresman, J. B.; Cioslowski, J.; Stefanov, B. B.; Nanayakkara, A.; Challacombe, M.; Peng, C. Y.; Ayala, P. Y.; Chen, W.; Wong, W.; Andres, J. L; Replogle, E. S.; Gomberts, R.; Martin, R. L.; Fox, D.J.; Binkley, J. S.; DeFrees, D. J.; Baker, J.; Stewart, J. P. P.; Head-Gordon, M.; Gonzalez, C.; Pople, J.A. Gaussian Inc., Pittsburgh PA, **1995**.

9. GAMESS, Schmidt, M.W.; Baldridge, K.K.; Boatz, J.A.; Elbert, S.T.; Gordon, M.S.; Jensen, J.H.; Koseki, S.; Matsunaga, N.; Nguyen, K.A.; Su, S.J.; Windus, T.L.; Dupuis, M.; Montogomery,J.A. *J. Comput. Chem.* **1993**, *14*, 1347.

10. (a) George,P.; Trachtman, M.; Bock, C.W.; Brett, A.M. *Tetrahedron* **1976**, *32*, 317. (b) Hehre, W. J.; Rarom, L.; Schleyer, P. v. R.; Pople, J. A. *Ab Initio Molecular Orbital Theory*, Wiley, New York, **1986**.

11. ACESII, product of the Quantum Theory Project, University of Florida, by: Stanton, J. F.; Gauss, J.; Watts, J. D.; Nooijen, M.; Oliphant, N.; Perrera, S. A.; Szalay, W. J.; Lauderdale, W. J.; Gwaltney, S. R.; Beck, S.; Balkova, A.; Bernhold, D. E.; Baeck, K.-K.; Rozyczko, P.; Sekino, H.; Huber, C.; Bartlett, R. J. Integral Packages: VMOL (Almlöf, J. and Taylor, P. R.); VPROPS (Taylor, P. R.); ABACUS (Helgaker, T.; Jensen, H. J. Aa.; Jorgensen, P.; Olsen, J. and Taylor, P.R.).

12. (a) Raghavachari, K.; Stefanov, B. B.; Curtiss, L. A. *J. Chem. Phys.* **1997**, *106*, 6764.

13. (a) Dresselhaus, M. S.; Dresselhaus, G.; Eklund, P. C. *Science of Fullerenes and Carbon Nanotubes*; Academic Press: San Diego, CA, **1996**. (b) Ebbesen T. W. *Physics Today*, June **1996**.

14. Padney, *Phys. Rev. Lett.* **1981**, *28*, 1913. (b) Private communication.

15. (a) West, R.; Fink, M. J.; Michl, J. Science, 1981, 214, 1343. (b) Brook, A. G.; Abdesaken, F.; Gutenkunst, B.; Gutenkunst, A.; Kallury, R. K. Chem. Soc. 1981, 191, 1981.

16. (a) Bakshi, A. K. *Solid State Communications*, **1993**, *88*, 401 and references therein. (b) Mann, J. "The Structure, Dynamics, and Function of Interfaces, and Thin Films", 1st Hansen Lecture, Physcial Chemistry Seminar, Spring 1999, Iowa State University.

17. (a) Schaeffer, H. F. III *Acc. Chem. Res.* **1982**, *15*, 283. (b) Baldridge, K. K.; Boatz, J. A.; Koseki, S.; Gordon, M. S. *Ann. Rev. Phys. Chem.* **1987**, *38*, 211.

18. (a) Murrll, J. N.; Kroto, H. W.; Guest, M. F. *J. Chem. Soc., Chem. Commun.*, **1977**, 619. (b) Hopkinson, A.C.; Lien, M. H. J. *Chem. Soc., Chem. Commun.*, **1980**, 107. (c) Gordon, M. S.; Pople, J. A. *J. Am. Chem. Soc.* **1981**,*103*, 2945.

19. For example see, Chance, R. R.; Patel, G. N.; Turi,E. A.; Khanna, Y. P. *J. Am. Chem. Soc.* **1978**, *100*, 1307.

20. Chase, M. W.,Jr. *NIST-JANAF Thermochemical Tables*, 4th Ed., *J. Phys. Chem.* Ref. Data, Monograph 9, **1998**, 1-1951.

Table 1A. HF-optimized energies, single-point MP2 energies at HF geometries, and zero-point energies, in Hartrees. Thermal corrections in kcal mol^{-1}.

Molecule	HF//6-31G(d)	MP2/6-31G(d)	ZPE (HF)	Thermal correction
($D_{\infty h}$) H_2	-1.126828	-1.144102	0.010580 (0.009450)	2.1
(T_d) CH_4	-40.195172	-40.332444	0.047777 (0.042368)	2.4
($D_{\infty h}$) C_2H_2	-76.817827	-77.064625	0.029448 (0.026297)	2.3
(D_{2h}) C_2H_4	-78.031718	-78.284343	0.054772 (0.048911)	2.5
(D_{3d}) C_2H_6)	-79.228755	-79.494513	0.079759 (0.071225)	2.8
($D_{\infty h}$) C_4H_2	-152.497928	-152.987469	0.042006 (0.037450)	3.1
(D_{6h}) C_6H_6	-230.703137	-231.456504	0.107673 (0.096152)	3.4
(C_{2v}) 	-307.378250	-307.376102	0.117863 (0.105252)	4.7
(D_{2h}) $C_2Si_2H_2$ (S=0)[a]	-654.547788	-654.992395	0.030515 (0.027250)	3.9
(D_{2h}) $C_2Si_2H_2$ (UHF, S=1)[a]	-654.598812	-654.980067	0.030494 (0.027231)	3.7
(D_{2h}) $C_2Si_2H_2$ (ROHF, S=1)[a]	-654.569431	-654.996774	0.032024 (0.028597)	3.6
(C_{2v}) $C_4Si_4H_4$ (S=0)[a]	-1309.224656	-1309.120289	81.83 I cm^{-1}	TS
(C_{2v}) $C_4Si_4H_4$ (UHF, S=1)[a]	-1309.236779	-1310.113923	0.074933 (0.066692)	6.0
(C_{2v}) $C_4Si_4H_4$ (ROHF, S=1)[a]	-1309.238256	-1310.054932	0.071150 (0.063537)	6.0

[a]S denotes the multiplicity of the state, S=0 for singlet, and S=1 for UHF or ROHF triplet respectively.

Table 1B. MP2-full core optimized energies and MP2, QCISD(T) and CCSD(T) single-point energies.

Molecule	$MP2^{FU}$// 6-31G(d)[b]	MP2/6-31G(d)[c]	MP2/ 6-311+G(3df,2p)[c]	QCISD(T)/ 6-31G(d)[c]
($D_{\infty h}$) H_2	-1.144141	-1.144141	-1.162735	-1.151648
(T_d) CH_4	-40.337043	-40.332552	-40.405661	-40.355947
($D_{\infty h}$) C_2H_2	-77.076215	-77.066790	-77.156341	-77.094095
(D_{2h}) C_2H_4	-78.294286	-78.284222	-78.392997	-78.320783
(D_{3d}) C_2H_6	-79.503970	-79.494740	-79.620234	-79.534559
($D_{\infty h}$) C_4H_2	-153.01255	-152.992786	-153.150278	-153.035930
(D_{6h}) C_6H_6	-231.487188	-231.457720	-231.720499	-231.531283
(C_{2v}) 	-307.419412	-307.379781	-307.725339	-307.469645
(D_{2h}) $C_2Si_2H_2$ (S=0)[a]	-655.024651	-654.992826	-655.189961	-655.040502
(D_{2h}) $C_2Si_2H_2$ (UHF, S=1)[a]	-655.011372	-654.980356	-655.161907	-655.044786
(C_{2v}) $C_2Si_2H_2$ (ROHF, S=1)[a]	-655.030769	-654.995927	-655.179212	-655.044928[d]
(C_{2v}) $C_4Si_4H_4$ (S=0)[a]	-1310.187714	--	--	--
(C_{2v}) $C_4Si_4H_4$ (UHF, S=1)[a]	-1310.186788	-1310.118106	-1310.501392	-1310.206522
(C_{2v}) $C_4Si_4H_4$ (ROHF, S=1)[a]	-1310.198386	-1310.067776	-1310.526310	-1310.205925[d]

[a]S denotes the spin multiplicity of the state, S=0 for singlets and S=1 for triplets (UHF or ROHF). [b]MP2 full core optimized energies at 6-31G(d). [c]Single bar denotes single-point, frozen-core MP2 and QCSD(T) energies. [d]For ROHF triplets, QCISD(T), which is UHF-based, was been substituted by CCSD(T) single-points.

Table 2. Zero-point corrected energies and heats of formation of the primary fragments.

Molecule	Thermal correction	E_0(MP2) /6-31G(d)[b]	E_0[G2(MP2,SVP)]	$\Delta H_f^0(298.15)$[c]	$\Delta H_f^{0,exp}$[c]
H	1.481[a]	-0.499809	-0.500000[e]	--	52.10316
C	1.562[a]	-37.746841	-37.782330[e]	--	171.288
SI	1.804[a]	-288.895868	-288.930360[e]	--	108.0±2.0
H_2	2.1	-1.134652	-1.166112	-0.89	0.0
CH_4	2.4	-40.290076	-40.407968	-17.98	-17.8951
C_2H_2	2.3	-77.038328	-77.184449	54.07	54.19010
C_2H_4	2.5	-78.235432	-78.412567	12.37	12.53990
C_2H_6	2.8	-79.423288	-79.626068	-20.06	-20.04±0.07
C_4H_2	3.1	-152.950019	-153.203839	108.38 108.67[f]	110.0
C_6H_6	3.4	-231.360352	-231.777710	16.83 18.5[f]	19.82±0.12
	4.7	-307.270850	-307.806191	65.23 68.20[f]	73.27±0.64
$C_2Si_2H_2$ (S=0)	3.9	-654.965145	-655.258267	133.45	--
$C_2Si_2H_2$ (S=1,UHF)	3.7	-654.952836	-655.242046	143.43	--
$C_2Si_2H_2$ (S=1,ROHF)	3.6	-654.968177	-655.242555	143.01	--
$C_4Si_4H_4$ (S=0)	(TS)	-1310.057459[d]	--	--	--
$C_4Si_4H_4$ (S=1,UHF)	6.0	-1310.0472310			--
$C_4Si_4H_4$ (S=1,ROHF)	6.0	-1309.991395	-1310.691742		--

[a]This number includes only the translational correction for atoms. Values taken from ref (JANAF). [b]MP2 energies at HF//6-31G(d) optimized geometries, corrected for zero-point. [c]In kcal mol^{-1}. [d]This energy has been corrected, for (3N-7) normal modes, since it corresponds to a transition state. [e]From reference 5c. [f]The second number is computed from appropriate homodesmic reactions.

Table 3. Energies (in Hartrees), zero-point energies and standard heats (gas) of formation (in kcal mol^{-1}).

Molecule	Thermal corrections[a]	HF//6-31G(d)[b]	MP2/6-31G(d)[b]	ZPE (HF) (scaled)	E_0(MP2)	$\Delta H_f^{0,298.15}$
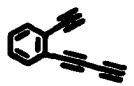	7.1	-457.731282	-459.220310	0.139890 (0.124922)	-459.095388	176.32
	7.7	-535.938678	-537.690239	0.205603 (0.183603)	-537.506636	85.98 (Exp 92.0±0.64[c])
$C_{36}H_{16}$ (D_2, S=0)[c]	18.6	-1372.292441	-1376.785421	0.414322 (0.369990)	-1376.415431	372.40
$C_{36}H_{16}$ (D_{2h}, S=0)	TS	-1372.280564	-1376.773088	0.413674 (0.369411)[d]	-1376.403616[d]	{379.91}[d]
$C_{36}H_{16}$ (graphitic sheet) (D_{2h}, S=0)	14.7	-1372.693247	-1377.258078	0.426314 (0.380698)	-1376.877380	44.15
$C_{32}Si_4H_{16}$ (D_2, S=0)	20.3	-2376.377139	-2380.825534	0.392166 (0.350204)	-2380.475330	271.40
$C_{32}Si_4H_{16}$ (C_1, S=0)	18.9	-2376.474033	-2380.909262	0.396158 (0.353769)	-2380.555493	--
$C_{32}Si_4H_{16}$ (C_1, S=1)[e]	19.2	-2376.457711	-2380.877909	0.394693 (0.352461)	-2380.525448	
$C_{72}H_{36}$ (D_2, S=0)	37.4	-2744.575705	-2753.632905	0.831445 (0.742480)	-2752.890425	[707.6][f]

[a]In kcal mol^{-1}. [b]HF optimized geometries, MP2 at the HF geometries. [c]From ref. 20. [d]Only (3N-7) normal modes were included in the correction of the transition state. The computed heat of formation corresponds to ΔH^0_f(0K). [e]S denotes the multiplicity of the state, for S=1, restricted open-shell calculation was performed. [f]This estimate here is given most for comparison, as this number was computed from the dimerization reaction and not any iso- or homodesmic reaction.

Table 4. Singlet-triplet state splittings, and 1st Koopmans ionization potentials.

Molecule	ΔE(Singlet-Triplet)[a]	1st Koopmans[b]
$C_{36}H_{16}$ (D_2)	--	7.8
$C_{36}H_{16}$ (D_{2h})$_{(graph)}$	--	5.1
$C_{32}Si_4H_{16}$ (S=0, D_2)	+31.5	6.7
$C_{32}Si_4H_{16}$ (S=0, C_1)	-18.9	6.6
$C_{32}Si_4H_{16}$ (S=1, C_1)	--	3.3

[a]Energy differences taken as (singlet-triplet) in kcal mol^{-1}, at MP2/HF//6-31G(d), corrected to zero-point. [b]In eV's.

Figure captions: Bond distances are given in Å, angles in degrees. For transition states, the Imaginary frequency is given in parenthesis, in cm^{-1}.

Figure 1. The homodesmic reaction used in the evaluation of $\Delta H^0_f(298)$ of $C_{36}H_{16}$ (D_2)

Figure 2.RHF//6-31G(d) (F1-F10) and MP2-FU//6-31G(d) (F1-F7) geometries for the all-C fragments. F10 is a transition state with one Imaginary frequency (10.0 cm^{-1}).

Figure 3. RHF and MP2-FU//6-31G(d) geometries for various wavefunctions of $C_2Si_2H_2$.

Figure 4. A selected set of geometrical parameters of $C_4Si_4H_4$, at the HF and MP2 levels of theory, and for various wavefunctions.

Figure 5. RHF//6-31G(d) geometrical parameters for the three $C_{36}H_{16}$ isomers (5a and 5b). Selected Boys localized (pi and sigma components) orbitals (5c and5d).

Figure 6. RHF//6-31G(d) geometry of the second singlet state of $C_{32}Si_4H_{16}$, ^1A-D_2 (6a) and Boys localized orbitals (6b).

Figure 7. ROHF//6-31G(d) geometry of the triplet state of $C_{32}Si_4H_{16}$, ^3A-C_1 (7a). Boys localized orbitals, lone pairs (7b) and single electrons (7c).

Figure 8. RHF//6-31G(d) geometry of the ground state singlet of $C_{32}Si_4H_{16}$, ^1A-C_1 (8a). Boys localized orbitals (8b and 8c).

Figure 9. RHF//6-31G(d) geometry of the ground state of the dimer $C_{72}H_{32}$, ^1A-D_2 (9a). Boys localized orbitals, π-type interactions (9b) and σ-type (9c).

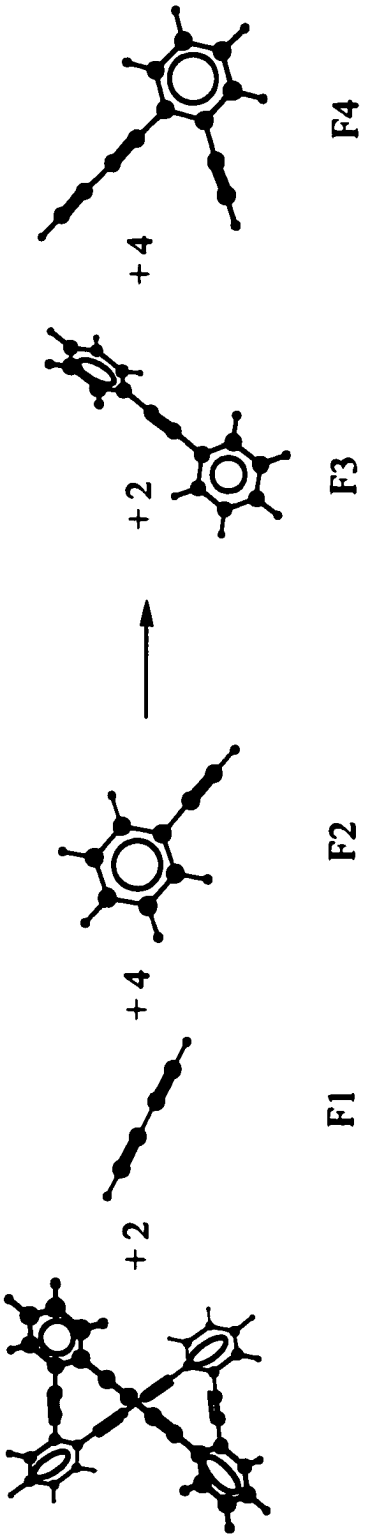

Figure 1

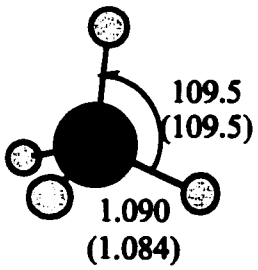

1

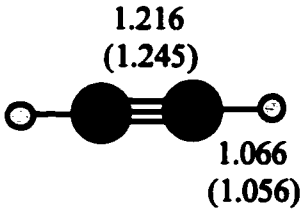

2

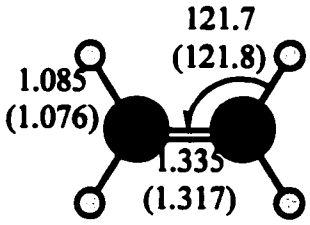

3

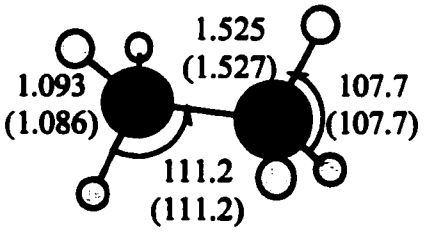

4

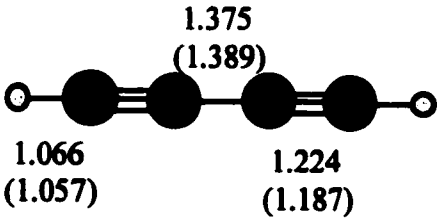

5

Figure 2a

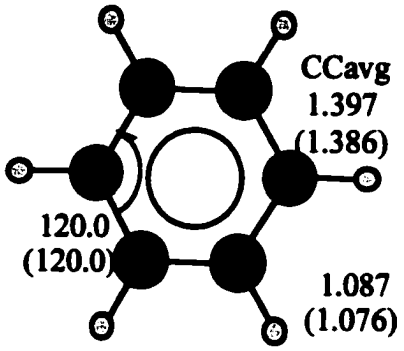

6

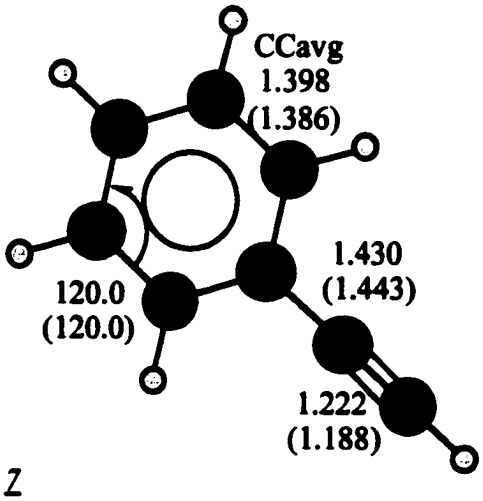

7

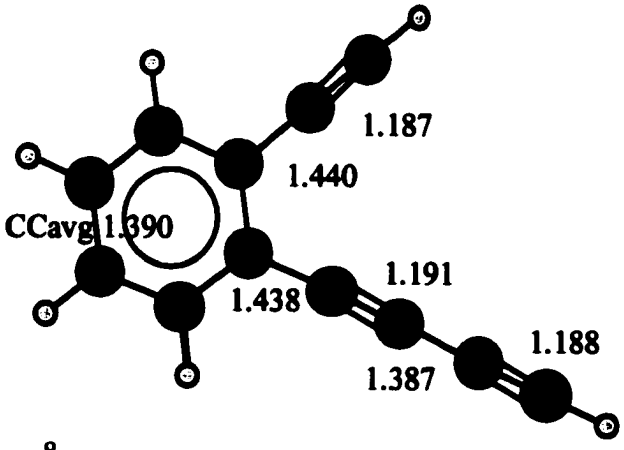

8

Figure 2b

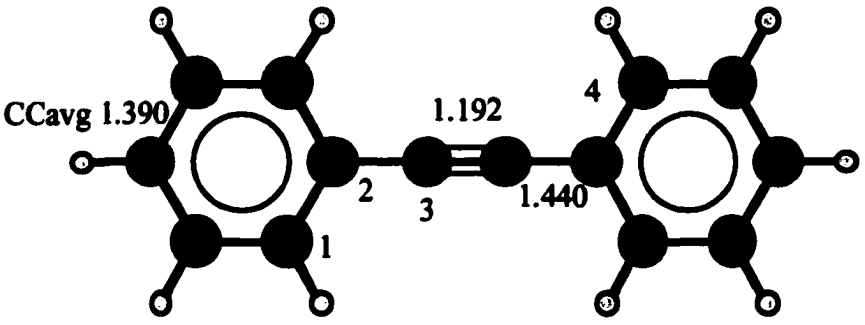

Dihedral 1234=179.9°

9

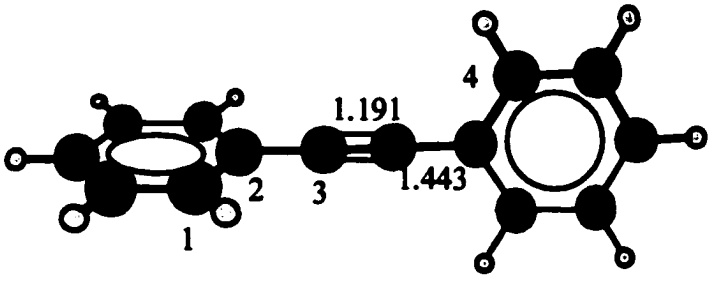

Dihedral 1234= -100.1°

10

Figure 2c

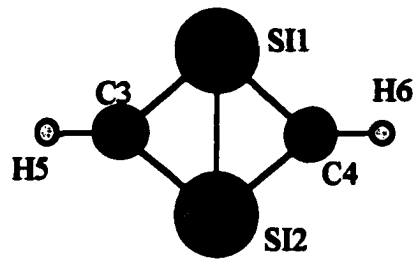

Singlet, D_{2h}

Parameters	RHF (minimum)	MP2(-362.89 cm^{-1})
SI1-SI2	2.327	2.327
SI1-C3	1.788	1.799
C3-C4	2.716	2.739
C3-H5	1.065	1.018
SI1-C3-SI2	81.1	80.7
C3-SI1-C4	98.9	99.3

ROHF triplet ($^3A_2$) C_{2v}, ($^3A_{1u}$) D_{2h} and ROMP2 ($^3A_2$) C_{2v}

Parameters	C_{2v} (minimum)	D_{2h} (-287.39 cm^{-1})	ROMP2
SI1-SI2	2.583	2.583	2.592
SI1-C3	1.805	1.824	1.824
C3-C4	2.576	2.576	2.619
C3-H5	1.071	1.071	1.084
SI1-C3-SI2	90.2	90.2	89.4
C3-SI1-C4	91.1	89.8	90.6

UHF triplet ($^3B_{2u}$)D_{2h}

Parameters	UHF (minimum)	UMP2 (minimum)
SI1-SI2	2.593	2.590
SI1-C3	1.839	1.831
C3-C4	2.608	2.589
C3-H5	1.072	1.083
SI1-C3-SI2	89.7	90.0
C3-SI1-C4	90.3	90.0

Figure 3

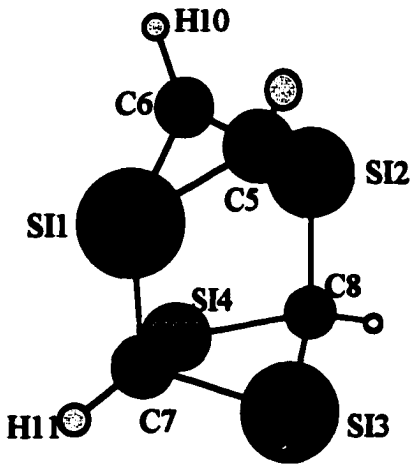

RHF/MP2

Singlet, C_{2v}, RHF and MP2 optimized geometries.

Parameter	RHF (81.83 cm^{-1})	MP2
SI1-SI2	2.671	2.706
SI3-SI4	2.705	2.693
SI1-C5	1.836	1.846
SI1-C7	1.920	1.901
SI3-C7	1.923	1.920
C5-C6	1.709	1.701
C7-C8	2.561	2.573
C6-H10	1.071	1.086
C7-H11	1.082	1.093
C5-SI1-C6	55.5	54.9
SI1-C5-SI2	93.4	94.3
SI4-C7-SI3	105.4	89.1
C7-SI3-C8	83.6	84.1
SI1-C7-SI3	105.5	105.5
SI1-C5-C6-SI2	-110.6	-111.4
C7-SI3-SI4-C8	139.3	140.1

Figure 4a

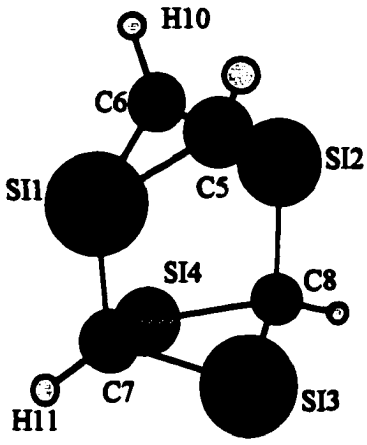

UHF

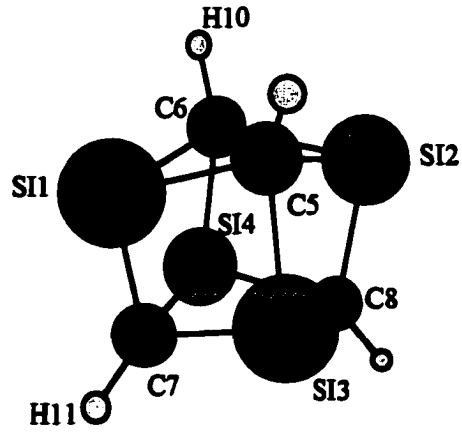

UMP2

Triplet, C_{2v}, UHF and UMP2 optimized geometries.

Parameter	UHF	UMP2
SI1-SI2	2.781	3.515
SI3-SI4	2.724	2.703
SI1-C5	1.842	1.979
SI1-C7	1.898	1.903
SI3-C7	1.930	1.935
C5-C6	1.647	2.781
C7-C8	2.570	2.707
C6-H10	1.075	1.088
C7-H11	1.083	1.087
C5-SI1-C6	53.1	47.2
SI1-C5-SI2	98.1	125.3
SI4-C7-SI3	89.8	88.6
C7-SI3-C8	83.5	88.7
SI1-C7-SI3	129.6	89.9
SI1-C5-C6-SI2	-115.2	-151.5
C7-SI3-SI4-C8	140.2	-155.3

Figure 4b

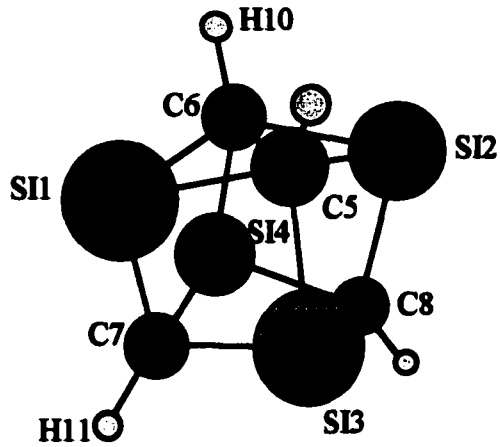

ROHF/ROMP2

Triplet, C_{2v}, ROHF and ROMP2 optimized geometries.

Parameter	ROHF	ROMP2
SI1-SI2	3.514	3.502
SI3-SI4	2.756	2.689
SI1-C5	1.975	1.976
SI1-C7	1.943	1.892
SI3-C7	1.941	1.929
C5-C6	1.609	1.591
C7-C8	2.655	2.710
C6-H10	1.076	1.088
C7-H11	1.075	1.087
C5-SI1-C6	48.1	47.5
SI1-C5-SI2	125.7	124.8
SI4-C7-SI3	90.4	88.4
C7-SI3-C8	86.3	89.2
SI1-C7-SI3	89.2	90.3
SI1-C5-C6-SI2	-153.9	-151.1
C7-SI3-SI4-C8	-152.1	156.7

Figure 4c

D_2 bonds in Å, angles in deg:

C2-C3 : 1.438
C3-C4 : 1.191
C4-C5 : 1.384
C8-C9 : 1.439
C9-C10: 1.190
avg C-C(benz) : 1.390
torsion C1-C2-C7-C8 : 91.7

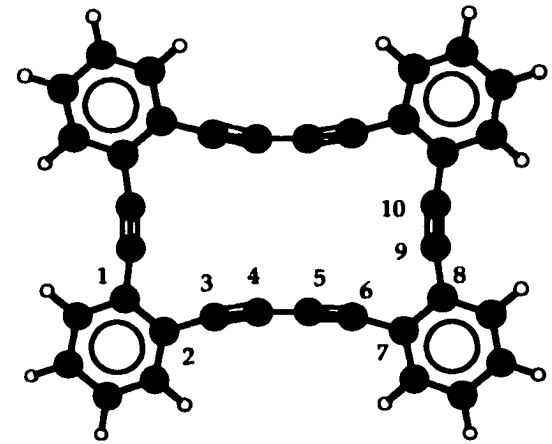

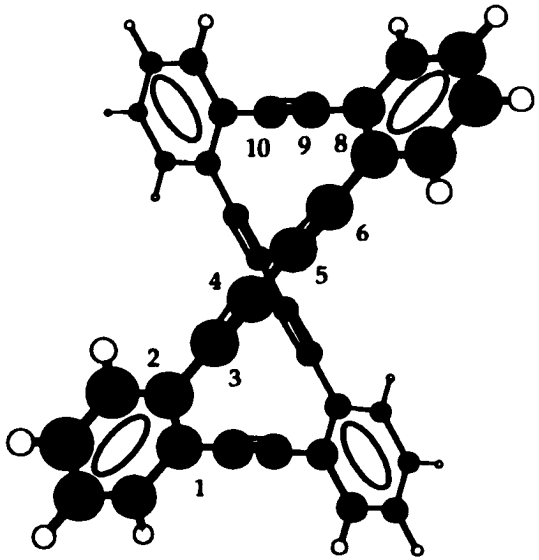

D_{2h}

$\Delta E = 7.34$ kcal mol^{-1}

ΔE_0(MP2/6-31G(d)//RHF/6-31G(d)
$= 10.1$ kcal mol^{-1}

D_2

D_{2h} bonds in Å, angles in deg:

C2-C3 : 1.438
C3-C4 : 1.192
C4-C5 : 1.385
C8-C9 : 1.438
C9-C10: 1.191
avg C-C(benz) : 1.390
C4-C5-C6 : 173.4
C5-C6-C7 : 171.2
C6-C7-C8 : 123.7
C7-C8-C9 : 123.6
C8-C9-C10: 172.6

Figure 5a

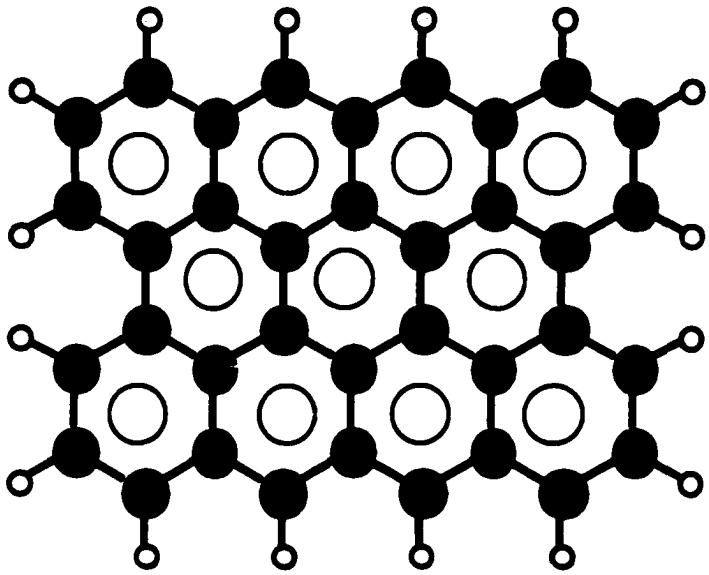

Average bond lengths (in Å)

C-C	1.386
C-H	1.076

Isodesmic scheme for the evaluation of the standard heat of formation:

$$C_{36}H_{16}(\text{"graphitic"}) + 56CH_4 \rightarrow 18C_2H_4 + 28C_2H_6$$

Figure 5b

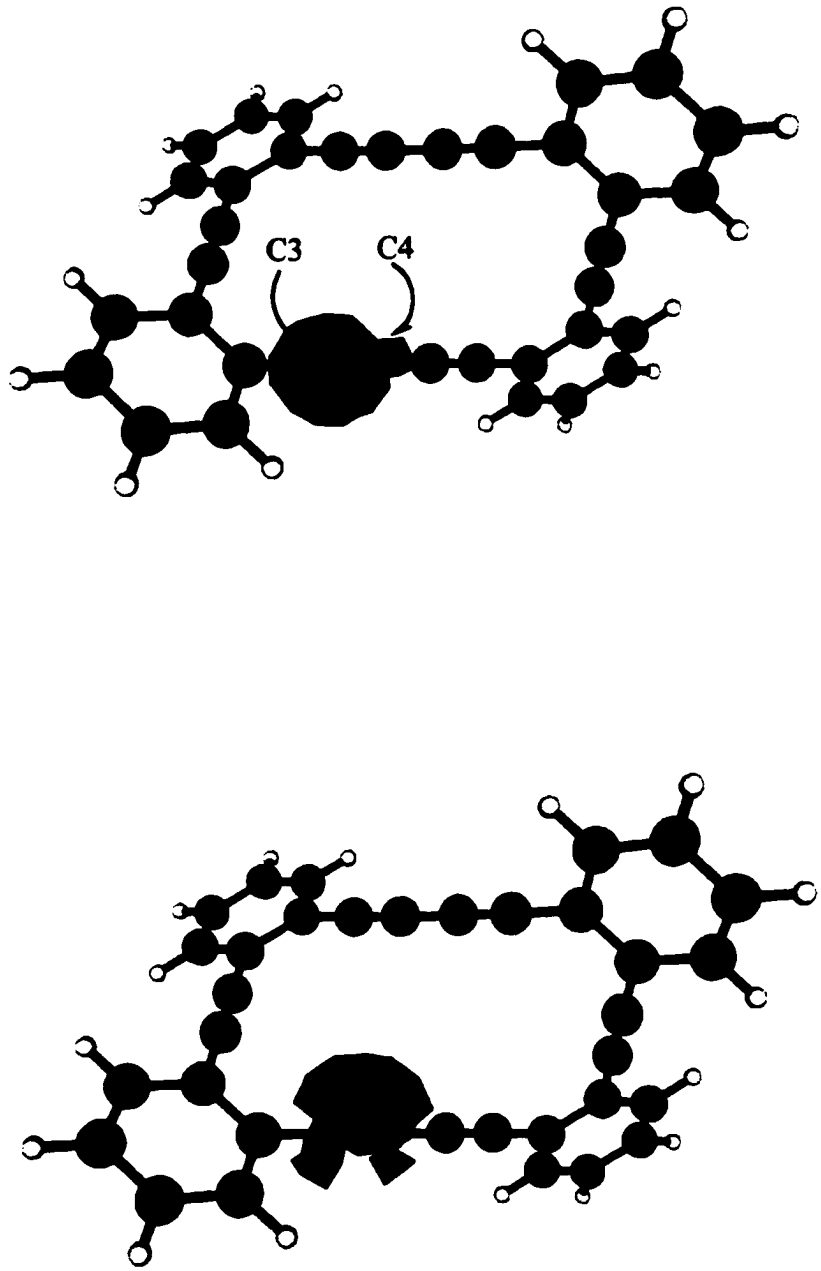

Figure 5c

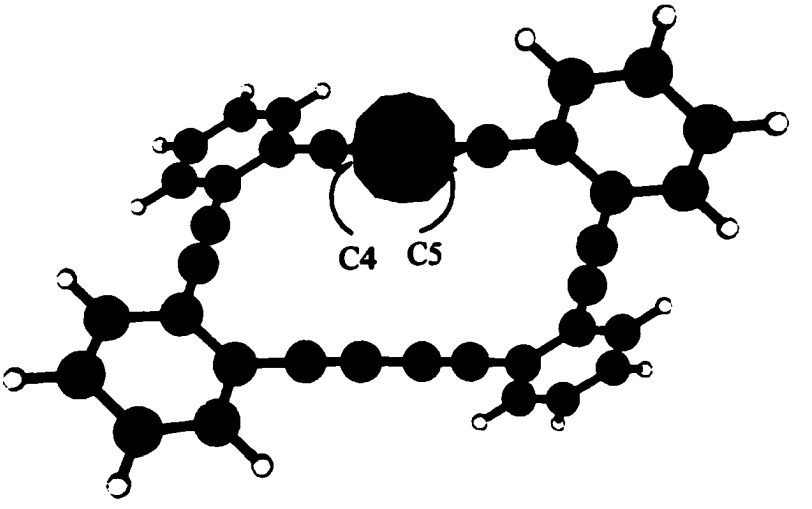

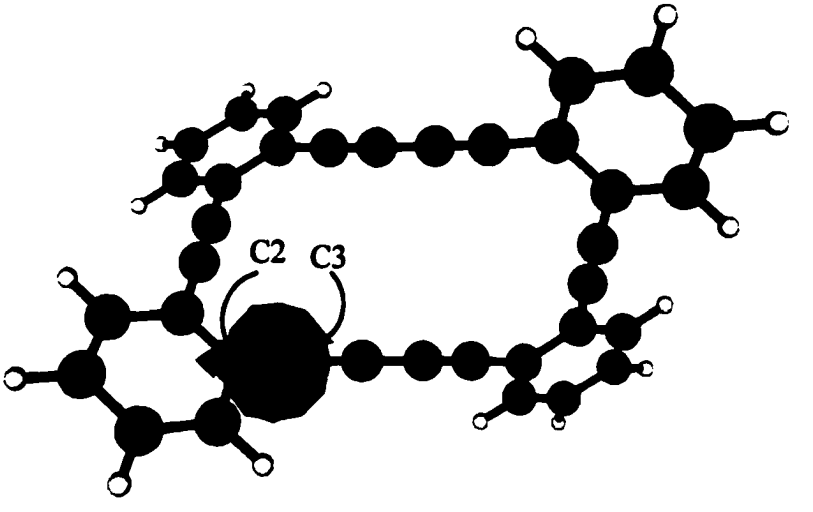

Figure 5d

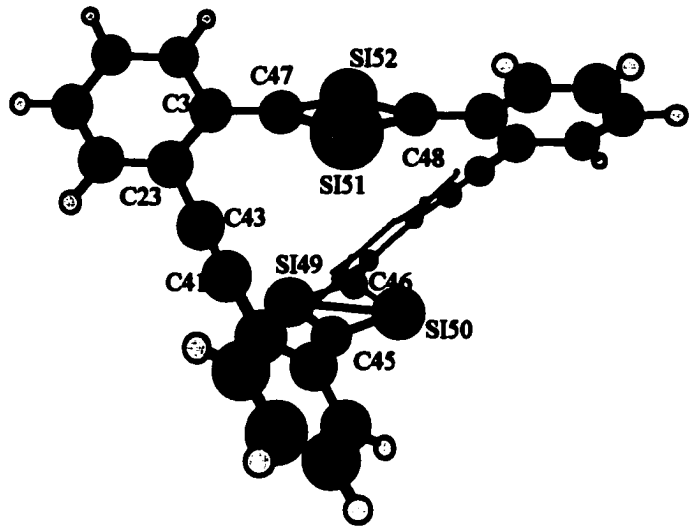

A selected set of geometric parameters of $C_{32}Si_4H_{16}$, ^1A D_2.

SI51-C48	1.784	SI51-C48-SI52	82.
SI51-SI52	2.365	C48-SI51-C47	100.
C45-C46	2.721	SI51-C47-C3	141.4
C47-C3	1.454	C47-C3-C23	122.2
C23-C43	1.439	C23-C43-C41	178.6
C41-C43	1.194	C47-C3-C23-C43	-2.6

Figure 6a

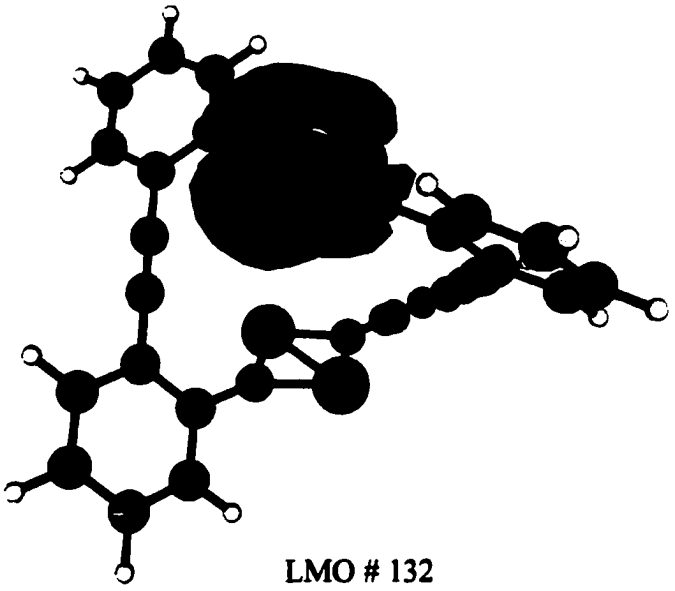

LMO # 132

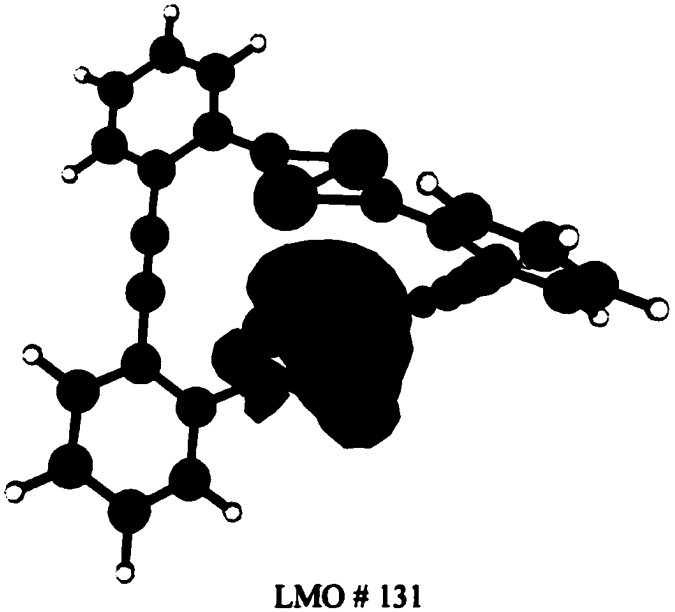

LMO # 131

Figure 6b

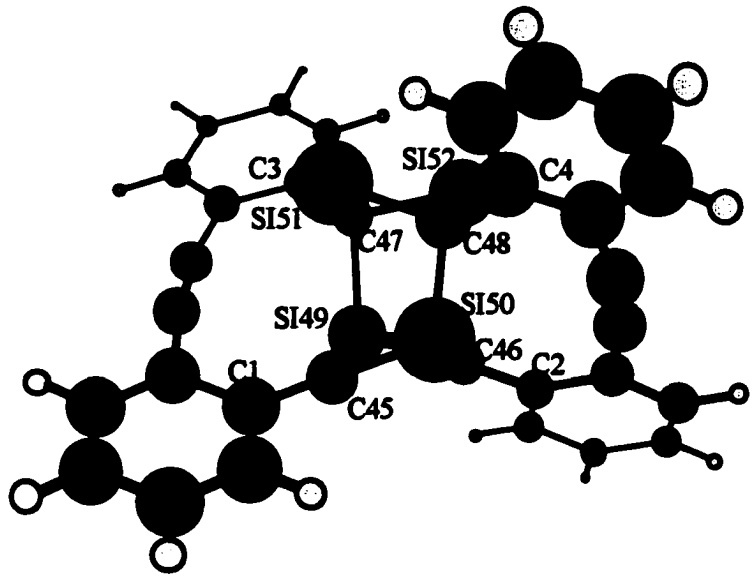

A selected set of geometrical parameters. Bonds are in Å, angles in degrees.

C45-SI50	1.834	C45-C1	1.459	C41-C43-C23	169.3
C45-SI49	1.944	C46-C2	1.451	C42-C44-C24	170.8
C46-SI50	1.833	C47-C3	1.506	C21-C1-C5	117.9
C46-SI49	1.945	C48-C4	1.506	C21-C17-C13	120.7
C47-SI51	1.900	C41-C43	1.194	C17-C13-C9	119.7
C47-SI52	1.920	C42-C44	1.196	C1-C5-C9	121.4
C47-C48	2.631	C21-C1	1.413	C22-C2-C46	120.3
C48-SI50	1.890	C21-C17	1.392	C21-C1-C45	121.9
C48-SI51	1.945	C17-C13	1.380	C4-C24-C44	117.8
C48-SI52	1.982	C1-C5	1.397	C24-C4-C8	117.2
SI47-C47	2.006	C22-C2	1.415		
SI47-SI50	2.498				

Figure 7a

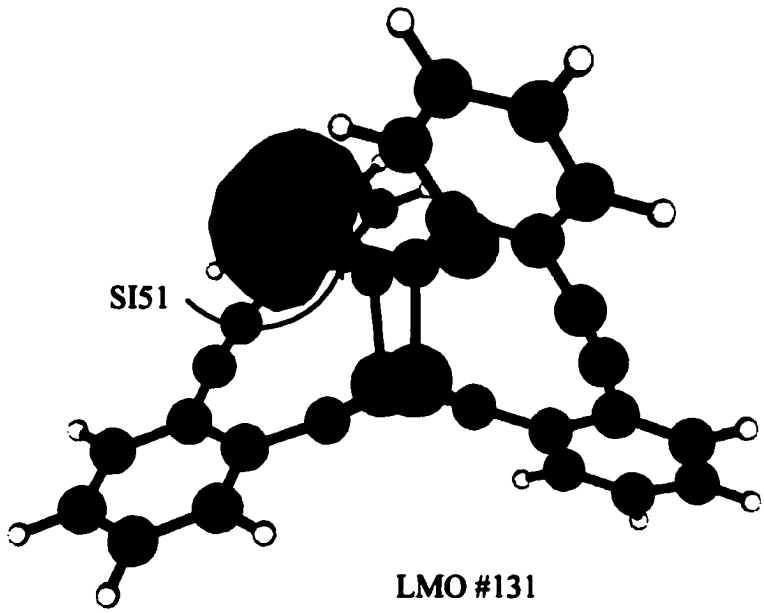

LMO #131

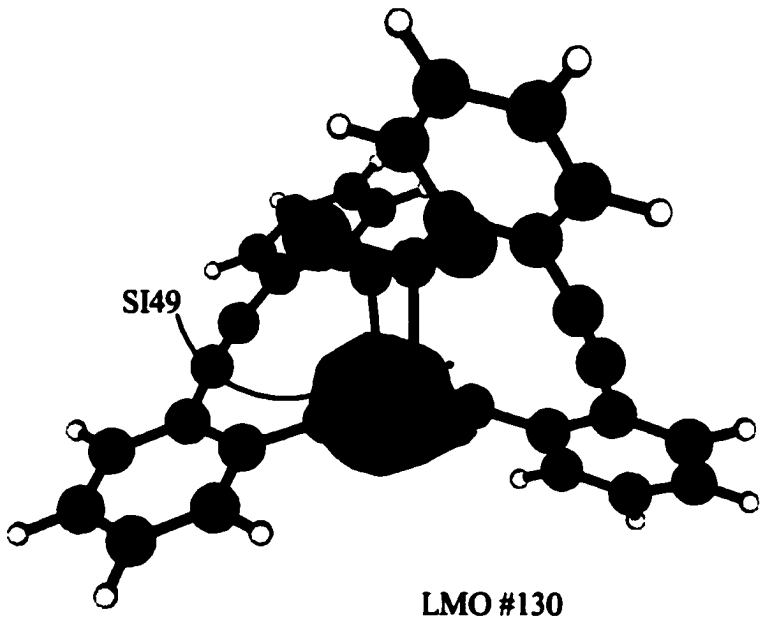

LMO #130

Figure 7b

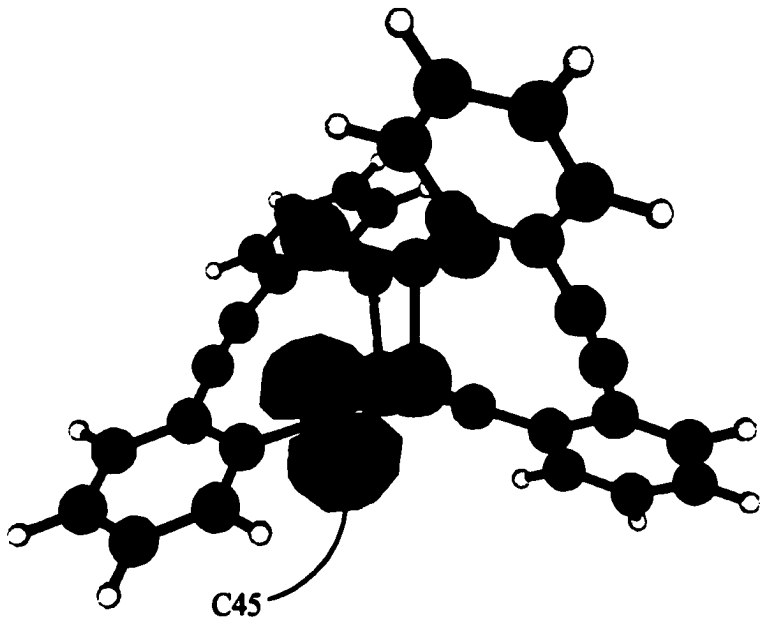

LMO #132

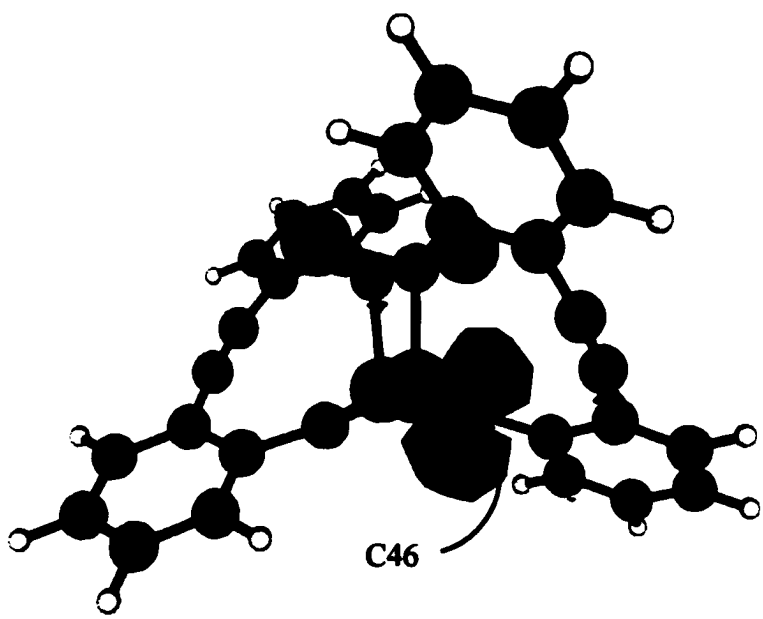

LMO #133

Figure 7c

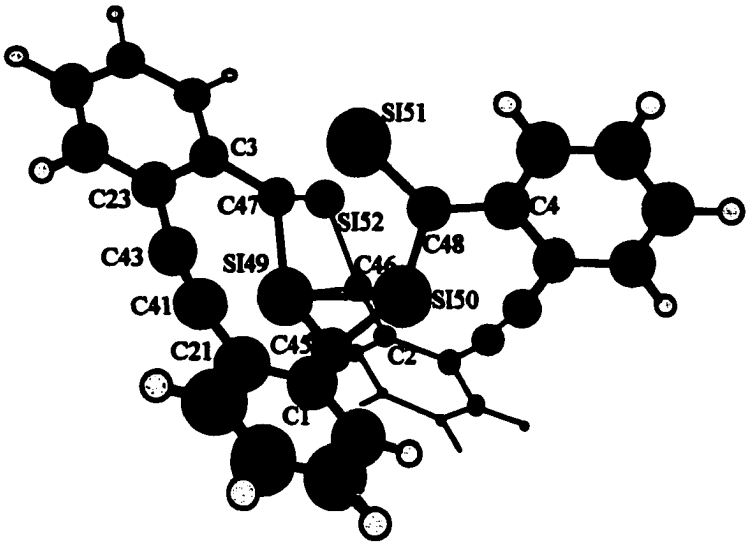

A selected set of geometric parameters, for the second singlet of $C_{32}SI_4H_{16}$. Bond lengths are in Å, angles in degrees.

C47-C3	1.487	SI49-C47-SI50	90.0
C47-SI52	1.929	C47-SI52-C46	86.3
C48-CI50	1.815	SI49-C46-SI52	88.9
C48-SI51	1.784	C46-SI49-C47	88.1
SI49-C45	1.776	SI50-C48-SI51	113.3
SI49-C46	1.917	C48-C50-SI49	108.9
SI49-C47	1.859	C50-C46-SI49	74.8
SI49-SI50	2.315	C21-C41-C43	171.3
C21-41	1.431	C46-SI49-C47-SI52	-152.2
		SI50-C46-SI49-C45	-29.7
		C21-C41-C43-C23	-7.9

Figure 8a

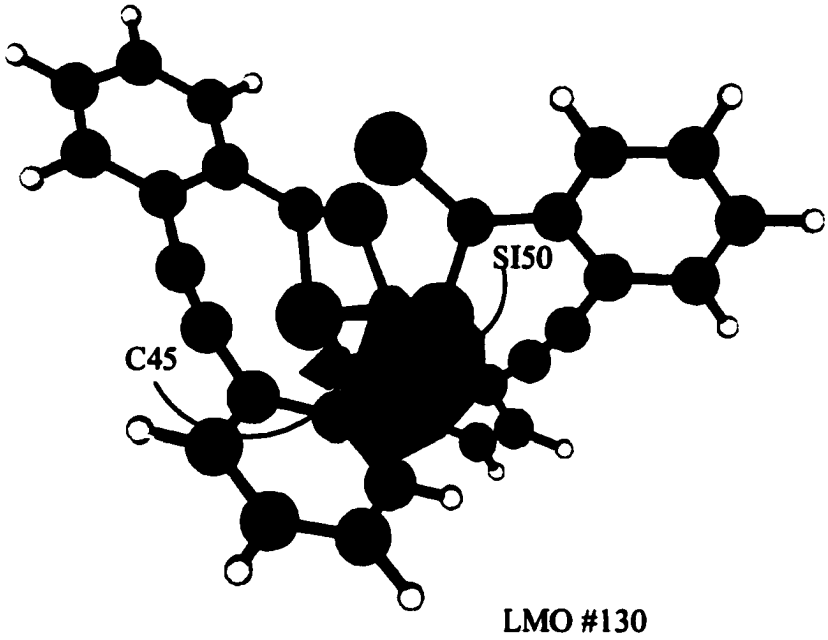

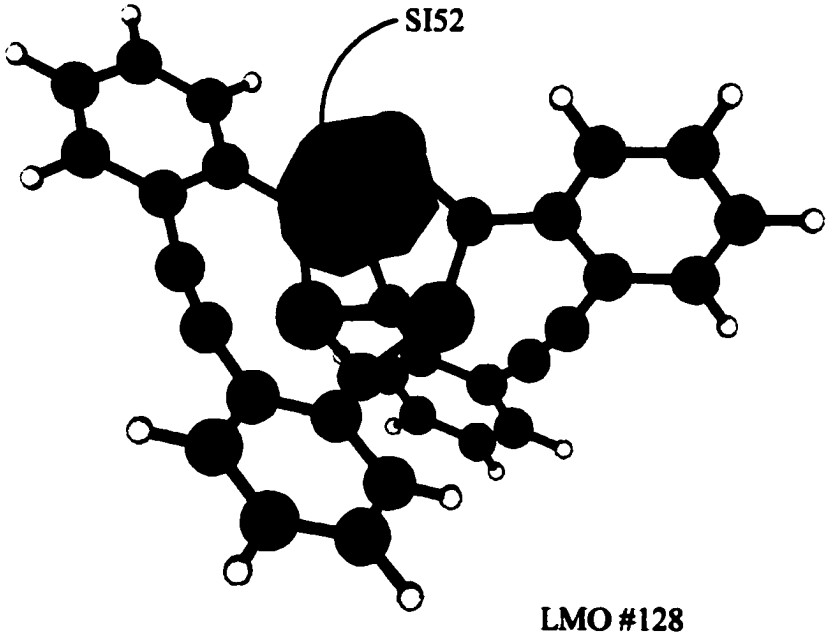

Figure 8b

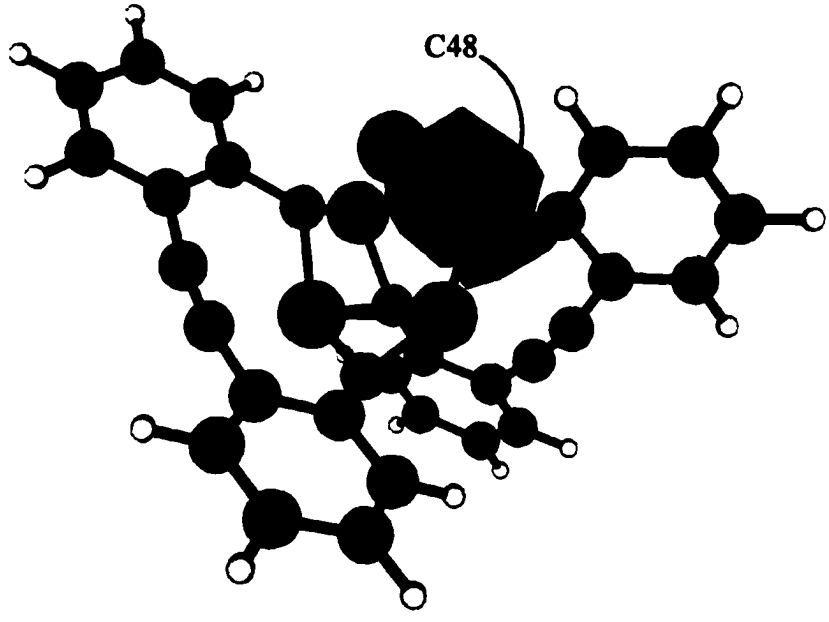

LMO #132

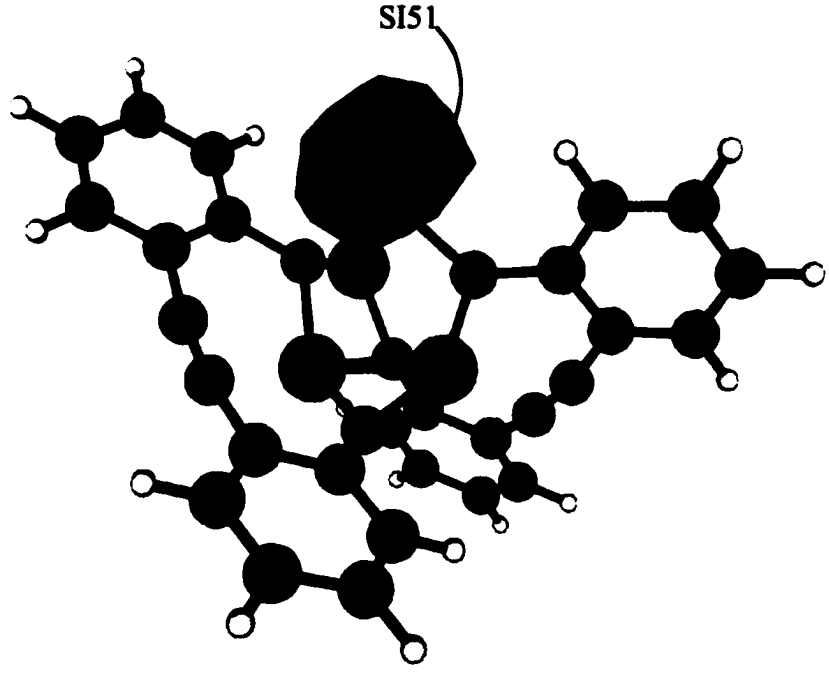

LMO #131

Figure 8c

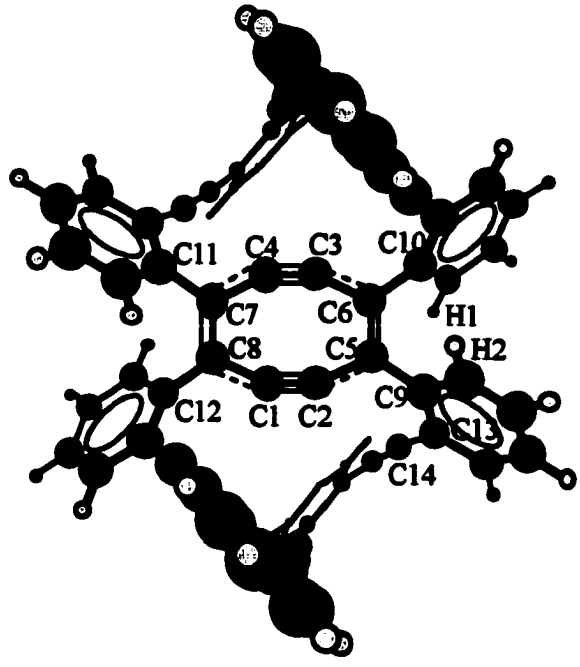

A set of selected geometric parameters of $C_{72}H_{32}$ dimer. Bond distances in Å, angles in degrees.

C1-C2	1.192
C1-C8	1.459
C6-C10	1.494
C7-C8	1.353
C9-C10	3.022
H1-H2	4.063
C1-C8-C12	121.7
C1-C2-C5	155.3
C2-C5-C6	114.6
C5-C6-C8	123.6
C1-C2-C5-C9	57.5
C5-C9-C13-C14	-0.42
C9-C5-C6-C10	15.1

Figure 9a

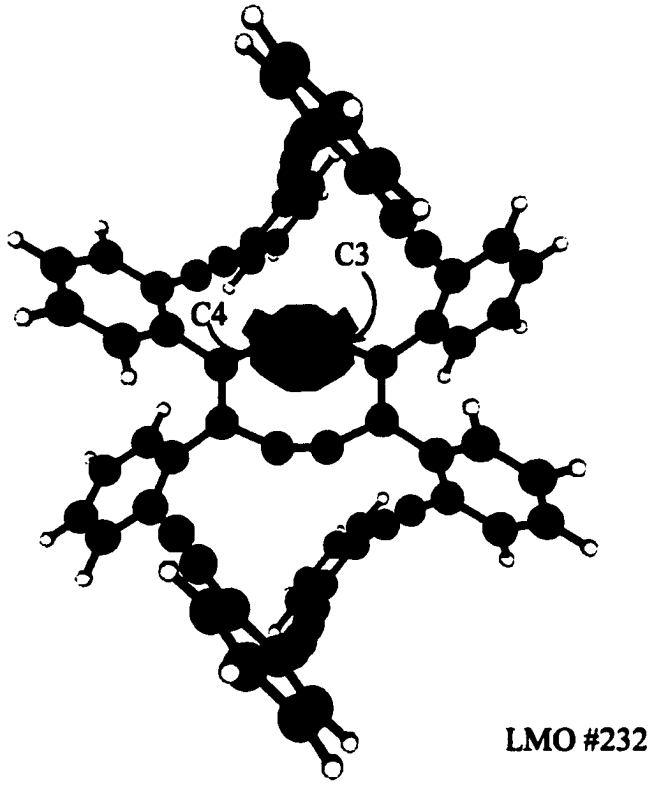

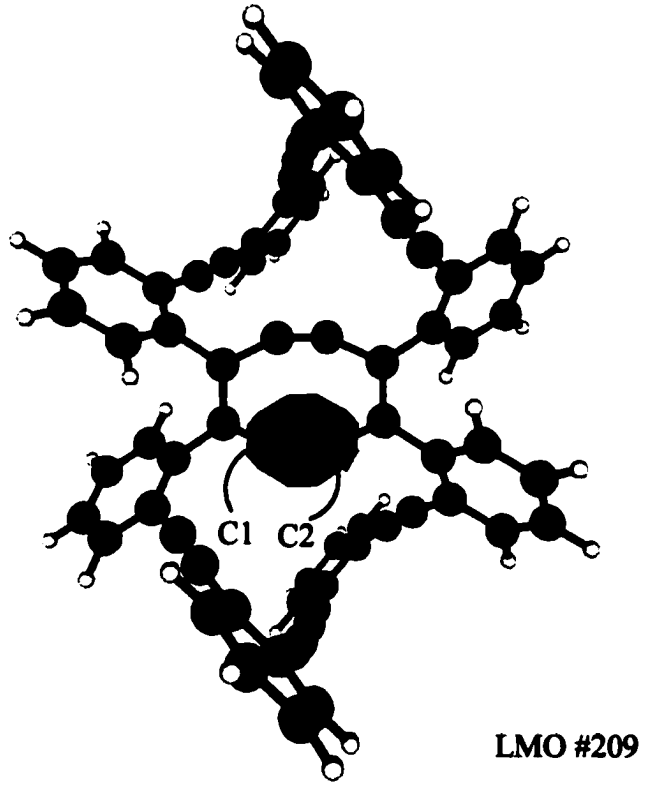

Figure 9b

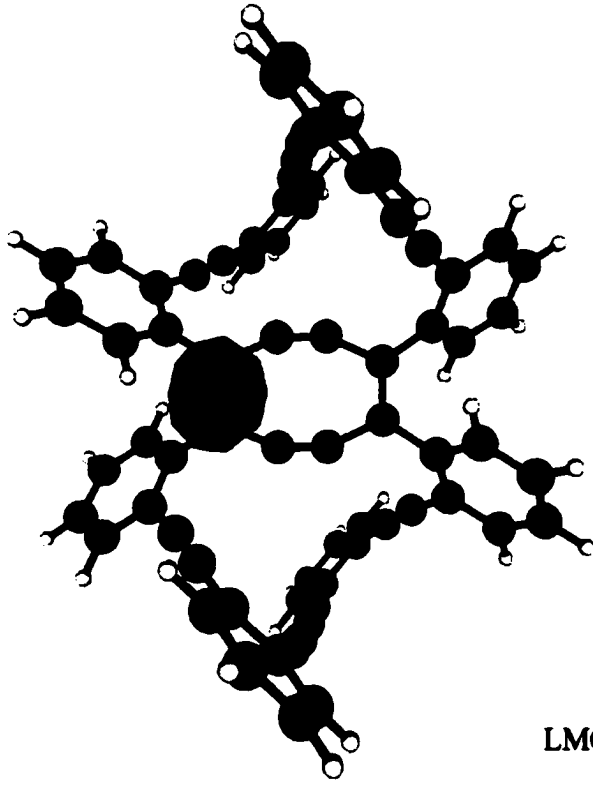

LMO #208

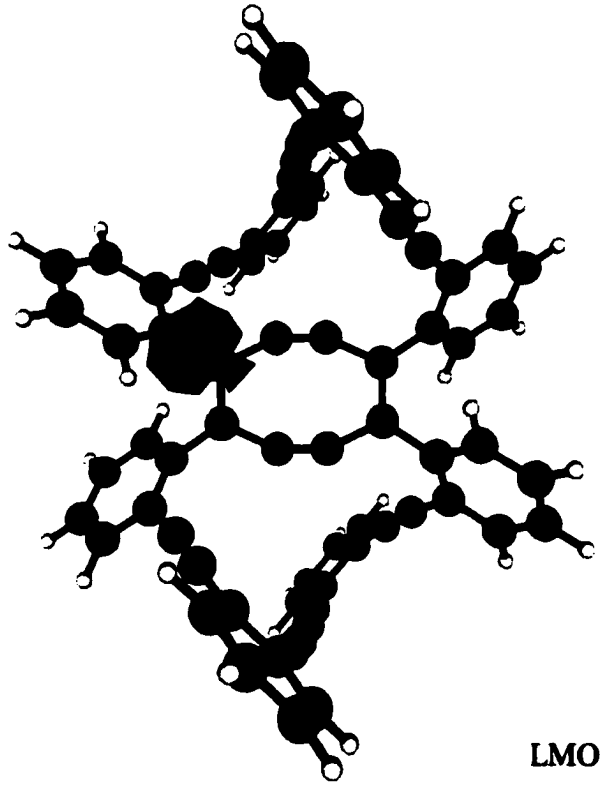

LMO #195

Figure 9c

Appendix I. Cartesian coordinates for $C_{36}H_{16}$, ^1A - D_2.

C	-2.7640	-2.1321	1.8401
C	2.7640	-2.1321	-1.8401
C	-2.7640	2.1321	-1.8401
C	2.7640	2.1321	1.8401
C	-2.8267	-3.0082	2.9214
C	2.8267	-3.0082	-2.9214
C	-2.8267	3.0082	-2.9214
C	2.8267	3.0082	2.9214
C	-3.9584	-3.0755	3.7110
C	3.9584	-3.0755	-3.7110
C	-3.9584	3.0755	-3.7110
C	3.9584	3.0755	3.7110
C	-5.0473	-2.2650	3.4284
C	5.0473	-2.2650	-3.4284
C	-5.0473	2.2650	-3.4284
C	5.0473	2.2650	3.4284
C	-4.9984	-1.3908	2.3594
C	4.9984	-1.3908	-2.3594
C	-4.9984	1.3908	-2.3594
C	4.9984	1.3908	2.3594
C	-3.8640	-1.3101	1.5555
C	3.8640	-1.3101	-1.5555
C	-3.8640	1.3101	-1.5555
C	3.8640	1.3101	1.5555
H	-1.9793	-3.6333	3.1323
H	1.9793	-3.6333	-3.1323
H	-1.9793	3.6333	-3.1323
H	1.9793	3.6333	3.1323
H	-3.9909	-3.7566	4.5419
H	3.9909	-3.7566	-4.5419
H	-3.9909	3.7566	-4.5419
H	3.9909	3.7566	4.5419
H	-5.9306	-2.3128	4.0391
H	5.9306	-2.3128	-4.0391
H	-5.9306	2.3128	-4.0391
H	5.9306	2.3128	4.0391
H	-5.8376	-0.7585	2.1373
H	5.8376	-0.7585	-2.1373
H	-5.8376	0.7585	-2.1373
H	5.8376	0.7585	2.1373
C	-3.8442	-0.3870	0.4521
C	3.8442	-0.3870	-0.4521
C	-3.8442	0.3870	-0.4521
C	3.8442	0.3870	0.4521
C	-1.5740	-2.0958	1.0346
C	1.5740	-2.0958	-1.0346
C	-1.5740	2.0958	-1.0346
C	1.5740	2.0958	1.0346
C	-0.5779	-2.0918	0.3810
C	0.5779	-2.0918	-0.3810
C	-0.5779	2.0918	-0.3810
C	0.5779	2.0918	0.3810

Appendix II. Cartesian coordinates of $C_{32}Si_4H_{16}$, ^1A - D_2.

C	-2.1800	-2.1398	1.7784
C	2.1800	-2.1398	-1.7784
C	-2.1800	2.1398	-1.7784
C	2.1800	2.1398	1.7784
C	-2.2111	-2.9789	2.8987
C	2.2111	-2.9789	-2.8987
C	-2.2111	2.9789	-2.8987
C	2.2111	2.9789	2.8987
C	-3.2870	-2.9994	3.7617
C	3.2870	-2.9994	-3.7617
C	-3.2870	2.9994	-3.7617
C	3.2870	2.9994	3.7617
C	-4.3936	-2.1975	3.5159
C	4.3936	-2.1975	-3.5159
C	-4.3936	2.1975	-3.5159
C	4.3936	2.1975	3.5159
C	-4.3969	-1.3675	2.4142
C	4.3969	-1.3675	-2.4142
C	-4.3969	1.3675	-2.4142
C	4.3969	1.3675	2.4142
C	-3.2998	-1.3135	1.5549
C	3.2998	-1.3135	-1.5549
C	-3.2998	1.3135	-1.5549
C	3.2998	1.3135	1.5549
H	-1.3697	-3.6220	3.0795
H	1.3697	-3.6220	-3.0795
H	-1.3697	3.6220	-3.0795
H	1.3697	3.6220	3.0795
H	-3.2714	-3.6509	4.6172
H	3.2714	-3.6509	-4.6172
H	-3.2714	3.6509	-4.6172
H	3.2714	3.6509	4.6172
H	-5.2406	-2.2188	4.1775
H	5.2406	-2.2188	-4.1775
H	-5.2406	2.2188	-4.1775
H	5.2406	2.2188	4.1775
H	-5.2427	-0.7354	2.2145
H	5.2427	-0.7354	-2.2145
H	-5.2427	0.7354	-2.2145
H	5.2427	0.7354	2.2145
C	-3.3246	-0.3908	0.4514
C	3.3246	-0.3908	-0.4514
C	-3.3246	0.3908	-0.4514
C	3.3246	0.3908	0.4514
C	-1.0308	-2.1441	0.8881
C	1.0308	-2.1441	-0.8881
C	-1.0308	2.1441	-0.8881
C	1.0308	2.1441	0.8881
Si	-0.7526	-2.1070	-0.9122
Si	0.7526	-2.1070	0.9122
Si	-0.7526	2.1070	0.9122
Si	0.7526	2.1070	-0.9122

Appendix III. Cartesian coordinates of $C_{32}Si_4H_{16}$, ^1A - C_1.

C	-1.4517	-1.6502	1.4243
C	2.0489	-1.4274	-2.0649
C	-2.3502	1.7771	-2.1579
C	1.8840	1.7560	1.8308
C	-1.0220	-2.3433	2.5642
C	2.1019	-2.0881	-3.2911
C	-2.4392	2.8421	-3.0549
C	1.8424	2.8509	2.7107
C	-1.9149	-2.7612	3.5259
C	3.0935	-3.0112	-3.5676
C	-3.6634	3.3355	-3.4630
C	2.7979	3.0223	3.6844
C	-3.2793	-2.5215	3.3781
C	4.0704	-3.3123	-2.6272
C	-4.8463	2.7802	-2.9919
C	3.8468	2.1136	3.8482
C	-3.7339	-1.8386	2.2719
C	4.0533	-2.6727	-1.4053
C	-4.7895	1.7344	-2.0956
C	3.9284	1.0321	3.0056
C	-2.8335	-1.3850	1.3081
C	3.0626	-1.7348	-1.1328
C	-3.5580	1.2398	-1.6702
C	2.9734	0.8627	2.0017
H	0.0246	-2.5640	2.6694
H	1.3482	-1.8825	-4.0297
H	-1.5373	3.2857	-3.4349
H	1.0362	3.5560	2.6248
H	-1.5563	-3.2896	4.3913
H	3.1012	-3.5076	-4.5215
H	-3.6967	4.1572	-4.1565
H	2.7288	3.8713	4.3416
H	-3.9734	-2.8623	4.1245
H	4.8341	-4.0351	-2.8477
H	-5.7959	3.1644	-3.3162
H	4.5795	2.2599	4.6201
H	-4.7814	-1.6309	2.1508
H	4.8029	-2.8864	-0.6654
H	-5.6918	1.2966	-1.7089
H	4.7290	0.3210	3.1020
C	-3.2595	-0.5843	0.2009
C	3.0546	-0.9873	0.1112
C	-3.4710	0.1911	-0.6913
C	3.0699	-0.2079	1.0403
C	-0.5348	-1.2762	0.3644
C	1.0082	-0.4227	-1.7053
C	-1.0539	1.2040	-1.7067
C	0.8945	1.4646	0.7984
Si	-0.8447	-0.5833	-1.2407
Si	0.9503	-0.2416	0.1806
Si	-0.3572	2.4616	0.0091
Si	0.5757	1.1277	-2.7363

Appendix IV. Cartesian coordinates of $C_{32}Si_4H_{16}$, ^3A - C_1.

C	-2.0215	-1.8013	1.7010
C	2.0908	-1.7683	-1.7890
C	-2.1004	1.6860	-1.7709
C	2.0227	1.6524	1.7542
C	-1.7680	-2.6524	2.7796
C	1.8815	-2.5570	-2.9223
C	-1.8875	2.5962	-2.8016
C	1.7949	2.6277	2.7214
C	-2.7853	-3.0911	3.6042
C	2.9452	-3.0589	-3.6463
C	-2.9402	3.1162	-3.5376
C	2.8266	3.1387	3.4913
C	-4.0917	-2.6829	3.3771
C	4.2498	-2.7807	-3.2614
C	-4.2450	2.7434	-3.2613
C	4.1258	2.6904	3.3171
C	-4.3697	-1.8292	2.3278
C	4.4858	-1.9887	-2.1545
C	-4.4885	1.8404	-2.2438
C	4.3835	1.7237	2.3649
C	-3.3540	-1.3807	1.4889
C	3.4241	-1.4749	-1.4182
C	-3.4368	1.3130	-1.5040
C	3.3521	1.2074	1.5877
H	-0.7588	-2.9755	2.9574
H	0.8735	-2.7769	-3.2217
H	-0.8841	2.9035	-3.0354
H	0.7961	2.9912	2.8796
H	-2.5602	-3.7494	4.4238
H	2.7587	-3.6674	-4.5129
H	-2.7370	3.8168	-4.3280
H	2.6114	3.8900	4.2301
H	-4.8851	-3.0216	4.0181
H	5.0760	-3.1717	-3.8269
H	-5.0612	3.1491	-3.8310
H	4.9259	3.0883	3.9143
H	-5.3749	-1.4939	2.1517
H	5.4912	-1.7528	-1.8584
H	-5.4934	1.5355	-2.0151
H	5.3838	1.3618	2.2123
C	-3.6247	-0.4507	0.4280
C	3.6301	-0.5958	-0.3022
C	-3.6606	0.3546	-0.4530
C	3.6026	0.2036	0.5869
C	-0.9371	-1.4061	0.8078
C	0.9849	-1.2953	-0.9775
C	-0.9830	1.1299	-0.9277
C	0.9143	1.1024	0.8955
Si	-0.9118	-0.8708	-1.0610
Si	0.7860	-0.7791	0.7696
Si	-0.9432	1.6803	0.9113
Si	0.8917	1.5305	-1.0398

Appendix V. Cartesian coordinates of $C_{72}H_{32}$, $^1A - D_2$.

C	0.4594	-5.1566	-3.2532
C	-0.4594	-5.1566	3.2532
C	0.4594	5.1566	3.2532
C	-0.4594	5.1566	-3.2532
C	3.1545	-1.4885	0.2596
C	-3.1545	-1.4885	-0.2596
C	3.1545	1.4885	-0.2596
C	-3.1545	1.4885	0.2596
C	-0.2427	-5.8351	-4.2433
C	0.2427	-5.8351	4.2433
C	-0.2427	5.8351	4.2433
C	0.2427	5.8351	-4.2433
C	3.9611	-1.1796	1.3521
C	-3.9611	-1.1796	-1.3521
C	3.9611	1.1796	-1.3521
C	-3.9611	1.1796	1.3521
C	-0.0408	-5.5340	-5.5780
C	0.0408	-5.5340	5.5780
C	-0.0408	5.5340	5.5780
C	0.0408	5.5340	-5.5780
C	5.1123	-1.8940	1.6245
C	-5.1123	-1.8940	-1.6245
C	5.1123	1.8940	-1.6245
C	-5.1123	1.8940	1.6245
C	0.8650	-4.5483	-5.9366
C	-0.8650	-4.5483	5.9366
C	0.8650	4.5483	5.9366
C	-0.8650	4.5483	-5.9366
C	5.4818	-2.9457	0.8026
C	-5.4818	-2.9457	-0.8026
C	5.4818	2.9457	-0.8026
C	-5.4818	2.9457	0.8026
C	1.5716	-3.8672	-4.9613
C	-1.5716	-3.8672	4.9613
C	1.5716	3.8672	4.9613
C	-1.5716	3.8672	-4.9613
C	4.6883	-3.2759	-0.2773
C	-4.6883	-3.2759	0.2773
C	4.6883	3.2759	0.2773
C	-4.6883	3.2759	-0.2773
C	1.3816	-4.1600	-3.6159
C	-1.3816	-4.1600	3.6159
C	1.3816	4.1600	3.6159
C	-1.3816	4.1600	-3.6159
C	3.5220	-2.5635	-0.5577
C	-3.5220	-2.5635	0.5577
C	3.5220	2.5635	0.5577
C	-3.5220	2.5635	-0.5577
H	-0.9470	-6.5938	-3.9571
H	0.9470	-6.5938	3.9571
H	-0.9470	6.5938	3.9571
H	0.9470	6.5938	-3.9571
H	3.6720	-0.3719	1.9974

H	-3.6720	-0.3719	-1.9974
H	3.6720	0.3719	-1.9974
H	-3.6720	0.3719	1.9974
H	-0.5900	-6.0647	-6.3344
H	0.5900	-6.0647	6.3344
H	-0.5900	6.0647	6.3344
H	0.5900	6.0647	-6.3344
H	5.7135	-1.6322	2.4764
H	-5.7135	-1.6322	-2.4764
H	5.7135	1.6322	-2.4764
H	-5.7135	1.6322	2.4764
H	1.0224	-4.3109	-6.9731
H	-1.0224	-4.3109	6.9731
H	1.0224	4.3109	6.9731
H	-1.0224	4.3109	-6.9731
H	6.3749	-3.5089	1.0048
H	-6.3749	-3.5089	-1.0048
H	6.3749	3.5089	-1.0048
H	-6.3749	3.5089	1.0048
H	2.2765	-3.1043	-5.2345
H	-2.2765	-3.1043	5.2345
H	2.2765	3.1043	5.2345
H	-2.2765	3.1043	-5.2345
H	4.9580	-4.0950	-0.9176
H	-4.9580	-4.0950	0.9176
H	4.9580	4.0950	0.9176
H	-4.9580	4.0950	-0.9176
C	2.1353	-3.4794	-2.5948
C	-2.1353	-3.4794	2.5948
C	2.1353	3.4794	2.5948
C	-2.1353	3.4794	-2.5948
C	2.7377	-2.9985	-1.6877
C	-2.7377	-2.9985	1.6877
C	2.7377	2.9985	1.6877
C	-2.7377	2.9985	-1.6877
C	0.2358	-5.4392	-1.8620
C	-0.2358	-5.4392	1.8620
C	0.2358	5.4392	1.8620
C	-0.2358	5.4392	-1.8620
C	1.9204	-0.6751	0.0435
C	-1.9204	-0.6751	-0.0435
C	1.9204	0.6751	-0.0435
C	-1.9204	0.6751	0.0435
C	0.0844	-5.5622	-0.6869
C	-0.0844	-5.5622	0.6869
C	0.0844	5.5622	0.6869
C	-0.0844	5.5622	-0.6869
C	0.5955	-1.2851	0.0193
C	-0.5955	-1.2851	-0.0193
C	0.5955	1.2851	-0.0193
C	-0.5955	1.2851	0.0193

CHAPTER 4: THE VERTICAL IONIZATION POTENTIAL OF Ti_8C_{12} AND THE REACTION OF TI(I) WITH ETHENE

A paper in preparation for submission to *The Journal of Chemical Physics*

Vassiliki-Alexandra Glezakou and Mark S. Gordon

Department of Chemistry, Iowa State University, Ames, IA 50011

Abstract

The geometries of T_d ($^5A_2$) and T_h ($^1A_{1g}$) of the neutral Ti_8C_{12} are evaluated at the ROHF/TZV+f level of theory and the vertical ionization of the ground state is compared to the available experimental data. Two different reaction channels of Ti (^{3}F) and Ti (^{5}F) with C_2H_4 are studied also at the same level of theory. Correlation is included in through MP2, MCSCF wavefunctions and coupled cluster techniques.

Introduction

The interaction of bare transition metal atoms with small hydrocarbons is very intimately related to homogeneous and heterogeneous catalytic processes, such as the hydrogenation of unsaturated hydrocarbons and polymerization of olefins[1]. For instance, Ti(IV) is the catalytic species in the well-known Ziegler-Natta polymerization, a process which produces more polyethylene than any other organic process[1a].

A common step in such processes is the C-H or C-C bond insertion of the metal centre and ultimately H_2 elimination[2-3]. Obviously, information on the reaction channels of metal atoms with small hydrocarbons can offer very useful insight for such important processes. Unfortunately, the available data, both experimental and theoretical, is scarce for the case of neutral atoms, especially of the first row transition metals.

There has been an abundance of studies performed on transition metal positive ions with hydrocarbons: experimental by Armentrout and co-workers[4], Bowers and co-workers[5a], Castleman and co-workers [5b], theoretical by Bauschlicher and co-workers[6]. Nonetheless, there are only a few papers on neutral atoms[7,8].

How can cations be so drastically different from the neutral atoms? Reactions with ions involve long-range ion-induced dipole forces, which result in highly attractive potential energy surfaces (PES)[2a,9,10]. The electronic configuration of the metal atom can have a dramatic influence on its reactivity towards the hydrocarbons. The interactions with neutral atoms have a much shorter range and the barriers are comparable to the available energies. The behaviour of the neutral atoms therefore is expected to be very sensitive to the topography of the PES[2a,10]. Also, because the interactions are of a shorter range, they are expected to resemble more closely those in the homogeneous catalysis[2a,10].

The formation of Metcars[11], M_8C_{12} clusters that were discovered by Castleman and co-workers in 1992, from the reaction of bare metal atoms with small hydrocarbons, is a closely related process. The structure and bonding of these clusters is very little understood, and of today, there is no uniform agreement as to what their structure is. There are several, well founded reasons why this is so. The isolation of pure samples is still a hard task; consequently, no definite spectroscopic measurements are available. Theoretical studies that

would adequately describe these systems are also very difficult to conduct. The application of correlation methods in combination with the appropriate size basis sets make such endeavors very hard, and all too often, simply impossible. Still, very early on a plethora of theoretical work[12-16] appeared in the literature, giving useful insights into the complicated nature of these systems.

The Ti_8C_{12} cluster is currently thought to be a closed cage structure, of T_d symmetry with a $^5A_2$ ground state. For a long time, it was debated, based on indirect experimental evidence[16], that the $^1A_{1g}$ state in T_h symmetry is the ground state. Dance[13b] presented an indirect but quite convincing argument that the latter is not even a minimum on the PES. Although not conclusive at this point, our calculations based on second derivatives of the energy tend to agree with this result. The first part of this paper presents calculations that verify this conclusion, making use of the second derivatives of the energy. Because of the recent successful experiments that measure the vertical ionization potential[17], we are also undertaking the task of a theoretical estimate of this value.

The second part of this study focuses on various reaction channels of the neutral Ti atom with ethene. Castleman and co-workers[11] also present evidence that the building blocks of the clusters are small Ti/C clusters, i.e. TiC_2, Ti_2C_2, and Ti_2C_3. In addition to the theoretical interest in understanding the interaction of Ti(I) with C_2H_4, our goal is also to investigate possible reaction channels that lead to the formation of TiC_2.

Computational details

The TZVP[18] (triple zeta valence plus polarization) basis set was selected for Ti, augmented by a set of f polarization functions (α_f=0.591)[19] for Ti. For C, the standard Pople 6-31(d)[20] basis was used.

This basis results in 676 basis functions for Ti_8C_{12} and 126 for Ti/C_2H_4. RHF and ROHF optimizations were performed for the $^1A_{1g}$, T_h and $^5A_2$, T_d structures. Second derivatives of the energy (Hessians) were calculated for the stationary points to determine whether they are minima or saddle points.

We also report preliminary results on the interaction of the ground state ^3F Ti atom, and the first excited state ^5F with C_2H_4. Two kinds of complexes are studied: the titana-cyclopropane complex, and the planar $HTiC_2H_3$, resulting from direct insertion of Ti into a C-H bond. From data available for Zr and Nb with C_2H_4[8b], it is likely that these complexes are species (minima) on the PES for the reaction:

$$M + C_2H_4 \rightarrow \rightarrow MC_2H_2 + H_2 \rightarrow \rightarrow MC_2 + H_2$$

All calculations were performed with the GAMESS[21] set of programs.

Results and discussion

I. Ti_8C_{12}

Figures 1 and 2a show the HF//TZV+P, 6-31G(d) geometries for the $^1A_{1g}$ (T_h) and $^5A_2$ (T_d) states of the Ti_8C_{12} cluster. As noted in the literature, the $^5A_2$ state is much more stable than the $^1A_{1g}$.

The cubic structure has essentially no M-M bonds, and the cluster is held together with the C_2-units. This arrangement involves 24 σ-type interactions between the Ti atoms and the C atoms. The tetra-capped tetrahedral structure T_d, is the result of a butterfly folding of the two opposite sides of the cube, and simultaneous rotation of the C_2-units by 45 degrees. An inner tetrahedron is formed (Ti^i atoms), whose sides are capped by the atoms of an outer one, (Ti^o). The C_2-units bridge the edges of the outer tetrahedron (head-on σ-type interactions), and interact sideways (side-on π-type interactions) with the inner tetrahedron. In this conformation, the cluster has a total of 36 interactions and is indeed expected to be more stable. These include 12 Ti^i-Ti^o interactions and 24 (12 head-on and 12 side-on) Ti-C interactions. The outer Ti atoms, Ti^o, are far enough so that they do not interact.

The energy difference between these structures is quite large, 658.3 kcal mol^{-1} at the HF level of theory, an even larger energy difference than that previously reported in the literature, 350.0 kcal mol^{-1} [12b]. Given the inadequacies of the HF method, this value may well change at the MP2 level (calculations in progress).

The quintet state was verified to be a minimun with numerical Hessians. We were unable to complete the corresponding calculations for the singlet state, as several of the displacements did not converge. This instability appears to agree with Dance's prediction[13a] that this state is not a well-defined species on the PES of Ti_8C_{12}.

Recent experimental data estimate the vertical excitation of Ti_8C_{12} to about 4.4 eV. In the quintet, the unpaired electrons occupy the orbitals:

$$\ldots a_1^1\ t_2^1\ t_2^1\ t_2^1$$

These are all dz^2-type combinations (Figure 2b), localized on the inner tetrahedron Ti^i atoms, with a_1 more stable, being a bonding interaction[12c]. Removal of one electron would result

into a partially occupied triply degenerate shell. Any attempt to average these 2 remaining electrons on the 3 orbitals in order to avoid Jahn-Teller distortions, leads to an unstable wavefunction that does not converge. Re-ordering of the orbitals and restricting them, to remove the electron from the singly degenerate orbital a_1, results in a more stable wavefunction. The ionization potential calculated in this manner, gives a value of 9.9 eV. No Hessians were computed for the cation, as the geometry of the cation was constrained to that of the neutral. This result is not reliable and a more refined wavefunction is needed.

An estimate of the first ionization potential can be inferred from Koopmans theorem. The orbital energies of the singly occupied shells are:

a_1 -0.1308 H=-3.6 eV

t_2 -0.0343 H=-0.93 eV

Bénard *et al.*[12c] report -4.16 and -1.55 eV for the corresponding orbital energies. These come from a CI expansion which correlates the 20 electrons that belong to the cluster. The energy difference between a_1 and t_2 orbital energies is ~ 2.6 eV from both calculations, since the reference wavefunction is single-determinant.

II. Ti(I) + C_2H_4

We also report some preliminary results on the interaction of Ti(I) with ethylene. First-row transition metals have filled 4s orbitals that are bigger than the 3d, and therefore exhibit noble-gas behaviour. The result is usually highly repulsive potential energy surfaces.

The simplest model for metal-ethylene bonding is the Dewar-Chatt-Duncanson (DCD) model[23], which involves two simultaneous interactions. The first is a sigma interaction involving transfer of electron density from the C=C π-orbital to the 4s of the

metal. Naturally, this is favoured for s^0 or s^1 occupancies. The other interaction is back-donation from the d-orbitals of the metal to the π^* of the ethylene. This is favoured by double occupancies of the d orbitals and dsp and dp hybridization. *Ab initio*[24] calculations indicate that sd hybridization of the metal centre facilitates bond formation in the DCD mechanism. According to Ritter, Carroll and Weisshaar (RCW)[7b], Sc, Ti and V have very similar reaction towards alkenes and oxidants[24]. The sd promotion does not require any change of spin and the sp promotion is relatively small, and it is expected that both hybridizations schemes will contribute. Kinetics experiments that follow the depletion of $Ti(^3F)$ and $Ti(^5F)$ by ethylene[7a], are in agreement with the RCW findings and indicate possibly reaction through intersystem crossing with the same spin (i.e. the ground term ^3F of Ti and the first excited ^3F term), and therefore with substantial barriers. Figure 3 is reproduced from ref.7a.

Table 1 and Figure 4 summarizes the results of ROHF//TZV+f, 6-31G(d) and single point MP2 calculations for the first three terms of Ti. The experimental terms for the first five terms of Ti(I) are include for comparison and evaluation of the basis set. At the MP2 level of theory, the triplet-quintet splitting is underestimated by ~ 30%. This basis set will be used for geometry optimizations, while a correlation consistent basis set will be used for the final refinement. Figures 5a-5c, show the relative energies of the $Ti\cdots C_2H_4$, $Ti\cdots C_2H_2$ and $Ti\cdots C_2$ complexes, for the triplet and quintet states, with respect to the various asymptotic limits. The appropriate number of H_2 molecules is included to scale the energies. For Ti, the unpaired electrons were averaged for the single-reference wavefunctions. Higher-level correlation calculations are imperative and are in progress. At the current level of theory we find:

(i) For the triplet state complex $Ti^{\cdots}C_2H_4$ at least two minima were found. At the Hartree-Fock level of theory, addition of Ti is endothermic by ~ 29.0 and 33.0 kcal mol^{-1} respectively. $Ti^{\cdots}C_2H_2$ is slightly unbound with respect to $Ti(^3F)$ and C_2H_2. At the MP2 level, both $^3A_1$ and $^3B_1$ states of $Ti^{\cdots}C_2H_4$ the are slightly bound, by ~1.0 kcal mol^{-1}. $Ti^{\cdots}C_2H_2$ is considerably bound (19.4 kcal mol^{-1}), which agrees with observations that addition of metal atoms in general to C_2H_2 is much easier[7a,b] than to C_2H_4 and more so than C_2H_6. The dehydrogenation of TiC_2H_4 and TiC_2H_2 is predicted to be exothermic in ref. 7a (estimated -19 kcal mol^{-1} for the first reaction, no estimate available for the second). Although the dehydrogenation reaction predicted here is endothermic even at the MP2 level, inclusion of correlation moves the heat of the reaction in the direction inferred form the experiment.

(ii) The quintet state complex, $^5A_2$, is bound with respect to the quintet asymptotic limit for both HF and MP2 levels of theory. Depletion of Ti (^5F) by C_2H_2 is exothermic for both HF and MP2 (Figure 3c, also in reference 7a).

References

1. (a)Anderson, J. R.; Boudart, M. *Catalysis: Science and Technology*; Springer-Verlag: Berlin, **1984**; *Vol. 6*, Chapter 1. (b) Mathey, F.; Sevin, A. *Molecular Chemistry of the Transition Metal Elements*; John Wiley and sons: NY, **1996**;p. 189.
2. (a) Carroll, J. J.; Weisshaar, J. C. *J. Phys. Chem.* **1996**, *100*, 12355. (b) Carroll, J. J.; Weisshaar, J. C.; Siegbahn, P. E. M.; Wittborn, C. A. M.; Blomberg, M. R. A. *J. Phys. Chem.* **1995**, *99*, 14388. (c) Carroll, J. J.; Hauge, K.L; Weisshaar, J. C.; Blomberg, M. R.A.; Siegbahn, P. E. M.; Svensson, M. *J. Phys. Chem.* **1995**, *99*, 13955.

3. (a) Wen, Y.; Perembski, M.; Ferret, T. A.; Weisshaar, J. C. *J. Phys. Chem. A.* **1998**, *102*, 8362.

4. (a) Armentrout, P.B.; Kickel, B. L. *Organometallic Ion chemistry*; Freiser, B. S., Ed.: Kluwer Academic Publishers: Dordrecht, **1996**; p. 1. (b) Armentrout, P. B. (1) *Annu. Rev. Phys. Chem.* **1990**, *41*, 313. (2) *Polyhedron* **1988**, *7*, 1573. (3) *Science*, **1991**, *251*, 175. (c) Georgiadis, R.; Armentrout, P. B. *J. Phys. Chem.* **1988**, *92*, 7060.

5. (a) Gidden, J.; van Koppen, P. A. M.; Bowers, M. T. *J. Am. Chem. Soc.* **1997**, *119*, 3935. (b) Guo, B.C.; Kerns, K.P.; Castleman, Jr., A. W. *J. Phys. Chem.* **1992**, *96*, 4879.

6. Sodupe, M.; Bauschlicher, Jr., C. W.; Langhoff, S. R.; Partridge, H. *J. Chem. Phys.* **1992**, *96*, 2118.

7. (a) Senba, K.; Matsui, R.; Honma, K. *J. Phys. Chem.* **1995**, *99*, 13992. (b) Ritter, D.; Carroll, J. J.; Weisshaar, J. C. *J. Phys. Chem.* **1992**, *96*, 10636. (c) Lee, Y. K.; Manceron, L.; Pápai, I. J. *Phys. Chem. A.* **1997**, *101*, 9650.

8. (a) Willis, P. A.; Stauffer, H. U.; Hinrichs, R. Z. Davis, H. F. J. Phys. Chem. A. 1999, 103, 3706. (b) Stauffer, H. U.; Hinrichs, R. Z.; Willis, P. A.; Davis, H. F. J. Chem. 1999, 111, 4101

9. (a) Weisshaar, J. C. *Adv. Chem. Phys.* **1992**, *82*, 213. (b) Weisshaar, J. C. *Acc. Chem. Res.* **1993**, *26*, 213.

10. Carroll, J. J.; Hauge, K. L.; Weisshaar, J. C. *J. Am. Chem. Soc.* **1993**, *115*, 6962.

11. Castleman, Jr., W. A.; Bowen, K. H. *J. Phys. Chem.* **1996**, *100*, 12911, and references therein.

12. (a) Rohmer, M.-M.; de Vaal, P.; Bénard, M. J. Am. Chem. Soc. 1992, 114, 9696. (b) Rohmer, M.-M.; Bénard, M.; Henriet, C.; Bo, C.; Poblet, J.-M. *J. Chem. Soc., Chem.*

Commun. **1993**, 1182. (c) Bénard, M.; Rohmer, M.-M.; Poblet, J.-M.; Bo, C. *J. Phys. Chem.* **1995**, *99*, 16913. (d) Rohmer, M.-M.; Bénard, M.; Bo, C.; Poblet, J.-M. *J. Am. Chem. Soc.* **1995**, *117*, 508.

13. (a) Dance, I. *J. Chem. Soc. Chem. Commun.* **1992**, 1779. (b) Dance, I. *J. Am. Chem. Soc.* **1996**, *118*, 6309.

14. (a) Hay, P. J. *J. Phys. Chem.* **1993**, *97*, 3081. (b) Lin, Z.; Hall, M. B. *J. Am. Chem. Soc.* **1993**, *115*, 11165.

15. Srinivas, G. N.; Srinivas, H.; Jemmis, E. D. *Proc. Indian Acad. Sci. (Chem Sci.)* **1994**, *106*, 169. (b) Reddy, B. V.; Khanna, S. N. *J. Phys. Chem.* **1994**, *98*, 9446. (c) Khan, A. *J. Phys. Chem.* **1995**, *99*, 4923.

16. (a) Guo, B. C.; Kerns, K. P.; Castleman, Jr., A. W. *Science* **1992**, *255*, 1411. (b) Kerns, K. P.; Guo, B. C.; Deng, H. T.; Castleman, Jr., A. W. *J. Am. Chem. Soc.* **1995**, *117*, 4026. (c) Deng, H. T.; Kerns, K. P.; Castleman, Jr., A. W. *J. Am. Chem. Soc.* **1996**, *118*, 446.

17. Kooi, S. E.; Castleman, Jr., A. W. *J. Chem. Phys.* **1998**, *108*, 8864, and references therein.

18. (a) TZV for Li-Ne, Dunning, T.H. *J. Chem. Phys.* **1971**, *55*, 716. (b) TZV for Na-Ar, McLean, A.D; Chandler, G.S. *J.Chem.Phys.* **1980**, *72*, 5639. (c) TZV for Sc-Zn (from HONDO 7.0), Wachter, A.J.H. *J. Chem. Phys.* **1970**, *52*, 1033. This is basically Wachter's basis (14s9p5d) extended to triple zeta quality by using (6d) contracted to [411] according to Rappé, A.K.; Smedley, T.A.; Goddard, W.A., III, *J. Phys. Chem.* **1981**, *85*, 2607. Also, the most diffuse s (α_s=0.0333) was substituted by an s with α_s=0.2090 to better describe the 3s-4s region, while another two p were added

(α_p=0.1506 and α_p=0.0611) to acount for a 4p. (d) Single-polarization d-functions for C and Si from HONDO 7.0, α_d=0.720 and α_d=0.388 respectively.

19. Glezakou, V.-A.; Gordon, M. S. *J. Phys. Chem. A.* **1997**, *101*, 8714.

20. Hehre, W. J.; Ditchfield, R.; Pople, J. A. *J. Chem. Phys.* **1972**, *56*, 2257.

21. **GAMESS**, Schmidt, M.W.; Baldridge, K.K.; Boatz, J.A.; Elbert, S.T.; Gordon, M.S.; Jensen, J.H.; Koseki, S.; Matsunaga, N.; Nguyen, K.A.; Su, S.J.; Windus, T.L.; Dupuis, M.; Montogomery,J.A. *J. Comput. Chem.* **1993**, *14*, 1347.

22. (a) Chatt, J.; Duncanson, L. A. *J. Chem. Soc.* **1953**, 2939. (b) Dewar, M. J. S. *Bull. Soc. Chim. Fr.* **1951**, 79.

23. (a) Widmark, P.; Roos, B. O.; Siegbahn, P. E. M. *J. Phys. Chem.* **1985**, *89*, 2180. (b) Pierloot, K.; Persson, B. J.; Roos, B. O. J. *Phys. Chem.* **1995**, *99*, 3465.

24. Ritter, D.; Weisshaar, J. C. *J. Phys. Chem.* **1990**, *94*, 4907.

25. Moore, C. E. *Atomic Energy Levels*, **1949**, Circular of the National Bureau of Standards 467.

Table 1: Ti terms, C_2H_4 and asymptotic limits.

Species	Term	HF	MCQDPT
	^1D	-848.341767	-848.392566
Ti[a]	^3F	-848.389135	-848.432380
	^5F	-848.369583	-848.410760
H_2		-1.132627	-1.159851
C_2H_2	singlet	-76.847985	-77.114057
C_2H_4		-78.061763	-78.344978[c]
	^1D	-926.403530	-926.737544
Ti+C_2H_4	^3F	-926.450898	-926.777358
	^5F	-926.431346	-926.755738
Ti-||-C_2H_4[b]	triplet	-926.450898	-926.782157

[a]For Ti, the 2-d electrons were state-averaged in the 5d-orbitals of each term. [b]Calculation on the complex at "infinity" (~30. Å). [c]This number corresponds to MP2.

Figure captions

Figure 1. RHF//TZV+f,6-31G(d) geometry of Ti_8C_{12}, $^1A_{1g}$ (T_h). Bond distances in Å, angles in degrees. Ti atoms are at the corners of the cube.

Figure 2a. ROHF//TZV+f,6-31G(d) geometry of Ti_8C_{12}, $^5A_2$ (T_d). Bond distances in Å, angles in degrees.

Figure 2b. Localized orbitals on Ti^{i}'s.

Figure 3. Schematic representation of the interaction of Ti(I) with C_2H_4.

Figure 4. Comparison of experimental data for the first few terms of Ti(I) (ref. 25) with the calculated values. Energy differences in kcal mol^{-1}.

Figure 5a. Hartree-Fock relative energies of the triplet states, with respect to the asymptotic limits as shown. Quintet states included for comparison.

Figure 5b. Same as Figure 5a, but for MP2 results.

Figure 5c. HF and MP2 relative energies, for the quintet states.

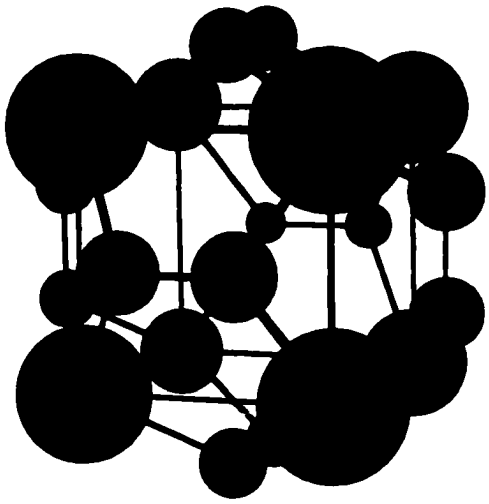

Ti_8C_{12}, $^1A_{1g}$ (T_h), RHF//TZV+f, 6-31G(d)

Ti-Ti	3.142
Ti-C	1.997
C-C	1.424
CCTi	115.5
TiCTi	103.8

Figure 1

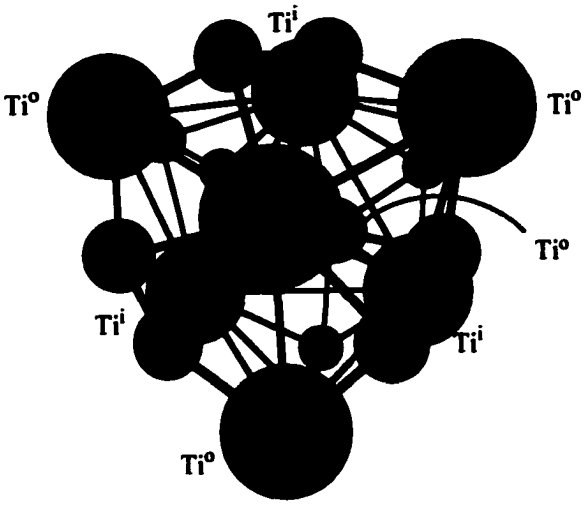

Ti_8C_{12}, $^5A_2$ (T_d), ROHF//TZV+f, 6-31G(d)

Ti^i-Ti^i	3.135
Ti^o-Ti^o	4.845
Ti^i-Ti^o	2.948
C-C	1.327
C-Ti^i	2.258
C-Ti^o	1.967
$Ti^oTi^iTi^o$	110.5
Ti^oCTi^i	88.2
CTi^iC	34.2
CTi^oC	99.5

Figure 2a

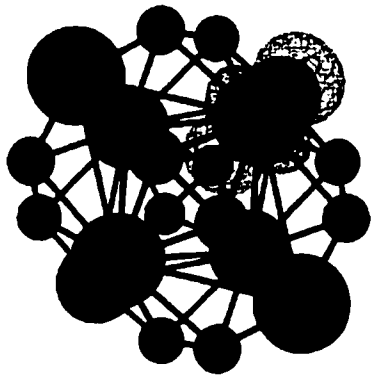

a_1

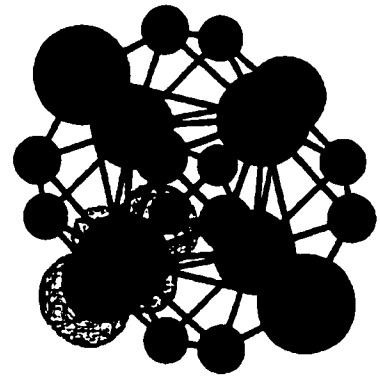

t_2

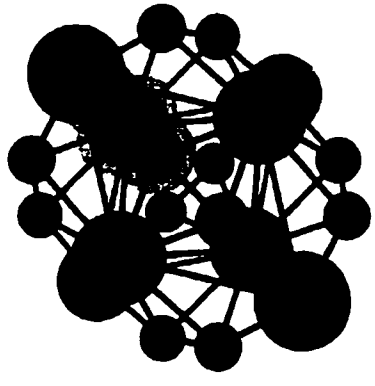

t_2

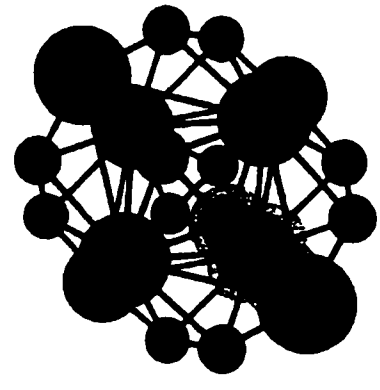

t_2

Figure 2b

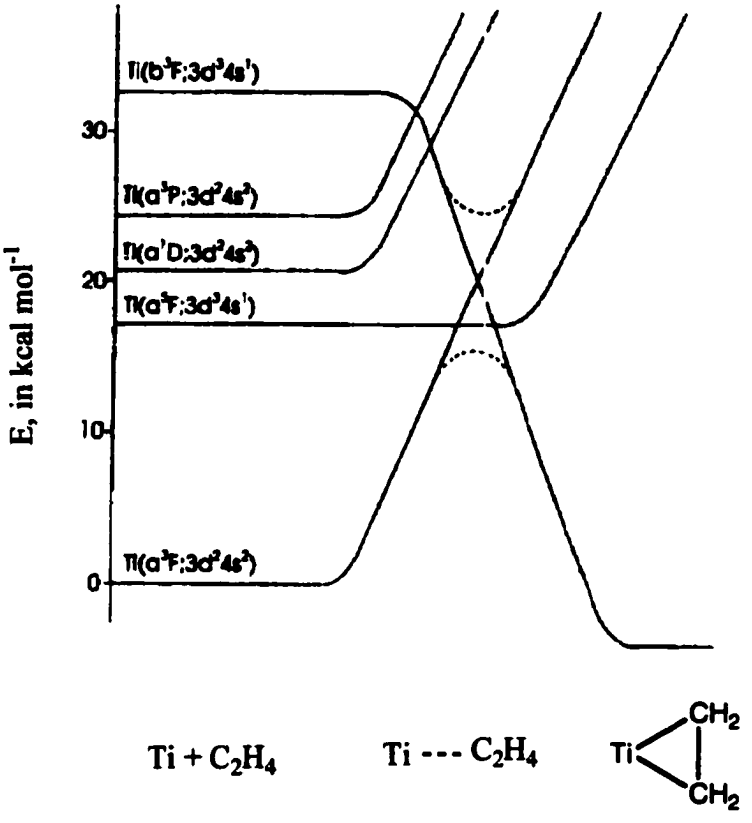

Figure 3

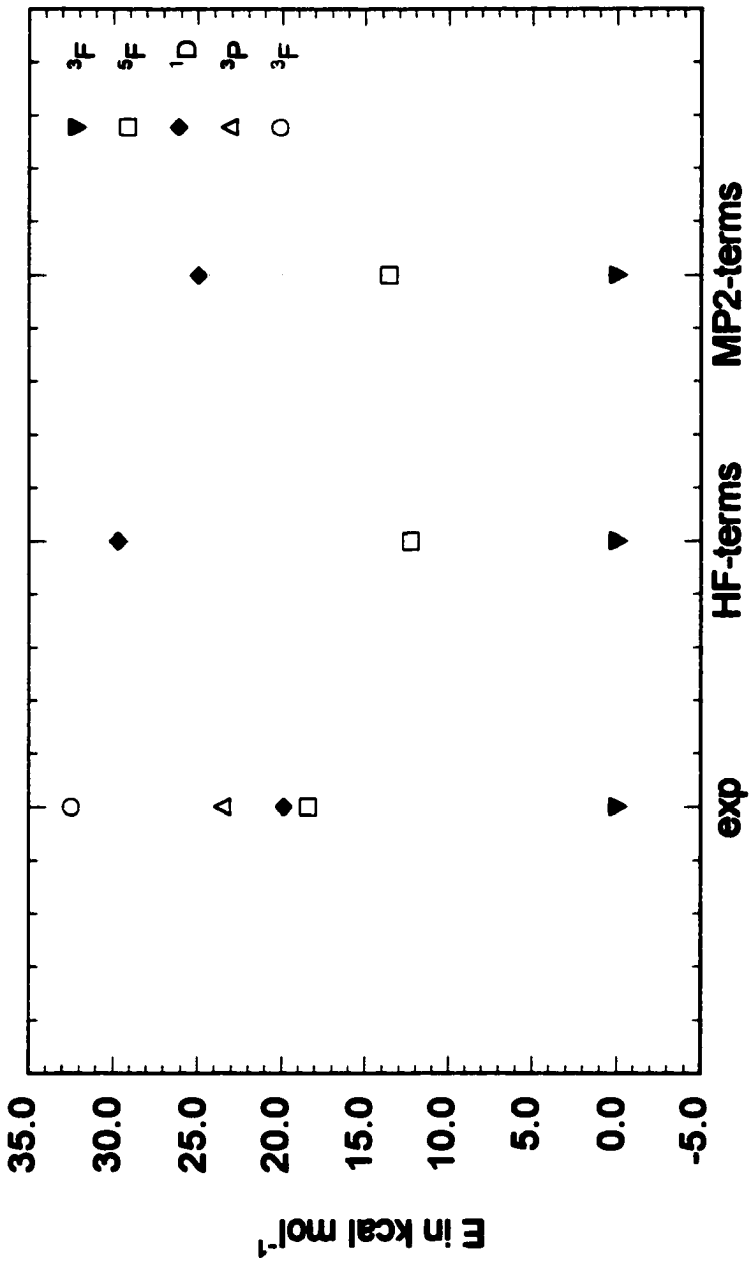

Figure 4

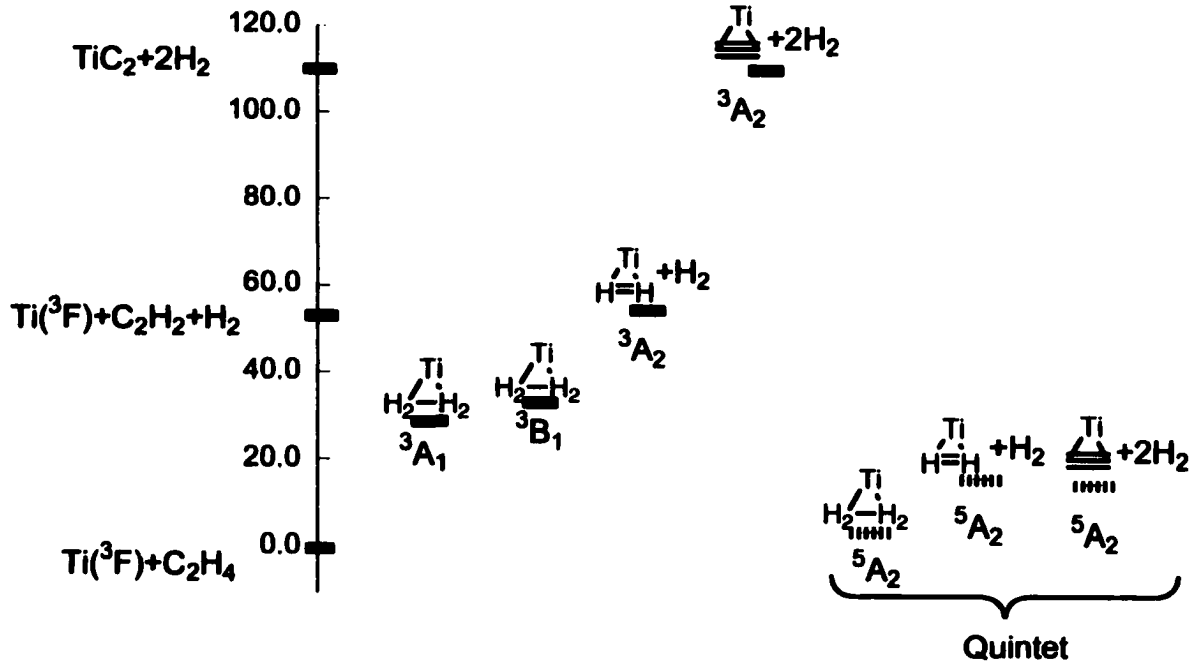

Figure 5a

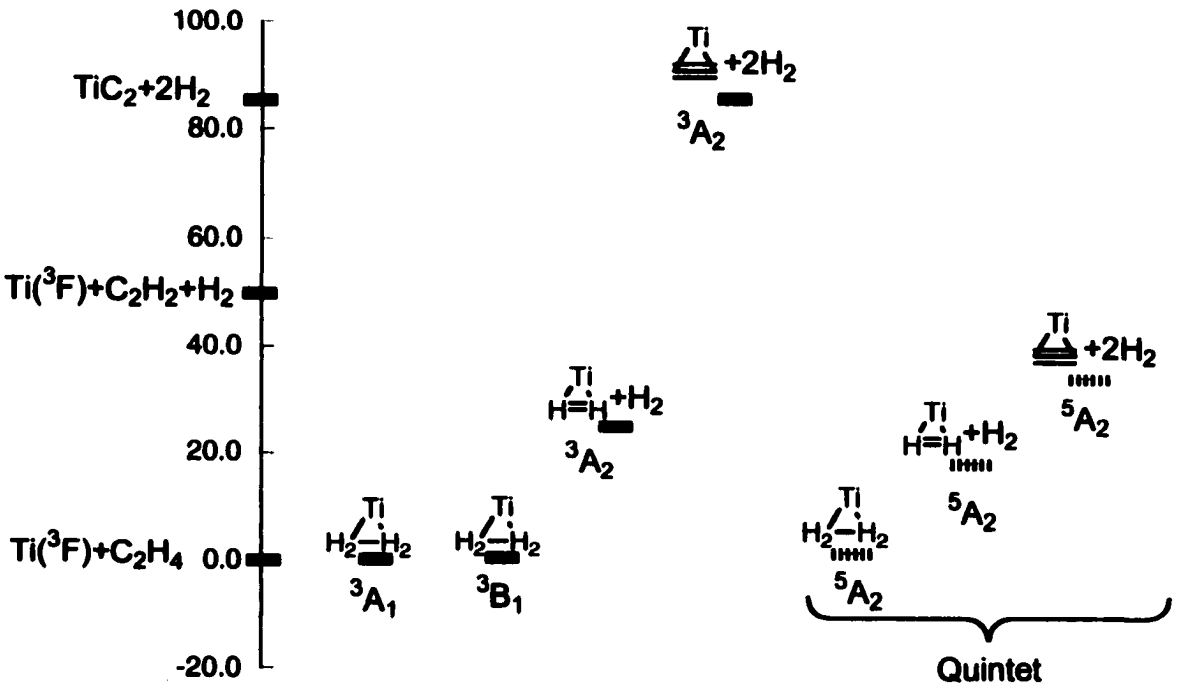

Figure 5b

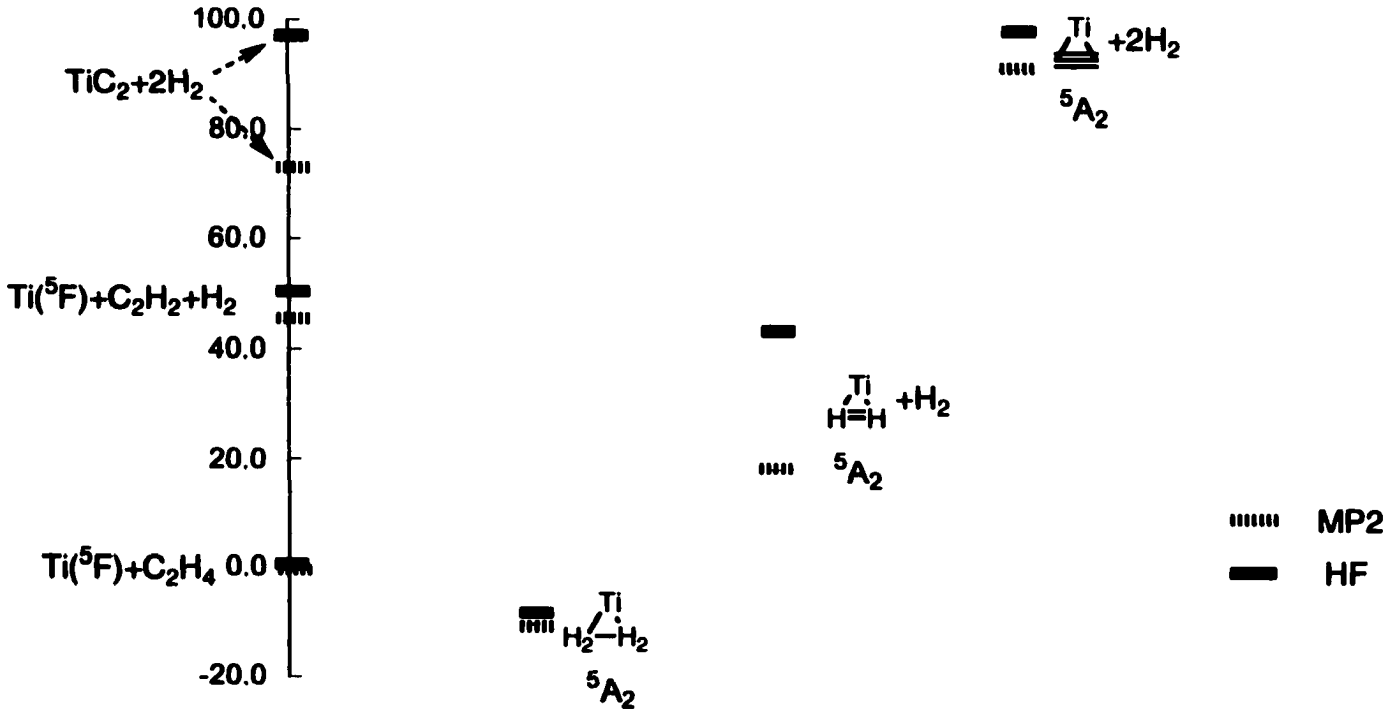

Figure 5c

CHAPTER 5: AN *AB INITIO* STUDY OF TWO REACTION CHANNELS OF B/H_2 AND THE EFFECT OF SURFACE CROSSING IN ITS ROLE AS A POTENTIAL HIGH ENERGY MATERIAL

A paper to be submitted for publication to the *Journal of Chemical Physics*

Vassiliki-Alexandra Glezakou and Mark S. Gordon

Department of Chemistry, Iowa State University, Ames IA 5001

David R. Yarkony

Department of Chemistry, The Johns Hopkins University, Baltimore, MD 21218

Abstract

In this work, we present the first *ab initio* study of the first two potential energy surfaces of atomic boron, with molecular hydrogen. Investigation of the two limiting insertion channels of boron into H_2, shows that the weak van der Waals complex crosses over to the molecular, strongly-bound region through a conical intersection that involves the first two (1A', 2A', C_s) states of the B/H_2 system. Light atoms react very exothermically with oxygen, consequently, they have been suggested as loosely-bound dopants in H_2-solid matrices as a means to store energy and improve the performance of H_2 as a fuel.

Introduction

The idea of doping H_2-cryogenic matrices is quite old, dating back to the 1950's when it was observed that energy associated with atomic recombination is much greater than the net energy difference resulting from bond energy changes in chemical reactions[1].

Atomic recombination is in general an exoergic process that increases the ratio of energy/unit volume of fuel, since atoms are lighter than their compounds. The issue of the fuel mass that a space-vehicle has to accommodate during the first stages is one of the most fundamental problems that need to be addressed for any space mission.

A number of low-mass elements have been evaluated as potential dopants[2] of cryogenic matrices (Li[3], Be[4], B[5], C[6], Al[7], Mg[8]), since their heats of oxidation are much larger than that of molecular hydrogen. Larger exoergicity can potentially result in a much larger specific impulse, I_{sp} , the most common performance gauge for rocket fuels[3]. The specific impulse is proportional to the quantity $[\Delta H_{rxn}/m]^{1/2}$, where ΔH_{rxn} is the heat of the reaction and m the mass of the products. All of the aforementioned metals tend to increase the Isp with respect to liquid H_2/liquid O_2, with boron being one of the best candidates[9]. The fact that boron is one of the lighter elements and does not create toxic products as in the case of Li and Be, makes it even more attractive. Recent experiments by Fajardo *et al.*[10a] show that co-deposition of B into a cryogenic matrix is not very efficient. This group is currently working on new, more promising methods of doping[10a,b].

The energetic material for the systems of interest here is the weak van der Waals complex B--H_2 with a D_e on the order of 10^2 wavenumbers. In this form, the process of oxidation of the metal does not have to overcome the strong binding energy of the diatom or that of the dihydride BH_2. In the literature, one can find a large number of theoretical as well

as experimental papers on these systems[5]. Alexander and Dagdigian in particular have reported on the stability of the van der Waals complex B--H_2[5b,d], found to be kinetically stable.

These complexes, apart from their great theoretical interst, have been proven to be computational challenges, as well. The location and determination of such weak complexes demands high level *ab initio* calculations with particular emphasis on the treatment of correlation and the size-consistency of the method. Furthermore, the existence of conical intersections and intersecting seams, and therefore the non-adiabatic character of the surfaces, plays a most important role in the understanding of the dynamics. For example, the photodissociation of water at 121.6 nm is a result of interference between two different surfaces that give the same product, OH +H[11a]. Likewise, the photodissociation of ammonia to H+ NH_2 is another example of diabatic behaviour[11b]. The subject of interstate crossing in triatomics is quite intriguing, and as shown in many different cases, seams (the *locus* of intersecting surfaces) although accidental, are symmetry allowed[12]. Small energy differences near a conical intersection may change the results of an adiabatic treatment[13-15]. In such instances, a non-adiabatic treatment beyond the Born-Oppenheimer approximation is necessary.

A good energetic material should be separated by a large barrier (~25 kcal mol^{-1}) from any other stable forms, such as the dihydride in this case, see Figure 1. The existence of a surface crossing may lower the barrier and lead to pre-dissociation. This aspect has been discussed recently for both Al and B complexes with H_2[5a,7].

In this paper, the two lowest-energy surfaces of the system B/H_2 are exploited with full optimized reaction space (FORS) multireference configuration interaction (MRCI)

wavefunctions, in order to characterize the important species and calculate the energetics on this potential energy surface. It is expected that an extensive characterization of the relevant potential energy surfaces will provide some impetus for future dynamics studies of this system. Indeed, in a recent paper[16] Niday and Weeks perform a dynamical treatment of this system based on the movement of a wave-packet on a potential surface constructed from ab initio data.

Reaction channels of B with H_2

There are two limiting reaction channels, one with T-shaped geometry (R1) and one that is linear (R2):

(R1) $B(^2P) + H_2 \rightarrow B\cdots H_2(1^2A_1, 2^2B_2) \rightarrow B\langle^{H}_{H}(X^2A_1)$

(R2) $B(^2P) + H_2 \rightarrow B\cdots H - H(^2A_1) \rightarrow BH(X^1\Sigma^+) + H$

In the first reaction, the section of the $1^2A'$ (1^2A_1) state in the van der Waals region, is repulsive and has a very high barrier for entrance into the molecular region. The crossing of this surface by the $2^2A'$ ($^2B_2$) state, is very critical for the stability of the van der Waals complex, as it lowers the aforementioned barrier by almost a factor of five. This second surface is where low energy pathways to the molecular region start, since it is very "flat" with a small well in the van der Waals region, see Figure 2. Similar behaviour has been observed for Al-H_2[7].

In a previous work[17], the two seams, one of C_{2V} and one of C_S symmetry have been located with the help of a numerical procedure[18]. Rüdenberg and co-workers[14], and Yarkony[18] have shown in practice that surface crossings in poly-atomics do exist not as isolated and accidental features, but rather as continuous seams.

Methods and computational considerations

The current investigation will determine the adiabatic surfaces for reactions R1 and R2 and the molecular and van der Waals and transition species. Such a task requires a reliable, flexible reference space that will ensure the correct dissociation channels and an appropriate treatment of the correlation energy. A fully optimized reaction space (FORS)[19], also referred to as complete active space self-consistent field (CAS-SCF)[20]. All six valence orbitals (three 2p on boron and σ and σ^* of H_2) and five valence electrons are included in the FORS wavefunction. Dynamic correlation is introduced with a multi-reference configuration interaction in which all single and double excitations from this FORS reference space into the virtual space are included, referred to as MR(SD)-CI in the contracted scheme of Werner and Knowles[21,22].

For reaction (R1) the FORS (5/6) space yields a total of 115 configuration state functions (CSF's) in C_S symmetry, and 59 ($^2A_1$) and 56 ($^2B_2$) in C_{2V}. With the use of symmetry, the MR(SD)-CI space spans ~103 000 configurations in the contracted scheme (408 000 uncontracted) in C_S and ~52 000 (204 000) in C_{2V}.

The augmented correlation consistent valence triple zeta (aug-cc-pVTZ) basis set[23] was used, which has been shown to give reliable results even in the absence of BSSE correction. The aug-cc-pVTZ basis for H and B consists of the generalized contractions[24]:

H: (6s 3p, 2d) → [4s, 3p, 2d]

B: (11s, 6p, 3d, 2f) → [5s, 4p, 3d, 2f]

resulting in a total number of 105 Cartesian basis functions.

The C_{2V} adiabatic surfaces, $^2A_1$ and $^2B_2$, were computed to locate the C_{2V} seam. The same procedure was followed for the $1^2A'$ and $2^2A'$ states that emerge for deviations from the

T-shaped geometry in order to analyze the C_S portion. The two surfaces give rise to two different, continuous seams that result in a trifurcation, since the C_{2V} symmetry can be broken in two directions. The van der Waals minima, transition states and two minimum-energy crossing points (MECP's) were located using grids, due to the lack of MRCI second derivatives with respect to the energy (Hessians). A short algorithm was written to transform from Jacobi coordinates to internal coordinates and then calculate the second derivatives of fitted second order polynomials for the areas of interest.

For the linear channel (R2), the reference space for the $^2\Sigma$ state includes 64 CSF's and ~55 000 contracted (211 000 uncontracted) configurations in the MR-CI (SD). For the $^2\Pi$ state there are 51 CSF's and ~52 000 (186 000) configurations, respectively.

The potential energy surfaces are expressed in terms of the Jacobi coordinates. These correspond to R,the distance of B from the mid-point of the H-H bond, r, the H-H bond distance, and γ, the angle between R and r, as shown in Figure 3.

All calculations were done using MOLPRO[25] and GAMESS[26].

Reaction channel (R1)

Figure 4a shows the splitting of the ^2P term of boron into $^2A_1$, $^2B_1$ and $^2B_2$ states as boron starts interacting with the hydrogen molecule. The H_2 distance was kept constant at the MR(SD)-CI equilibrium geometry in the preliminary investigation of the van der Waals complexes. Subsequently, both distances were relaxed within a very fine grid in order to determine the van der Waals minima and the transition states. The $^2A_1$ state is clearly repulsive, as it places the single electron in the orbital pointing directly towards the H_2 sigma bond (Figure 4b). Both $^2B_1$ and $^2B_2$ states form van der Waals complexes, $^2B_2$ being lower. The $^2B_2$

state has a single electron in the orbital parallel to the H_2 sigma bond, facilitating the interaction with the empty sigma antibonding (σ^*) H_2 orbital. In the $^2B_1$ state, the singly occupied orbital is perpendicular to the molecular plane; therefore the interaction, not surprisingly, is less strong.

The $^2A_1$ ($1a_1^2\ 2a_1^2\ 3a_1^2\ 4a_1^1$, at infinite separation) state correlates with the molecular dihydride species, BH_2, with the ground-state configuration of ($1a_1^2\ 2a_1^2\ 3b_2^2\ 4a_1^1$), and makes obvious the necessity for a flexible reference wavefunction. The C_{2V} path is symmetry forbidden and a high barrier is expected. The dyhidride region is indeed reached *via* a high barrier of 3.35 eV with respect to the asymptotic limit, see Figure 2. In the transition state the H-H bond is considerably stretched by ~23%. The transition state was located with a tight grid of points with increments of 0.01 bohr and a two-variable polynomial fit of a subset of these points. The transition geometry occurs at (R=1.551Å, r=0.9089Å, γ=90.°).

Figure 5 shows the contour plots of the transition area and the markers indicate the minimum energy path.

The dihydride minimum occurs at (R=2.147Å, r=0.5131Å, γ=90°). The B-H bond is 1.190Å and the ∢HBH angle is 128.9° (exp 131° from ref 28). The binding energy of the molecule with respect to the asymptotic limit is 2.55 eV.

Figure 6 shows the combined 2D (contour plot) surfaces of the $^2A_1$ and $^2B_2$ states. In general, two hypersurfaces of the same symmetry in the space of dimension Q, intersect along a hyperline of dimensionality (Q-2), and in the case of B/H_2 this is 3-2=1. Therefore, the two surfaces meet along a continuous line of dimension one, which is denoted as the seam of C_{2V} symmetry. As a result of this surface crossing, a number of lower energy pathways are now accessible to the van der Waals complex that can reach the molecular,

energetically favourable region without having to cross over the high barrier. The lowest energy crossing point along this seam (minimum energy crossing point, MECP1) lies only .56 eV higher than the asymptotic limit and at the geometry of (R=1.190Å, r=1.162Å, γ=90.°), Figure 2.

The second seam was located, this time by varying all three independent coordinates R,r and γ. Reducing the symmetry from C_{2V} to C_S reduces both $^2A_1$ and $^2B_2$ states to $^2A'$ (C_S). For each value of γ, the two same-symmetry states touch at one point only and the locus of these conical intersections for a smooth variation of the angle γ, forms another seam, this time of C_S symmetry. The two different symmetry seams intersect at one point, with γ=90.0° resulting in a trifurcation of the C_{2V} seam, since the symmetry can be broken left or right. This point is called a doubly diabolical point (DD)[18a], the common point of the *loci* of diabolical points (seams)[27]. This point lies 1.15 eV higher than the asymptotic limit and .58 eV higher than MECP1 (C_{2V} seam). The point of lowest energy on the C_S seam (MECP2), occurs at (R=1.372Å, r=1.686, γ=65.0°) and lies 0.50 eV higher than the MECP1 (Figure 7).

Tables 1 and 2 summarize the geometries and energetics for reaction channel (R1). The results of Table 1 have been determined with single-state wavefunctions. In Table 2, MECP2 and DD were determined by state-averaged wavefunctions to avoid root-flipping.

Reaction channel (R2)

The second limiting reaction channel is the linear one, which leads to abstraction of one H by B to form BH and H. In this channel, the B ^2P term splits into $^2\Sigma$ and $^2\Pi$ states.

Both states form van der Waals species, as shown in Figure 8a. Figure 8b gives a schematic representation of these weak interactions.

The products of reaction channel 2 correlate with the $^2\Sigma$ state, which is accessed by a transition state of about 1.2 eV with respect to the asymptotic limit (Figure 9a). Figure 9b shows the contour maps of the region between the transition state and the BH+H dissociation channel. The transition state occurs at the geometry of (BH=1.327 Å, HH=1.270Å) with a barrier of 1.207 eV from the asymptotic limit. This reaction is highly endoergic; the calculated endoergicity of 1.066 eV compares very well with the experimental values of 1.075 eV[28] and 1.084 eV[5f]. Table 3 summarizes the results for this reaction channel. As in previous cases, the minima and transition state are determined with a quadratic fit of the MR(SD)-CI calculated points.

Discussion

This work presents a detailed mapping of the first two adiabatic states of B/H_2 for two limiting reaction channels, at the FORS/MR(SD)-CI level of theory. The geometries and energies relative to the asymptotic limit were calculated with tight grids and fitted to quadratic polynomials of two and three variables, and subsequently used to calculate numerical Hessians and vibrational frequencies. The role of this system as a potential high energy material is discussed in relation to the results.

The ground state of Boron gives rise to a triplet of states in C_{2V} symmetry. Two of them ($^2B_1$ and $^2B_2$) form weak van der Waals minima. The remaining state ($^2A_1$) connects the asymptotic limit with the molecular dihydride region, over a high barrier of 3.38 eV. Because

the $^2A_1$ and $^2B_2$ states cross, as for Al/H_2, the effective barrier is decreased by a factor of five, a much more dramatic change than in Al.

There are two seams available to the B/H_2 system. One of these seams maintains C_{2V} symmetry, while the other breaks symmetry in the direction perpendicular to the C_{2V} ridge. There is a point of lowest energy on each one of these seams.

In Figure 10 is a representation of the two seams in the 3-dimensional space of the triatomic. The X-axis represents the H-H distance (r),Y-axis the B to H_2-midpoint distance and Z the angle γ. The two points marked MECP1 and MECP2 are the lowest energy crossing points on their respective seams, C_{2V} and C_S. MECP2 is higher than MECP1 by 0.47 eV (Figure 7). The point where the two seams cross is noted as DD (doubly diabolical) and lies ~0.60 eV higher than the first MECP1 (Figure 7). This region is expected to have important diabatic effects.

The importance of B/H_2 as a HEDM system relies on the longevity of the van der Waals complex. The interstate crossing reduces the barrier to the molecular region from 65.9 to 12.0 kcal mol^{-1}.

The second reaction channel leads to H abstraction to form BH and H. This channel is highly endoergic, with a relatively high barrier of 1.17 eV, only 3.3 kcal mol^{-1} higher than the products. Related experiments support that such thresholds are accessible, but the high endoergicity of the reaction is in general a favourable result: BH is also likely to increase the efficiency (Isp)[3] of the potential fuel.

Although the lowest possible energy crossing point is only 12.0 kcal mol^{-1}, a range of angles other than 94° will be also available to the system, and consequently other energy

pathways, like the linear channel, may be important. In this case, B/H_2 can be yet a promising reagent.

Conclusions

A complete investigation of the first two adiabatic states of the B/H_2 system that are crucial for its use as rocket fuel were mapped with high-level *ab initio* calculations. The global, fully optimized minima for the dihydride and the van der Waals complexes at the MR(SD)-CI level were computed. The structures were verified with numerical Hessians. With the same procedures, two transition states were found, one symmetry-allowed on the $^2A_1$ surface of the C_{2V} reaction channel, and one very similar to the MECP1, resulting from the relaxation of all three coordinates. This study complements the work presented in reference 9.

Acknowledgements

This collaboration was made possible through the AFOSR program in high energy density materials, grant No F49620-96-1-0017 to DRY and grant No F49620-95-1-0077 to MSG and V-AG.

References

1. A.T. Pritt, Jr., *et al* in *"Proceedings of the High Energy Density Matter (HEDM) Conference"*, p.245 and references therein, March 1989, New Orleans LA, Eds T.G. Wiley, R.A. van Opijnen.

2. (a) Fajardo, M. E. J. *Chem. Phys.* **1993**, *98*,110. (b) Fajardo, M. E.; Tam, S.; Thompson, T. L.; Cordonnier, M. E. *Chem. Phys.* **1994**, *189*, 351.

3. (a) Wagner, A. F.; Wahl, A. C.; Karo, A. M.; Krejei, R. *J Chem. Phys.* **1987**, *69*, 7356. (b) Hobza, P.; von R. Schleyer, P. *Chem. Phys. Lett.* **1984**,*105*, 830. (c) García-Pietro, J.; Feng, W. L.; Novaro, O. *Chem. Phys. Lett.* **1984**, *105*, 830. (d) Toyama, M.; Uchide, T.; Yasuda, T.; Kasai,T.; Matsumoto, S. *Bull. Chem. Soc. Jpn.* **1989**, *62*, 2781.

4. Kellö, V.; Sadlej, A. J. *Theor. Chim. Acta,* **1992**, *81*, 417.

5. (a) Chaban, G.; Gordon, M. S. J. *Phys. Chem.* **1996**, *100*, 95. (b) Xin, Y.; Hwang, E.; Dagdigian, P. J. *J. Chem. Phys.* **1996**, *104*, 8165. (c) Bauschlicher, C. W. Jr. *Chem. Phys. Lett.* **1996**, *261*, 637. (d) Xin, Y.; Hwang, E.; Alexander, M. H.; Dagdigian, P. J. *J. Chem. Phys.* **1995**, *103*, 7966. (e) Alexander, M. H.; Yang, M. *J. Chem. Phys.* **1995**, *103*, 7956. (f) Tague, T. J.; Andrews, L. *J. Am. Chem. Soc.* **1994**, *116*, 4970. (g) Alexander, M. H. *J. Chem. Phys.* **1993**, *99*, 6014. (h) Knight, L. B. Jr.; Wiminski, M.; Miller, P.; Arrington, C. A.; Feller, D. *J. Chem. Phys.* **1989**, *91*, 4468.

6. (a) Yarkony, D. R. *J. Chem. Phys.* **1998**, *109*, 7047. (b) Matsunaga, N.; Yarkony, D. R. *J. Chem. Phys.* **1997**, *107*, 7825.

7. Chaban, G.; Gordon, M. S.; Yarkony, D. R. *J. Phys. Chem. A* **1997**, *101*, 7953.

8. Augspurger, J. D.; Dykstra, C. E. *Chem. Phys. Lett.* **1989**, *158*, 399.

9. Carrick, P. G. in "*Specific Impulse Calculations of High Energy Density Solid Cryogenic Rocket Propellants. 1: Atoms in Solid H_2*". April 1993.

10. (a) Fajardo, M. E. HEDM Contractor's Meeting, June **1999**. (b) Fajardo, M. E.; Tam, S. *J. Chem. Phys.* **1998**, *108*, 4237.

11. (a) Dixon, R. N.; Hwang, D. W.; Yang, X. F.; Harich, S.; Lin, J. J.; Yang, X. *Science*, **1999**, *285*, 1249. (b) Dixon, R. N. *Mol. Phys.* **1996**, *88*, 949.

12. (a) von Neumann, I.; Wigner, E. *Z. Physik* **1929**, *30*, 467. (b) Teller, E. *J. Phys. Chem.* **1937**, *41*, 109. (c) Longuet-Higgins, H. C., F.R.S. *Proc. R. Soc. Lond. A* **1975**, *344*, 147

13. (a) Mead, C. A. *J. Chem. Phys.* **1979**, *70*, 2276. (b) Mead, C. A.; Truhlar, D. G. *J. Chem. Phys.* **1979**, *70*, 2284. (c) Mead, C. A. *Rev. Mod Phys.* **1992**, *64*, 51.

14. (a) Xantheas, S. S.; Elbert, S. T.; Rüdenberg, K. *J. Chem. Phys.* **1990**, *93*, 7519. (b) Xantheas, S. S.; Atchity, G. J.; Elbert, S. T.; Rüdenberg, K. *J. Chem. Phys.* **1991**, *94*, 8054.

15. Kuppermann, A.; Wu, Y.-S. M. *Chem. Phys. Lett.* **1993**, *205*, 577.

16. Niday, T. A.; Weeks, D. E. *Chem. Phys. Lett.* **1999**, *308*, 106.

17. Glezakou, V.-A.; Gordon, M. S.; Yarkony, D. R. J. *Chem. Phys.* **1998**, *108*, 5657.

18. (a) Yarkony, D. R. *Theor. Chim. Acc.* **1997**, *98*, 197. (b) Yarkony, D. R. *Molecular Structure*, in *"Atomic, Molecular and Optical Physics Handbook"*, G. L. Drake Ed., AIP, New York, **1996**, p. 357.

19. Rüdenberg, K.; Schmidt, M. W.; Gilbert, M. M.; Elbert, S. T. *Chem Phys.* **1982**, *71*, p. 41, p. 51, p.65.

20. Roos, B. O., *"The CASSCF Method and its Applications in Electronic Structure Calculations"*, in *Advances in Chemical Physics*, *69*, K.P. Lawley Ed., Wiley Interscience, New York, **1987**, p.339.

21. MCSCF/CASSCF: (a) Werner, H.-J.; Knowles, P. J. *J. Chem. Phys.* **1985**, *82*, 5053. (b) Knowles, P. J.; Werner, H.-J. *Chem. Phys. Lett.* **1985**, *115*, 259.

22. Internally contracted MRCI: (a) Werner, H.-J.; Knowles, P. J. *J. Chem. Phys.* **1988**, *89*, 5803. (b) Knowles, P. J.; Werner, H.-J. *Chem. Phys. Lett.* **1988**, *145*, 514.

23. (a) Dunning, T. H. Jr. *J. Chem. Phys.* **1989**, *90*,1007. (b) Kendall. R. A.; Dunning, T. H. Jr.; Harrison, R. J. *J. Chem. Phys.* **1992**, *96*, 6796. (c) Woon, D. E.; Dunning, T. H. Jr. *J. Chem. Phys.* **1993**, *98*, 1358.

24. Boys, S. F.; Bernardi, F. *Mol. Phys.* **1970**, *19*, 553.

25. **MOLPRO** is a package of *ab initio* programs written by H.-J. Werner and P. J. Knowles, with contributions from J. Almlöf, R. C. Amos, A. Berning, M. J. Deegan, F. Eckert, S. T. Elbert, C. Hampel, R. Lindh, W. Meyer, A. Nicklass, K. Peterson, R. Pitzer, A. J. Stone, P. R. Taylor, M. E. Mura, P. Pulay, M. Schuetz, H. Stoll, T. Thorsteinsson, and D. L. Cooper.

26. **GAMESS** is a package of *ab initio* programs written and maintained by Schmidt, M.W. with contributions from Baldridge, K.K.; Boatz, J.A.; Elbert, S.T.; Gordon, M.S.; Jensen, J.H.; Koseki, S.; Matsunaga, N.; Nguyen, K.A.; Su, S.J.; Windus, T.L.; Dupuis, M.; Montogomery,J.A. *J. Comput. Chem.* **1993**, *14*, 1347.

27. Berry, M. V., F.R.S; Wilkinson, M. *Proc. R. Soc. Lond. A* **1984**, *392*, 15.

28. Huber, K.P.; Herzberg, G. *"Molecular Spectra and Molecular Structure IV. Constants of Diatomic Molecules"*, van Nostrand Reinhold, New york, **1979**.

Table 1. Distances are in Å, angles in degrees and D_e in cm^{-1}. Minima were fitted to a second order quadratic fit.

State	R	r	γ	D_e
$^2A_1$	Repulsive, no van der Waals interaction			
$^2B_1$	3.393	0.7438	90.0	74.73
$^2B_2$	3.163	0.7442	90.0	121.93

Table 2. Distances are in Å, angles in degrees, energy differences in eV with respect to the asymptotic limit.

Species (state)	R	r	γ	ΔE^g
BH_2 ($^2A_1$, min)[a]	0.5131	2.1469	90.0	-2.51
TS1[b] ($^2A_1$)	1.5495	0.9053	90.0	+3.38
MECP1[c]	1.1902	1.1620	90.0	+0.563
TS2[d] ($^2A'$)	1.1959	1.2078	95.0	+0.521
MECP2[e] ($^2A'$)	1.3722	1.6865	65.0	+1.067
DD[f]	1.3647	1.6177	90.0	+1.145

[a]Dihydride. [b]TS1 is the "pure" $^2A_1$ transition state that connects the repulsive $^2A_1$ with the molecular region. [c]MECP1 is the minimum energy crossing point on the ridge between the states $^2A_1$ and $^2B_2$ (C_{2V} seam). MECP1 is a good estimate of TS2. [d]TS2 is the true transition state that connects the $1^2A'$ and the $2^2A'$ (C_S). [e]MECP2 is the minimum energy crossing point on the C_S seam. [f]DD is the point of trifurcation (diabolical point), where the two seams cross. TS1 and MECP1 have been determined with single-state calculations, while MECP2 and DD with state-average wavefunctions to avoid root-flipping. [g]The energy differences are taken with respect to the "infinite" separation of B and H2 (~ 30 Å) to avoid size-extensivity problems.

Table 3: van der Waals minima, transition state and products for linear channel (R2). Bond lengths are in Å and evengy differences in eV with respect to the asymptotic limit, except for the van der Waals complexes in cm^{-1}.

State	Species	R(BH)	R(HH)	ΔE	Exp./Lit.
$^2\Sigma$	vdW	3.516	0.7469	79.58[a]	
	TS	1.327	1.270	+1.207	
	BH+H	1.236	--	+1.066	1.075, R(BH)=1.2325[b]
					1.084, R(BH)=1.226[c]
$^2\Pi$	vdW	3.340	0.7461	28.68[a]	

[a] In cm^{-1}. [b]From reference 28. [c]From reference 5f.

Figure captions

Figure 1. A schematic illustrating the consequences of interstate crossing.

Figure 2. Qualitative diagram of reaction channel R1. Bond lengths in Å, angles in degrees, energy differences in kcal mol^{-1}.

Figure 3. Jacobi coordinates.

Figure 4. Reaction channel (R1), van der Waals interactions of B (^2P) with H_2 (Figures 4a and 4b).

Figures 5. Contour diagram of the $^2A_1$ transition state.

Figure 6. Contour diagram of the combined surfaces, $^2A_1$ and $^2B_2$. The red dot is the doubly diabolical point, the green ones, are points on the (C_{2v}) seam.

Figure 7. Relative energies of the seams, qualitative diagram. The energy differences, in eV are taken with respect to the lowest minimum-energy crossing point (MECP1), in this case on the C_{2V} seam.

Figure 8. Reaction channel (R2), van der Waals interactions of B (^2P) with H_2 (Figures 8a and 8b).

Figure 9. (9a), qualitative diagram of the linear reaction channel. Energy differences in kcal mol^{-1}. (9b) contour plots of the related transition state.

Figure 10. A "3D" representation of the two different seams and the trifurcation point (DD).

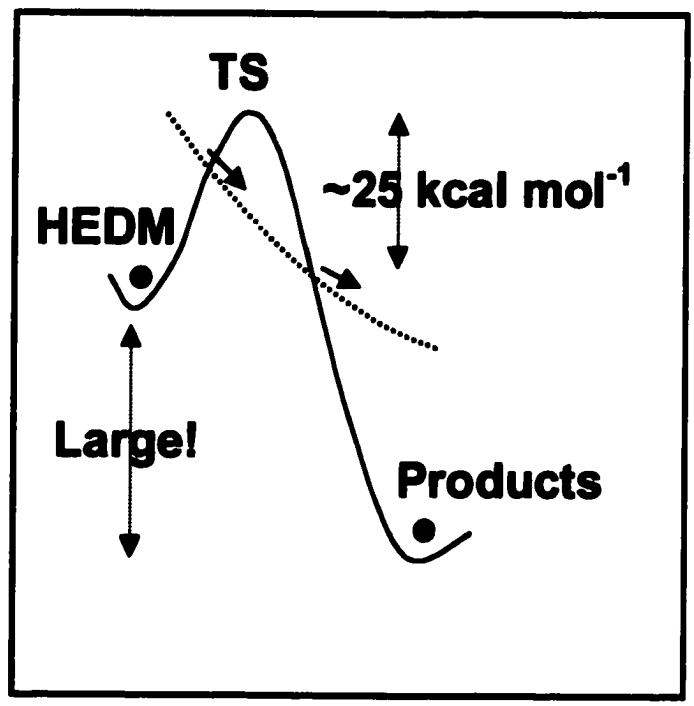

Figure 1

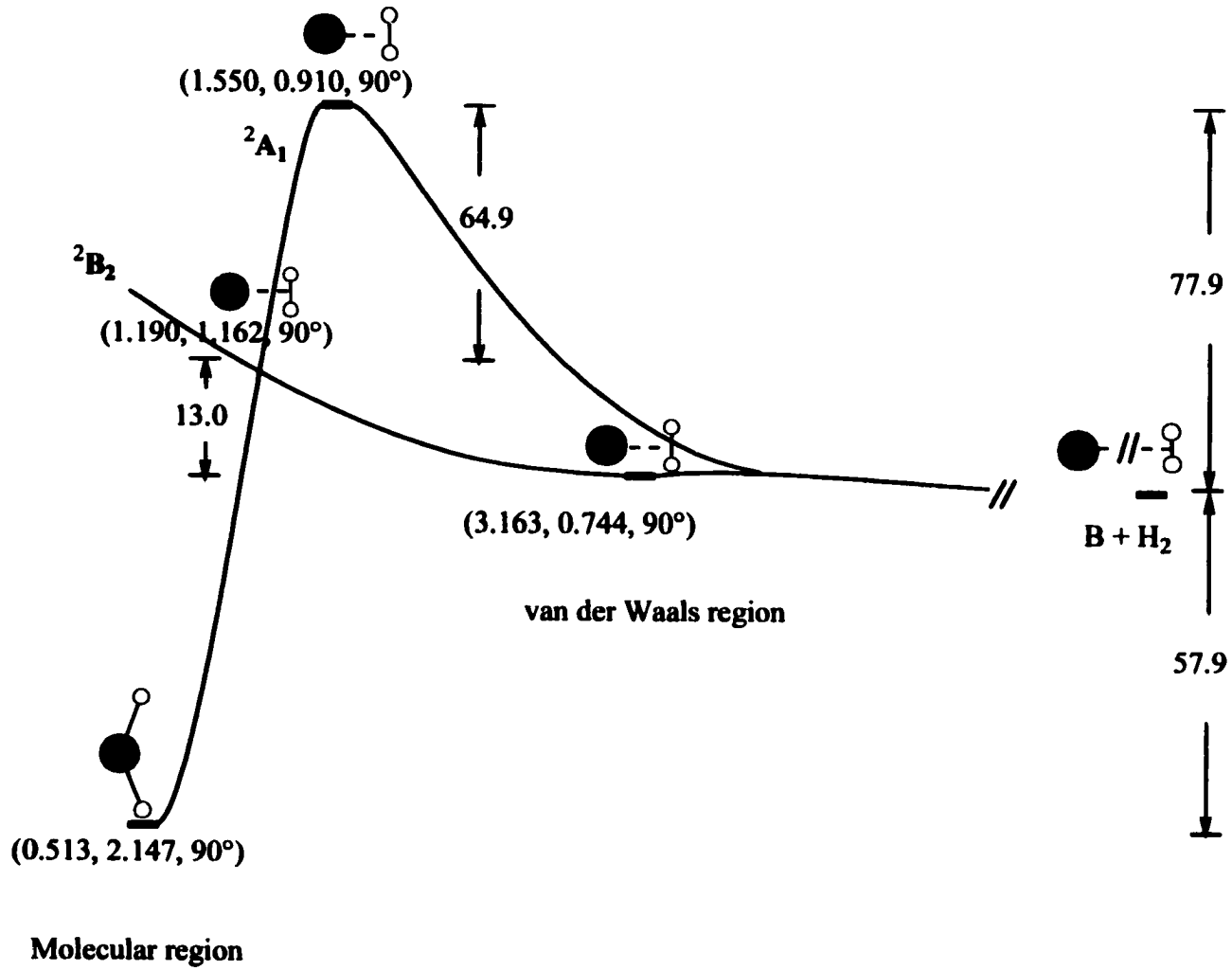

Figure 2

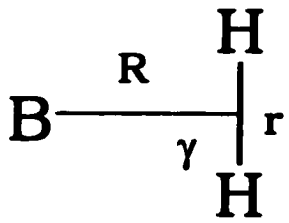

Figure 3

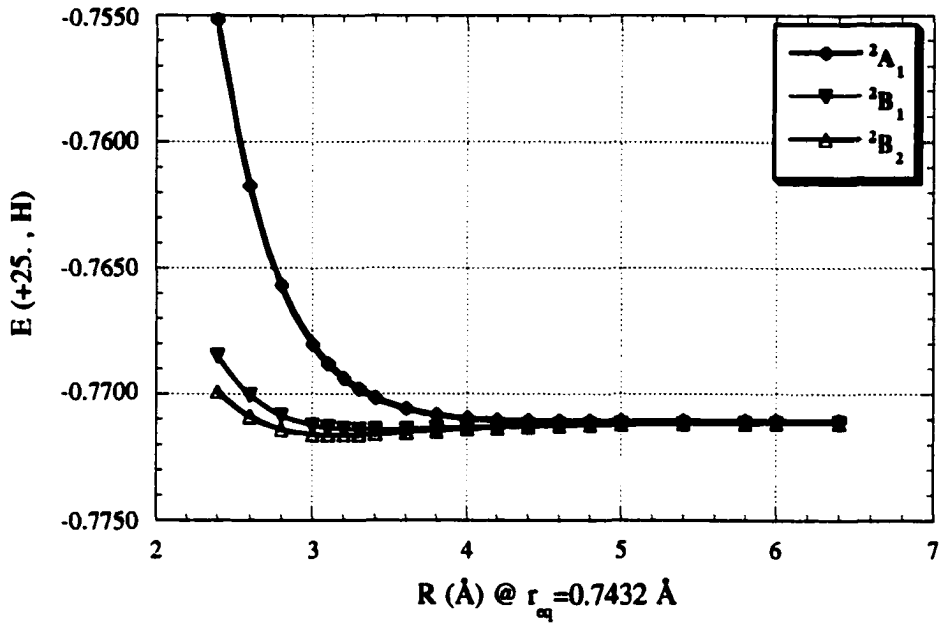

Figure 4a

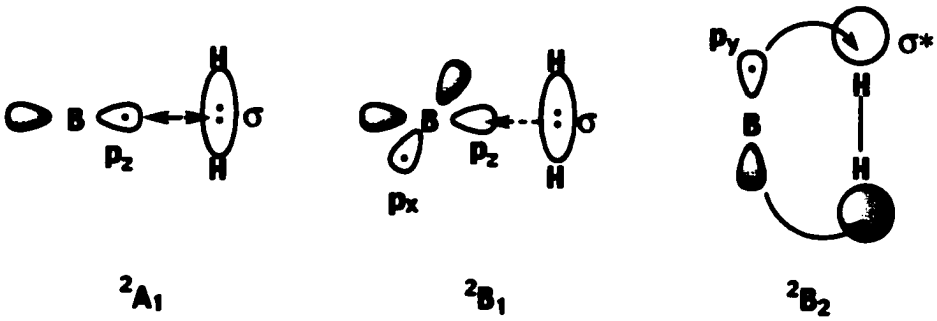

Figure 4b

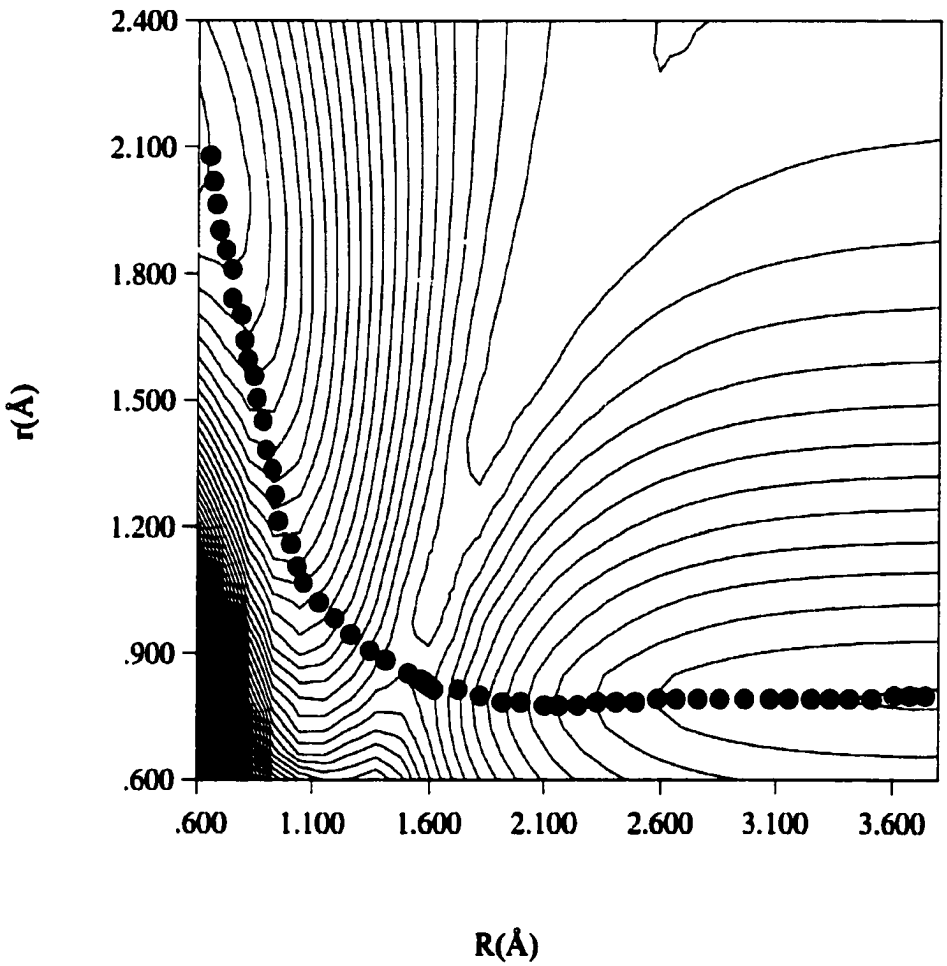

Figure 5

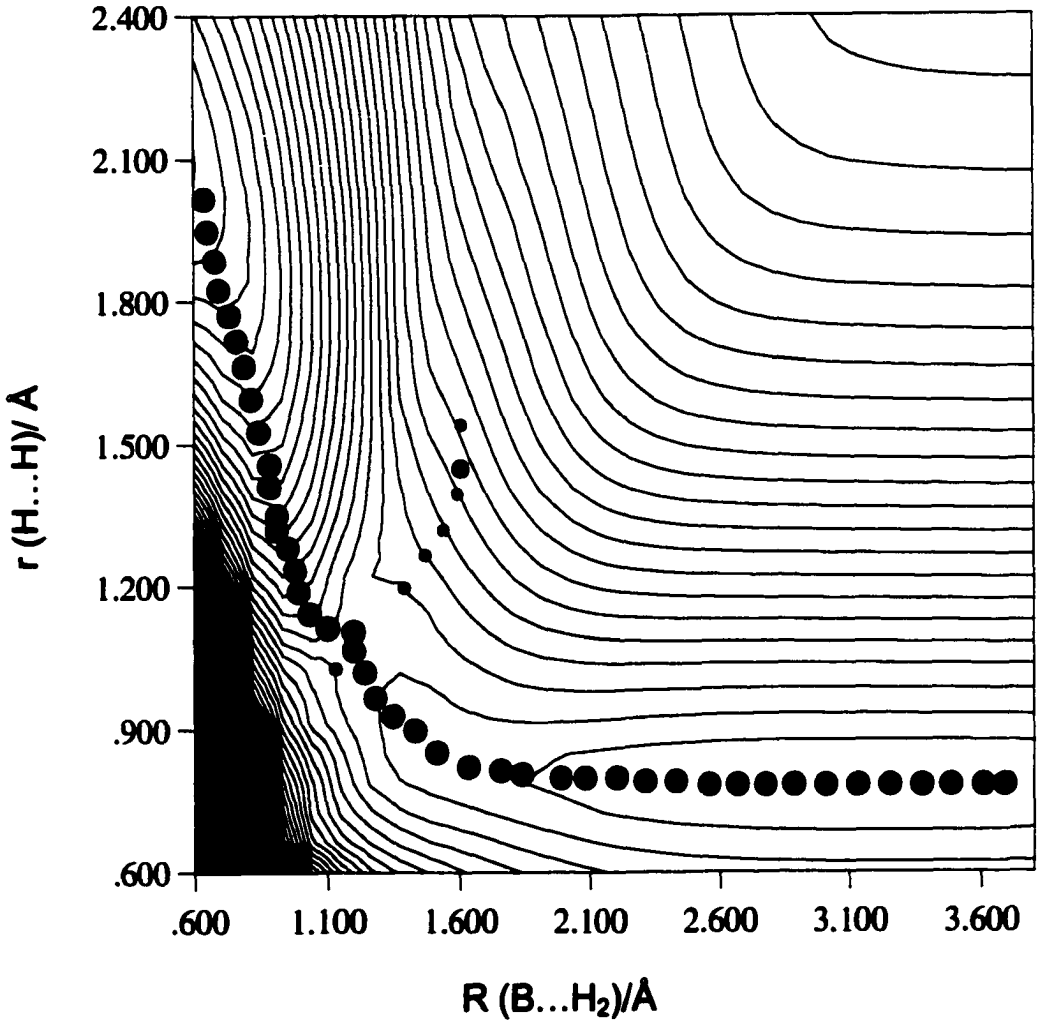

Figure 6

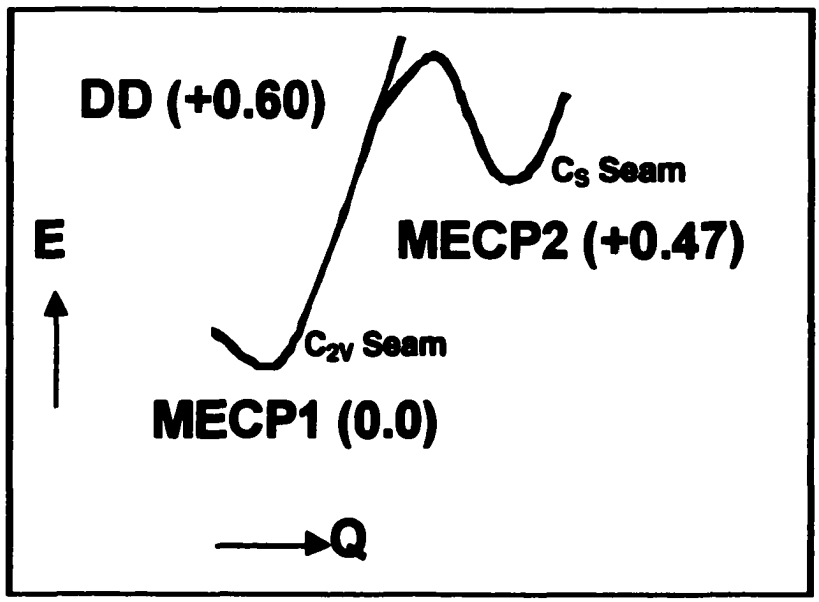

Figure 7

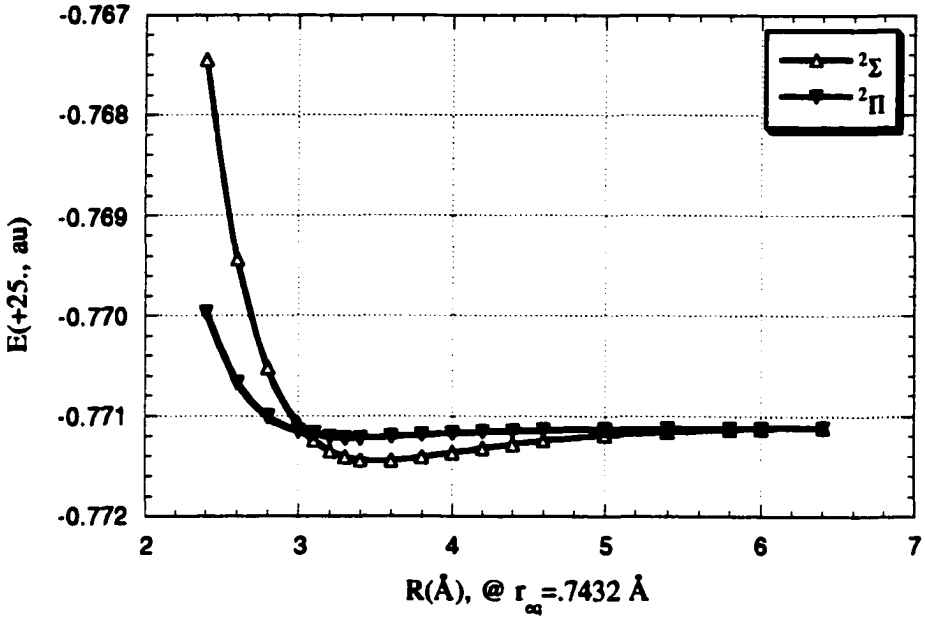

Figure 8a

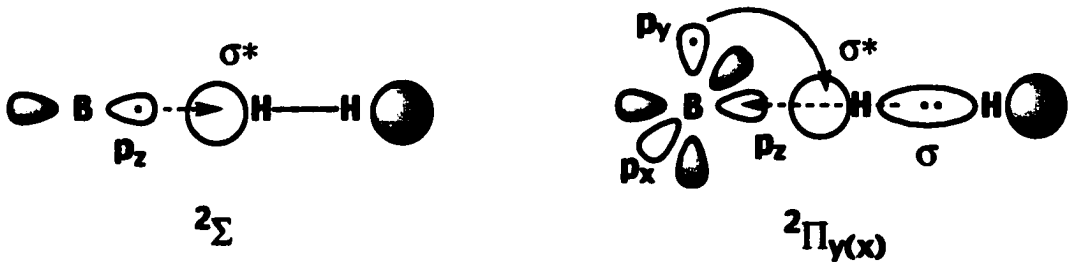

Figure 8b

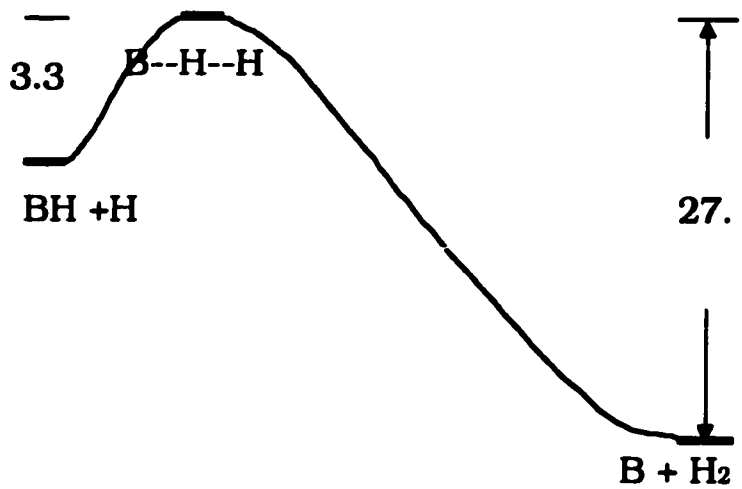

Figure 9a

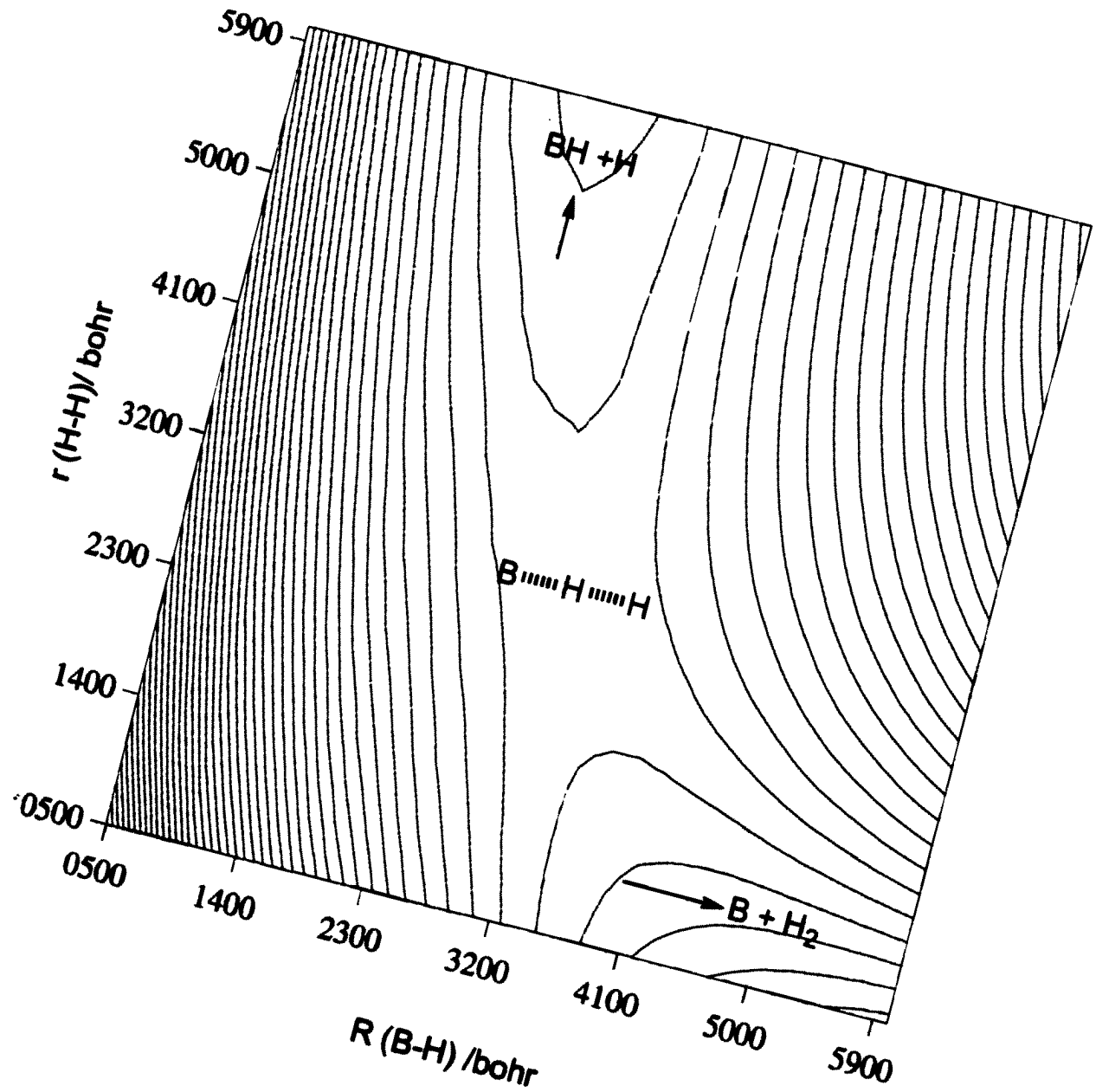

Figure 9b

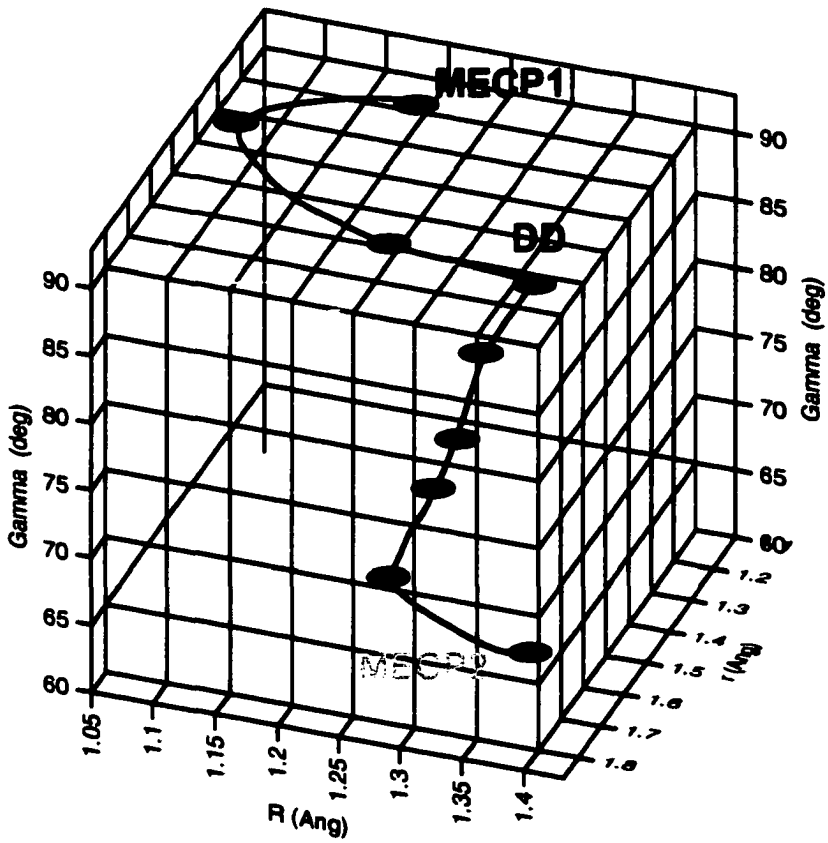

Green: C_{2V} Seam
Purple: C_S Seam

Figure 10

CHAPTER 6: CONCLUSIONS

Various aspects of the Ti and Si chemistry are presented in this compilation of papers. Although Si is isovalent with C, it reacts quite differently and often has a more fascinating behaviour. As a result, Si-compounds are elusive to synthesize and measure. The G2 scheme, in various forms (modifications) is being employed here, to make thermochemical predictions for Si/C systems.

Ti is often viewed as the metallic analogue of the previous two elements, but its behaviour is almost exclusive for each system that is encountered in. Appropriate treatment of Ti-compounds should include at least triple-zeta quality basis sets, for qualitative results, and definitely inclusion of correlation.

Triatomics have been in the centre of attention for many years now, either as theoretical problems, or more practical, like in the M/H_2 system, which has a potential use as rocket fuel. It seems that this application maybe limited by the existence of intestate crossings, and other diabatic phenomena. B/H_2, which is studied in this work, is one of the most promising candidates and therefore detailed information on the potential energy surfaces is of paramount importance.